Technische Universität München
TUM School of Medicine and Health

Evaluation of the DNA repair enzyme PARP1 as a biomarker for prostate cancer

Anna Hambarzumjan

Vollständiger Abdruck der von der TUM School of Medicine and Health der Technischen Universität München zur Erlangung einer Doktorin der Medizin (Dr. med) genehmigten Dissertation.

Vorsitz: apl. Prof. Dr. Stefan Thorban

Prüfer*innen der Dissertation:

1. Prof. Dr. Susanne Kossatz
2. Priv.-Doz. Dr. Julia Dorn

Die Dissertation wurde am 04.05.2024 bei der Technischen Universität München eingereicht und durch die Fakultät für Medizin am 30.09.2023 angenommen.

1 Summary

1.1 Zusammenfassung

Jedes Jahr wird bei 417.000 Männern Prostatakrebs diagnostiziert und über 100.000 Todesfälle lassen sich in Europa verzeichnen. Prostatakrebs ist eine sehr heterogene Krankheit mit Hochrisikopatienten, deren metastasierte Erkrankung derzeit unheilbar ist und eine schlechte Prognose hat. Diese Patienten benötigen neue Behandlungsmöglichkeiten, zu denen die kürzlich zugelassenen PARP-Inhibitoren und PARP-gerichteten Radioligandentherapien gehören. Hier stellen wir eine detaillierte Analyse der PARP1-Expression bei Prostatakrebs vor, um ihre Eignung für diagnostische und therapeutische Ansätze im Vergleich zu PSMA, einem wichtigen Biomarker für die Bildgebung und Radioligandentherapie, zu untersuchen. Wir analysierten formalinfixiertes, in Paraffin eingebettetes Gewebe aus chirurgisch entfernten radikalen Prostatektomie-Proben nach immunhistochemischer Färbung für PARP1 und PSMA. Wir extrahierten mehr als 500 Nahaufnahmen von 31 radikalen Prostatektomien und quantifizierten die PARP1- und PSMA-Färbung. Außerdem wurden 475 TMA-Spots von 248 Patienten angefärbt und auf PARP1-Expression quantifiziert. Bei beiden Ansätzen wurde die IHC-Quantifizierung mit dem Gleason-Score der einzelnen Nahaufnahmen korreliert. Die IHC-Färbung wurde mit ImageJ unter Verwendung einer automatischen Schwellenwertmethode quantifiziert, um den Prozentsatz der positiven Gewebefläche zu berechnen. Die statistische Analyse wurde mit dem D'Agostino & Pearson-Test, dem Kruskal-Wallis-Test und der Spearman-Korrelation in GraphPad Prism 9 durchgeführt. In den Prostatektomie-Proben war die PARP1-Expression im Krebsgewebe (11,4% pta) signifikant höher als bei krebsfreiem Prostatagewebe (4,6% pta; $p<0,05$) und nahm von Gleason 6 bis Gleason 9 stetig zu. Andererseits nahm die PSMA-Expression von Gleason 6 bis Gleason 8 zu. Der Vergleich der Expression von PARP1 und PSMA ergab eine schwache, aber signifikante positive Korrelation. In der TMA-Kohorte stieg die PARP1-Expression ebenfalls von Gleason 7a (3,4% pta) bis Gleason 9 (7,2% pta) an, verglichen mit 1,7% pta in der krebsfreien Prostata. Wir fanden eine weit verbreitete und konsistente Expression von PARP1 in den Prostatakrebsproben. Die mit fortschreitenden Tumorstadium zunehmende Expression von PARP1 in den Proben deutet darauf hin, dass PARP1 ein vielversprechender Biomarker für neue bildgebende und therapeutische Anwendungen bei Prostatakrebs ist, zusätzlich zur Therapie mit PARP-Inhibitoren. Interessanterweise war die Überexpression von PARP1 und PSMA bei Prostatakrebs nicht stark korreliert, was auf einen komplementären Wert hinweisen könnte.

1.2 Summary

Each year, prostate cancer (PC) is diagnosed in 417,000 men and accounts for over 100,000 deaths in Europe. PC is a very heterogeneous disease, with high-risk patients whose metastatic disease is currently incurable and has a poor prognosis. These patients need new treatment options, one of which are the recently approved PARP inhibitor- and PARP-targeted radioligand therapies (RLT). Here, we present a detailed analysis of the PARP1 expression in PC to examine its suitability for diagnostic and therapeutic approaches in comparison to PSMA, an important biomarker for imaging and RLT. We analyzed formalin-fixed paraffin embedded (FFPE) tissue from whole surgical radical prostatectomy biospecimens after immunohistochemical (IHC) staining for PARP1 and PSMA. We extracted more than 500 close-ups from 31 radical prostatectomies and quantified PARP1 and PSMA staining. In addition, 475 tissue microarray (TMA) spots from 248 patients were stained and quantified for PARP1 expression. In both approaches, IHC quantification was correlated to the Gleason score of each close-up. IHC staining was quantified with ImageJ using an automated thresholding method to calculate the percentage of positive tissue area (% pta). Statistical analysis was carried out using the D'Agostino & Pearson test, the Kruskal-Wallis test and the Spearman Correlation in GraphPad Prism 9. In the prostatectomy specimens, PARP1 expression was significantly higher in cancer tissue (11.4% pta) than in cancer free prostate tissue (4.6% pta; $p<0.05$) and increasing steadily from Gleason 6 to Gleason 9. On the other hand, PSMA expression was increasing from Gleason 6 to Gleason 8. Comparing the expression of PARP1 and PSMA, the results showed a weak but significant positive correlation. In the TMA cohort, PARP1 expression was as well increasing from Gleason 7a (3.4% pta) to Gleason 9 (7.2% pta), compared to 1.7% pta in cancer free prostate. We found a widespread and consistent expression of PARP1 in the PC specimens. The increasing expression of PARP1 in the specimens with progressing tumor stage indicates that PARP1 is a promising biomarker for emerging imaging and therapeutic applications in PC, in addition to PARP inhibitor therapy. Interestingly, PARP1 and PSMA overexpression in PC was not strongly correlated, which could indicate a complementary value.

2 List of figures and tables

2.1 Figures

2.2 Tables

2.3 Abbreviations

AR	Androgen receptor
ARPI	Androgen-receptor pathway inhibitor
ATM	Ataxia Telangiectasia Mutated
BRCA	Breast Cancer
BRIP1	BRCA1 Interacting Helicase 1
CHEK2	Checkpoint kinase 2
CRPC	Castration-resistant prostate cancer
DDR	DNA damage repair
DNA	Deoxyribonucleic acid
DSBs	Double-strand breaks
EMA	European Medicines Agency
FDA	Food and Drug Administration
FANCA	Fanconi anemia complementation group A
Ga	Gallium
HDAC2	Histone deacetylase 2
H&E/ HE	Haematoxylin and eosin
HG-PIN	High grade prostatic intraepithelial neoplasia
HRR	Homologous recombination repair
ibPFS	Imaging-based progression-free survival
Lu	Lutetium
mCRPC	Metastatic castration-resistant prostate cancer
PALB2	Partner and localizer of BRCA2
PARP1	Poly [ADP-ribose] polymerase 1
PARPi	PARP inhibitor
PET	Positron emission tomography
PC	Prostate cancer
PSMA	Prostate Specific Membrane Antigen
% pta	Percentage of positive tissue area
RLT	Radioligand therapy
RP	Radical prostatectomy
SUVs	Standardized uptake values
TMA	tissue microarray

Table of Contents

3 Introduction

3.1 Prostate cancer

Each year, PC is diagnosed in 417,000 men and accounts for around 100,000 deaths in Europe [1]. PC is a very heterogeneous disease, with high-risk patients, whose metastatic disease is currently incurable and has a poor prognosis [2]. This is demonstrated by a 5-year survival rate of only 34.1% for distant PC in the United States in Figure 1 [3].

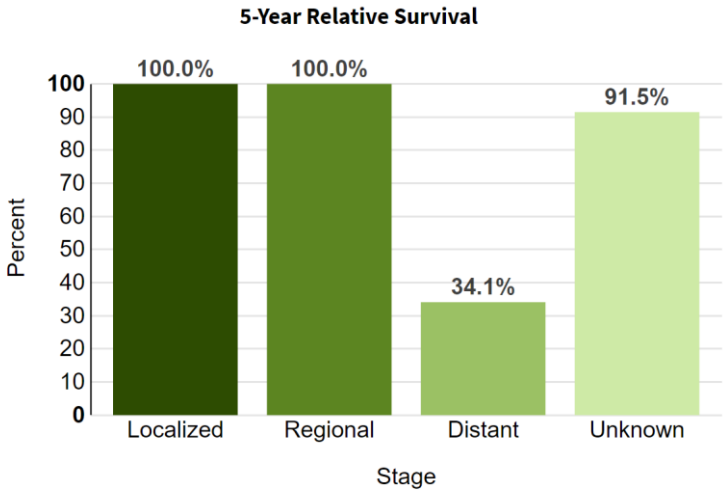

Figure 1: 5-Year Relative Survival for prostate cancer in the United States sorted by stage [3]

3.1.1 TNM-classification for PC

The TNM classification is an important factor in the staging of tumor diseases. It deals with the anatomical extent of the disease and therefore, helps to objective the probable outcome of the disease [4]. TNM is an acronym composed of T for tumor, N for lymph nodes and M for metastasis. The higher the TNM classification, the more the tumor has already progressed. An adapted TNM-classification was developed for each tumor type as can be seen in for PC. The TNM category is one of the three factors that are critical for prognosis. The other two are Gleason score and resection margins at surgery [5].

Table 1: TNM-classification for PC: standard for classifying the extent of spread of cancer [4]

T – Primary Tumor
TX Primary tumor cannot be assessed
T0 No evidence of primary tumor
T1 Clinically inapparent tumor that is not palpable
T1a Tumor incidental histological finding in 5% or less of tissue resected
T1b Tumor incidental histological finding in more than 5% of tissue resected
T1c Tumor identified by needle biopsy (e.g., because of elevated PSA)
T2 Tumor that is palpable and confined within prostate
T2a Tumor involves one half of one lobe or less
T2b Tumor involves more than half of one lobe, but not both lobes
T2c Tumor involves both lobes
T3 Tumor extends through the prostatic capsule
T3a Extracapsular extension (unilateral or bilateral) including microscopic bladder neck involvement
T3b Tumor invades seminal vesicle(s)
T4 Tumor is fixed or invades adjacent structures other than seminal vesicles: external sphincter, rectum, levator muscles, and/ or pelvic wall
N – Regional Lymph Nodes
NX Regional lymph nodes cannot be assessed
N0 No regional lymph node metastasis
N1 Regional lymph node metastasis
M – Distant Metastasis
M0 No distant metastasis
M1 Distant metastasis
M1a Non regional lymph node(s)
M1b Bone(s)
M1c Other site(s)

Further parameters used in this project to classify PC as accurately as possible are mentioned in Table 2.

Table 2: Further parameters for PC classification [6]

L – invasion into lymphatic vessels
L0 no invasion into lympathic vessels
L1 invasion into lympathic vessels
Pn – perineural invasion
Pn0 no perineural invasion
Pn1 perineural invasion
R – the completeness of the operation
R0 no residual tumor
R1 microscopic residual tumor
R2 macroscopic residual tumor
X – information not available

3.1.2 Gleason Score Grading

The Gleason score is a prognostic parameter for the evaluation of PC. It is based on the histological morphology of the glandular pattern. This is often heterogeneous in PC. The Gleason patterns go from Gleason 1 to 5, where Gleason 1 is well-differentiated adenocarcinoma and Gleason 5 is very polymorphic tumor cells with frequent mitoses. The use of Gleason pattern 1 and 2 is no longer recommended due to considerable interobserver variability. In a radical prostatectomy (RP) specimen, the most frequent and the second most frequent differentiation pattern are added together, resulting in a Gleason score from 6-10 [7]. An overview of this is provided by Table 3

Table 3: The Gleason score and Grade Groups [8]

Gleason score	**Grade Group**	**Description**
Gleason score 6 (3 + 3 = 6)	1	The cells look similar to normal prostate cells. The cancer is likely to grow very slowly, if at all.
Gleason score 7a (3 + 4 = 7)	2	Most cells still look similar to normal prostate cells. The cancer is likely to grow slowly.
Gleason score 7b (4 + 3 = 7)	3	The cells look less like normal prostate cells. The cancer is likely to grow at a moderate rate.

Gleason score 8 (4 + 4 = 8)	4	Some cells look abnormal. The cancer might grow quickly or at a moderate rate.
Gleason score 9 or 10 (4 + 5 = 9, 5 + 4 = 9 or 5 + 5 = 10)	5	The cells look very abnormal. The cancer is likely to grow quickly.

3.1.3 Overview over recent therapy options

For the choice of therapy, it is relevant whether the tumor is only localized, has already locally advanced, or metastasized. Figure 2 gives a rough overview of the possible therapies. The preparations used in this work were from RPs. Furthermore, in the context of Poly [ADP-ribose] polymerase (PARP) inhibitors, combination therapies with a prior hormonal treatment for patients with homologous recombination repair (HRR) gene-mutated metastatic castration-resistant prostate cancer (mCRPC) will be discussed. Regarding the biomarker Prostate Specific Membrane Antigen (PSMA), RLT plays an important role.

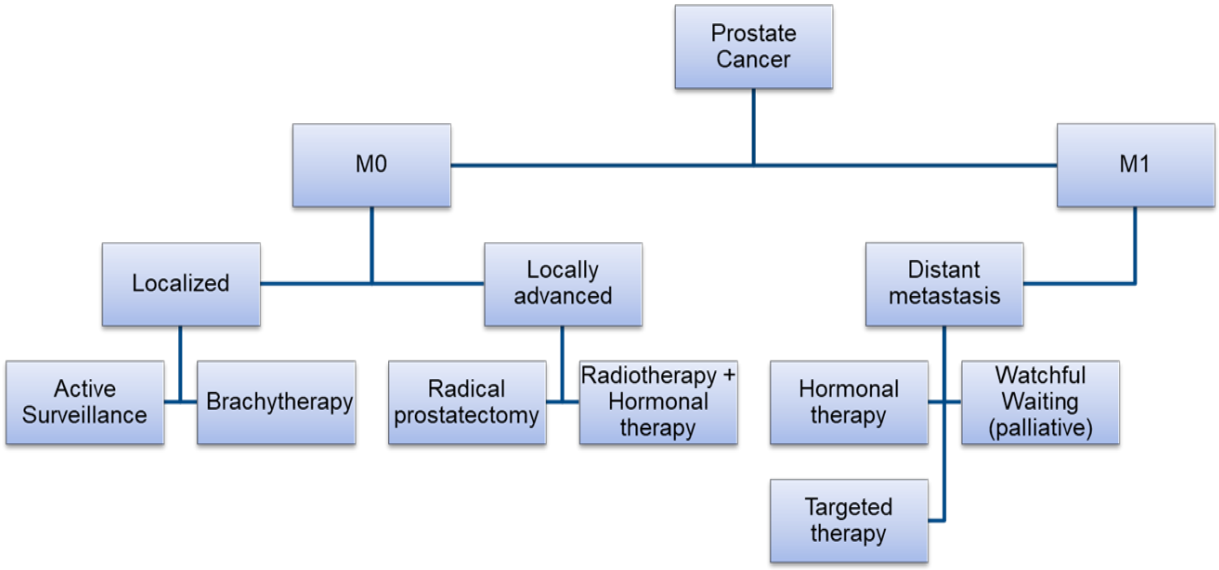

Figure 2: Overview over recent therapy options [7]

3.2 Prostate Specific Membrane Antigen (PSMA)

Currently, the most successful biomarker in imaging and in nuclear medicine therapy of PC is PSMA [9]. It is a type II integral membrane glycoprotein that has a strong expression in PSMA positive PC cells, but a weak one in healthy prostate tissue [10]. Studies show that PSMA expression was found to increase progressively in high grade prostate tumor cells and metastatic lesions [11]. Contrary to what the name suggests, PSMA is not completely specific to prostate tissue. Its expression has also been found in other tissues, like kidney, proximal small intestine and salivary gland, and therefore shows problems in terms of specificity and sensitivity [10]. PSMA appears to be a promising molecule for improved diagnosis and treatment of PC, which is why PSMA in its application will be further discussed in the following two chapters.

3.2.1 PSMA-PET/ CT and SPECT/CT

PSMA is a biomarker to improve diagnosis, staging and monitoring for recurrence in PC patients [12]. Gallium-68 (^{68}Ga) is a radiopharmaceutical that is being used in positron emission tomography (PET)-imaging for diagnostic purposes [13]. Combined as ^{68}Ga -PSMA-11, this tracer has been approved as a diagnostic imaging agent by the U.S. Food and Drug Administration (FDA) since December 2020 and by the European Medicines Agency (EMA) since December 2022 [14]. Another recently FDA approved drug for PET imaging of PSMA positive lesions in men with PC is Pylarify (piflufolastat F18) [15]. It received its approval in May 2021 in the USA for patients with suspected metastasis who are candidates for initial definitive therapy or with suspected recurrence based on elevated serum PSA level [16]. PSMA PET/CT is an important type of imaging for the detection of recurrence and has therefore a big impact on the planning of individualized radiotherapy.

A much newer approach is Technetium-99m (^{99m}Tc)-PSMA SPECT/CT [12]. Compared to PET/CT, it is cheaper and available in more countries, especially developing countries [12]. Clinical studies showed that ^{99m}Tc-PSMA SPECT-CT has a similarly high sensitivity to detect recurrence of PC in high-risk patients as ^{99m}Tc-PSMA PET/CT, and is extremely useful when PET/CT is not available [17]. In low-risk patients and when PET/CT is available, PET/CT is superior in the results according to the current state of research [17].

3.2.2 PSMA-ligand therapy

A novel therapeutic option for patients with mCRPC is the RLT with 177 Lutetium [Lu]-labelled PSMA-binding molecules [18]. 177Lu-PSMA-617, with the trade name Pluvicto®, was approved by the FDA in March 2022 [19] and by the EMA in December 2022 [20]. It appears to be a safe and effective option for reducing PSA and tumor burden in patients with mCRPC. In the final phase III trial VISION, 177Lu-PSMA-617, in combination with the standard therapy, showed a reduction of the overall mortality by 38% [21]. As every therapy option, 177Lu-PSMA-RLT has side-effects such as the risk for a critical radiation dose in organs like the kidneys, the lacrimal and the salivary glands [18], as well as tiredness, nausea, anaemia, decreased appetite and constipation [20].

Currently approved for the PSMA-RLT are only male patients with mCRPC progressing after standard treatments [21]. This is due to the fact that the recent approval of 177Lu-PSMA-617 is based on the phase III trial VISION. Consequently, the patients included so far have a poor prognosis due to the advanced diagnoses. The World Association of Radiopharmaceutical and Molecular Therapy demonstrated in a retrospective multicenter analysis study that applying this therapy on chemotherapy-naive PC patients had a better outcome, with longer overall survival rates (14.6 months) compared to patients with a history of chemotherapy (10.9 months and 8.9 months, depending on previous therapy) [22]. Therefore, ongoing phase III trials are investigating whether 177Lu-PSMA-617 can provide therapeutic benefit earlier in the treatment sequence in order to presumably improve the outcome of this therapy [23]. In addition, not all PSMA-positive patients responded to therapy or became resistant with ongoing therapy despite PSMA expression [24]. Therefore, new additional biomarkers need to be identified to help improve diagnostics and treatment.

3.3 Poly [ADP-ribose] polymerase (PARP1)

Another option is the treatment with PARP inhibitors (PARPis) which inhibit the deoxyribonucleic acid (DNA) repair and have entered the market of PC therapy in 2020 [25]. The first discovered and most analyzed PARP enzyme is PARP-1 [26]. It has a key role in the repair of single-strand breaks (SSB) which result from oxidative stress via the base excision repair/SSB repair (BER/SSBR) pathway [27]. According to the synthetic lethality hypothesis, two circumstances work together to induce cell death in

cancer cells (see Figure 3) [25]. On the one hand, the DNA damage repair (DDR) is efficiently blocked by inhibiting the activity of PARP enzymes. On the other hand, the cells are homologous recombination repair (HRR) deficient, for example with a breast cancer (BRCA) mutation in two alleles. Other gene mutations that have been examined for leading to genomic instability are ATM, FANCA, PALB2, CHEK2, BRIP1, HDAC2 [26]. They are still being researched and are not indications for PARPis approved by the FDA.

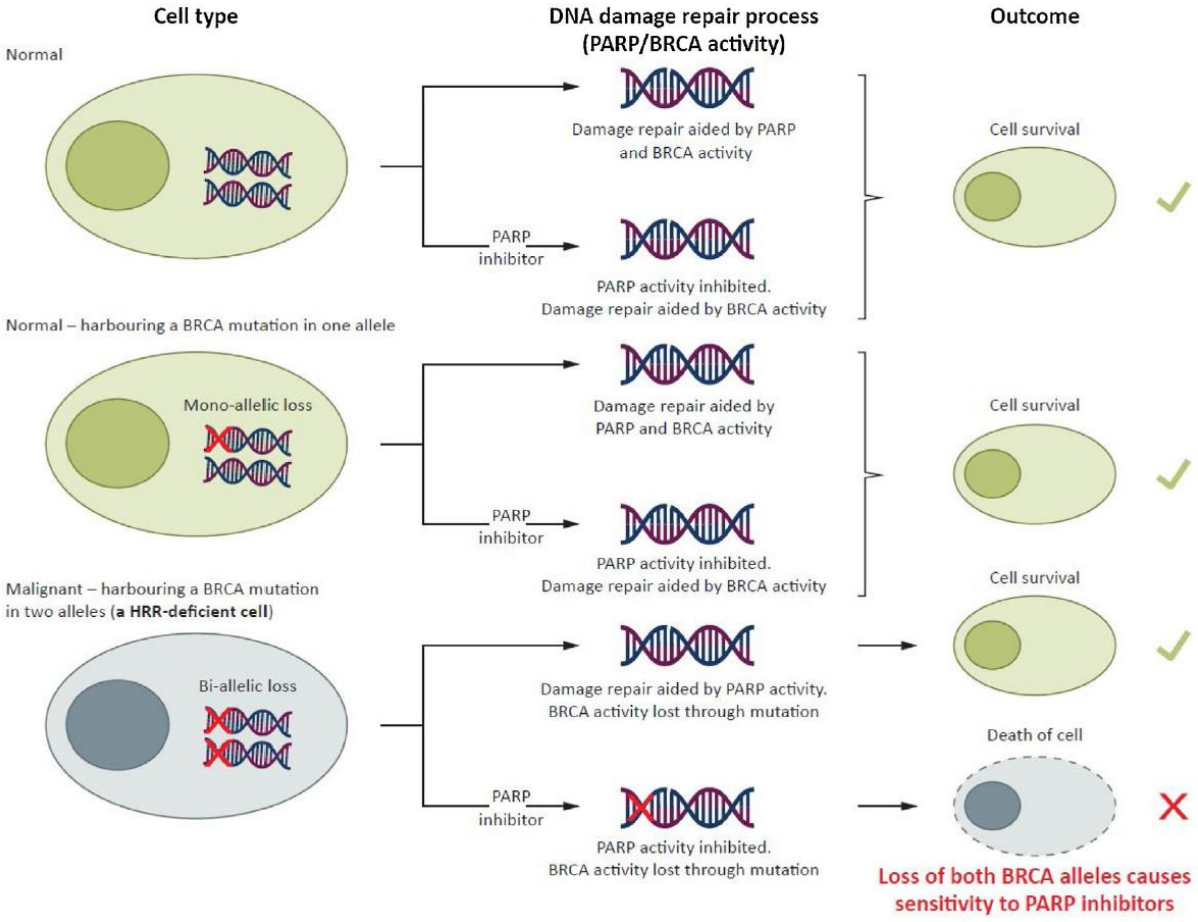

Figure 3: The role of PARP inhibitors and BRCA mutation status in DNA repair and apoptosis of cancer cells: the synthetic lethality hypothesis [25].

3.3.1 PARP inhibitors as monotherapy

The PARPis that have been approved for the longest time are olaparib and rucaparib. Approval was led by the multicenter, open-label, phase II TRITON2 trial (NCT02952534), which evaluated the response to rucaparib as monotherapy of 227 patients with mCRPC associated with HRR deficiency [28]. When the results were published, patients were divided into two groups according to HRR mutations. In the

BRCA group, rucaparib was found to have antitumor activity in patients with mCRPC, but with a manageable safety profile consistent with that reported in other solid tumor types [29]. In the non-BRCA group, there was a limited response to PARP inhibition in men with alterations in ATM, CDK12 [30]. Olaparib, on the other hand, was approved in the phase III, open label, randomized PROfound study (NCT02987543), which assessed the efficacy and safety of olaparib versus enzalutamide or abiraterone acetate in 387 patients with mCRPC, who had failed prior treatment with a new hormonal agent and had HRR gene mutations [31]. In cohort A, imaging-based progression-free survival (ibPFS) was significantly longer in the olaparib group than in the control group (median, 7.4 months vs. 3.6 months). The median overall survival in cohort A was 18.5 months in the olaparib group and 15.1 months in the control group. 81% of the patients in the control group who had progression crossed over to receive olaparib [32]. Both are FDA approved for the therapy of PC since May 2020 [25]. Olaparib was further approved by the EMA in November 2020, which means it is already being used in Germany and can be found in the S3 Guideline for PC (Version 6.2 - October 2021; recommendation 7.45) [33]. So far it is only indicated as monotherapy for patients with mCRPC and a BRCA1/2 mutation, who have progressed following prior treatment with a new hormonal agent [33]. This affects a lot of patients because the incidence of germline mutation in DDR genes among men with metastatic PC is significantly higher compared to the incidence in men with localized PC [34]. Studies showed that ~90% of mCRPC patients have clinically actionable germline and somatic alterations, whereof DDR defects represent 25% of these alterations [35]. The most frequent aberration is BRCA2 with around 5.3% [34]. It was noted that there is a tendency for a better outcome in homozygous BRCA alterations than in heterozygous [29]. Although, this was not confirmed because of the very small monoallelic subgroup in the referring study. Furthermore, studies distinguished between germline and somatic alterations. However, there are currently no conclusive results that could significantly prove a superiority in germline alterations in regard to a better outcome of therapy [29].

3.3.2 PARP inhibitors as combination therapies

Current studies showed that PARPi appears to be more effective in combination treatments with immunotherapy, targeted agents and radiation [36]. What has been frequently analyzed is the blockade of androgen receptors (AR) with androgen-receptor pathway inhibitors (ARPI) in combination with olaparib. As first-line treatment for mCRPC, the phase III study PROBel enrolled 796 patients to either olaparib or placebo, both combined with abiraterone and prednisolone [36]. At the first data cutoff, the analysis showed that abiraterone combined with olaparib significantly prolonged ibPFS compared to the placebo arm (24.8 vs. 16.6 months) irrespective of the patients HRR status [37].

PARP inhibition has, among others, an indirect effect on the upregulation of PD-L1, which is why in several studies anti-PD-L1 was combined with olaparib as an example of a combination therapy of PARPi and immunotherapy [38]. For a phase II trial olaparib and durvalumab (anti-PD-L1) were combined as a treatment in 17 mCRPC patients unselected for HRR alterations after prior treatment with ARPI. The study's conclusion was that durvalumab plus olaparib had acceptable toxicity and that for all patients the combination showed a median radiographic progression free survival (rPFS) of 16.1 months with a 12-month rPFS of 51.5% [39].

There already exists an approved PARPI combination therapy for advanced high grade epithelial ovarian cancer. Patients suffering from this condition can be treated through a combination of olaparib and bevacizumab as maintenance therapy [40]. According to the assessment of the Institute for Quality and Efficiency in Health Care in Germany, a substantial benefit regarding overall survival was found in patients without detectable tumor after primary surgery and patients without detectable tumor/ with complete response after chemotherapy [41]. For patients without detectable tumor/ with complete response after interval surgery and patients with partial response only minor benefits were identified [41].

PARPi has also been modified into agents for molecular imaging RLT [42]. It has been shown in models of oral cancer that PARPi-FL, a fluorescent PARP1-targeted small molecule, specifically binds to PARP1 with a similar affinity to olaparib and can be used to detect cancer as a targeted optical imaging agent [43].

4 Aims of the work

This thesis presents a detailed analysis of the PARP1 expression in PC to examine its suitability for diagnostic and therapeutic approaches in comparison to PSMA, an already clinically validated biomarker for imaging and RLT. More specifically, the PARP1 expression in PC will be analyzed sorted by the stage of cancer. The expressions in the same areas of RP specimen will be compared. In addition, many PARP1 stained TMAs will be examined to obtain average expression values of a large cohort of patients. This allows a better statistical representability of the PARP1 expression distribution. Its aim is to draw conclusions for appropriate use in research and later clinical settings.

Following structured questions will be addressed:

1) Does PARP1 expression increase steadily with progressing cancer stage?
2) Are the differences between the PARP1 expressions in increasing cancer stage significant?
3) Does PSMA expression increase steadily with progressing cancer stage?
4) Are the differences between the PSMA expressions in increasing cancer stage significant?
5) Do PARP1 expression and PSMA expression correlate?
6) How is the trend of PARP1 expression in the different tumor stages in TMAs?
7) How is the PARP1 expression in TMAs compared to RPs?

5 Material and methods

The project deals with basic medical research in the field of imaging and biomarkers in oncology. Included are FFPE preparations of RP specimens from PC patients from the submission material of the Institute of Pathology of the Technical University of Munich. The material is being analyzed retrospectively, after the completion of diagnostics and therapy. Patient data is used in accordance with Article 27 of the Bavarian Hospital Law for research purposes as defined in the positive vote of the ethics committee with the reference number 101/20S.

Our study included RP tissues (n=31 patients) stained for H&E, PARP1 and PSMA. Furthermore, TMA tissues (n=248 patients) derived from RP tissues stained for PARP1 were analyzed.

5.1 Technical equipment

Table 4: Technical equipment

Device	**Company**
Aperio AT2 scanner	Leica Biosystems, Nußloch, Germany
Aperio CS scanner	Leica Biosystems, Nußloch, Germany
BOND RXm: automatic IHC stainer used for PARP1 immunostaining	Leica Biosystems, Nußloch, Germany
Benchmark XT: automatic IHC stainer used for PSMA immunostaining	Ventana GmbH & Co. KG, Vreden, Germany
Leica ASP300S: fully enclosed tissue processor	Leica, Biosystems, Nußloch, Germany

5.2 Consumable supplies

Table 5: Consumable supplies

Consumable	**Company**
SuperFrost Ultra Plus Adhesion Slides	Engelbrecht GmbH, Edermünde, Germany

5.3 Reagents for H&E staining

Table 6: Reagents for H&E staining

Reagents
Aqua dest
Eosin alcoholic 1%
Ethanol 70%
Ethanol 96%
HTX-Mayer
Isopropanol
Tap water
Xylene

5.4 Antibodies used for IHC

Table 7: Antibodies used for IHC

	PARP1	**PSMA**
Manufacturer	proteintech	Agilent Dako
Order number	66520-1-Ig	M3620
Clone	142	3E6
Species	Mouse monoclonal	Mouse monoclonal
Reacts with	Human	Human
Working dilution	1:200	1:50
Working concentration	2,5µg/ml	3,4µg/ml

5.5 Kits

Table 8: Kits

Kit	**Produced by**
PARP1: Bond Polymer Refine Kit	Leica Biosystems, Nußloch, Germany
PSMA: ultraView Universal Kit	Roche Holding, Basel, Switzerland

5.6 Software

Table 9: Software

EndNote version 20
Microsoft Office (Word, Excel, PowerPoint) 2016
Image J version 1.53c
GraphPad Prism version 9.0
Leica Aperio ImageScope version 12.4.3.5008

5.7 Fixation, dehydration, paraffin embedding and section preparation

5.7.1 Fixation and dehydration

Fixation methods were used to ensure that tissues were preserved as naturally as possible and that they could be assessed in their original architecture. Tissues were fixed in aqueous formalin solutions containing 4% formaldehyde. This form of fixation is the most common type of tissue preservation. The tissues were fixed in the fixative solution for 8 to 24 hours at room temperature and then well immersed with 70% ethanol for another 8 to 24 hours. This was followed by the usual dehydration of the tissues overnight in the dehydration machine Leica ASP300.

5.7.2 Paraffin embedding and section preparation

The fixed tissues were then embedded in paraffin. The embedding temperatures were between 50°C and 70°C. From the hot paraffin, the tissues were poured into blocks and cooled to -20°C. In the next step, a microtome was used to make sections. The sections were cut in 1-2 micrometer thin slices.

The obtained sections were first collected on a cold-water bath (~ 20°C) and then stretched on a hot-water bath (~ 45°C) to be mounted smoothly on a slide. The mounted sections were then dried overnight at about 37°C to 45°C, which leads us to the last step, the staining.

5.8 Staining procedures

5.8.1 Haematoxylin and Eosin (H&E) staining

5.8.1.1 Staining

H&E is a survey stain routinely used for evaluation of histological specimens in histology. It is considered the gold standard. The deparaffinization of the sections and staining were done by hand. The working steps contain Xylene (5 min), Xylene (5 min), Isopropanol (5 min), Isopropanol (5 min), Ethanol 96% (2 min), Ethanol 96% (2 min), Ethanol 70% (2 min), Ethanol 70% (2 min), Aqua dest (25 s), HTX-Mayer (8 min), Tap water (10 min), Eosin alcoholic 1% (4 min), Ethanol 96% (30 s), Isopropanol (25 s), Isopropanol (25 s), Xylene (1.5 min), Xylene (1.5 min). With this staining, the nuclei were stained blue, other material pink. The sections were scanned with a Leica CS system to our e-slide database.

5.8.2 Immunohistochemistry (IHC) staining

5.8.2.1 PARP 1 staining

RP tissues and TMAs were both stained for PARP1 with the following IHC protocol. The antibody mentioned in Table 7 was used. The preparations were first pretreated with citrate buffer (30min) following an incubation with the PARP1 antibodies (15min). The next step was the detection with the PARP1 Kit (see Table 8), where the counterstaining was also included. The staining was performed on a fully automated stainer (see Table 4).

5.8.2.2 PSMA staining

For PSMA IHC staining, the antibody mentioned in Table 7 was used. The preparations were first pretreated with citrate buffer (60min) following an incubation with the PSMA antibodies (32min). The next step was the detection with the PSMA Kit (see Table 8). After that the specimen were counterstained with hematoxylin (8min). Here again, the staining was performed on a fully automated stainer (see Table 4).

6 Results

6.1 Patient epidemiology

Table 10: RP analysis - tumor classification and Gleason Score (X: no information available)

Patient	Age	T	N	L	Pn	R	Gleason 3 (%)	Gleason 4 (%)	Gleason 5 (%)	Tumor volume (%)
1	70	3b	1	1	1	X	20	80	-	45
2	73	3b	0	1	1	1	70	25	5	75
3	48	2c	0	0	1	0	55	45	-	15
4	66	2c	0	0	0	0	100	-	-	25-50
5	75	3b	1	1	1	1	30	70	-	40
6	76	3b	0	0	1	1	10	90	-	35
7	73	3a	0	0	1	0	-	100	-	30
8	72	3b	0	0	X	0	-	100	-	-
9	63	3b	1	0	1	1	-	-	100	80
10	72	3b	1	1	1	X	-	60	40	40
11	65	3b	1	0	1	1	-	30	70	90
12	79	3b	1	1	1	1	-	70	30	70
13	66	3b	1	1	1	1	-	60	40	75
14	66	3a	1	1	1	1	60	40	-	60
15	77	3b	0	1	1	1	15	80	5	80
16	72	2c	0	0	x	0	100	-	-	15
17	67	3b	1	1	1	1	15	80	5	75
18	76	3a	0	0	1	1	30	65	5	50
19	66	3b	1	1	1	0	5	9	-	40
20	80	3b	1	X	1	X	0	100	0	10
21	51	2c	1	X	1	0	5	95	-	X
22	70	HG-PIN	-	-	-	-	-	-	-	-
23	72	3b	1	X	1	1	25	75	-	X
24	69	3b	1	1	1	1	5	85	10	10-15
25	67	3b	1	1	1	1	40	50	10	30
26	70	3a	1	1	1	0	70	30	-	10

27	55	3b	1	1	1	1	20	55	25	X
28	78	3a	1	X	1	0	25	75	-	15
29	53	4	1	X	1	1	5	95	-	25-30
30	72	3b	1	1	1	1	-	85	15	90
31	63	3b	1	1	1	1	5	90	5	X

In Table 10, the age of the patient at the time of surgery, the TNM classification, the percentages of Gleason 3, 4, and 5, and the percentage of tumor volume can be found for each RP preparation. Patients No.1-18 were analyzed as cohort A in the first step. In the second step, patients No.19-31 (cohort B) were co-utilized from a PSMA study by AG Eiber and additionally analyzed for PARP according to the same scheme to have a comparison cohort. To control for cohort-specific differences, both were first analyzed as a separate cohort, compared, and then added to a common cohort in the last step. In the cohort A, the patients´ age ranged from 48 to 79 years with an average of 70 years. Tumor stages varied from pT2c, pT3a to pT3b according to the TNM classification. In the cohort B, patients ranged in age from 51 to 80 years, but averaged 66 years. Tumor stages according to the TNM classification ranged from pT2c, pT3a, pT3b to pT4.

Table 11: TMA analysis – Number of close ups per TMA block

TMA	Number of close-ups
1	102
2	126
3	132
4	95
5	99

As shown in Table 11, there were 5 TMA blocks for the second approach available, in which between 95 and 132 close-ups were taken.

6.2 Analysis of PARP1 and PSMA expressing in RP specimens

In the first approach, FFPE tissue from surgical RP specimens was analyzed after IHC staining with PARP1 and PSMA. Tumor areas were drawn onto the HE specimens (see Figure 4) by me and verified by an employee of the pathology department both using the Aperio ImageScope program. In the next step, the respective tumor areas were matched to the correct Gleason scores. Low-grade PIN was not selected as a single category, because clinically it is not considered a precancerous stage. The low number of samples scored as low-grade PIN were assigned to the tumor-free prostate category. Close-up images were then extracted at 20X magnification in all RP specimens each at the same position in HE, PARP1 and PSMA (see examples in Figure 5). All overview images of the RP specimens in HE, PARP1, and PSMA staining can be found in the appendix in chapter 10.2. A minimum of 10 and a maximum of 30 close-up images were taken per patient, with an average of 18. These were distributed across the entire specimen, in order to cover tumor areas as well as tumor-free areas.

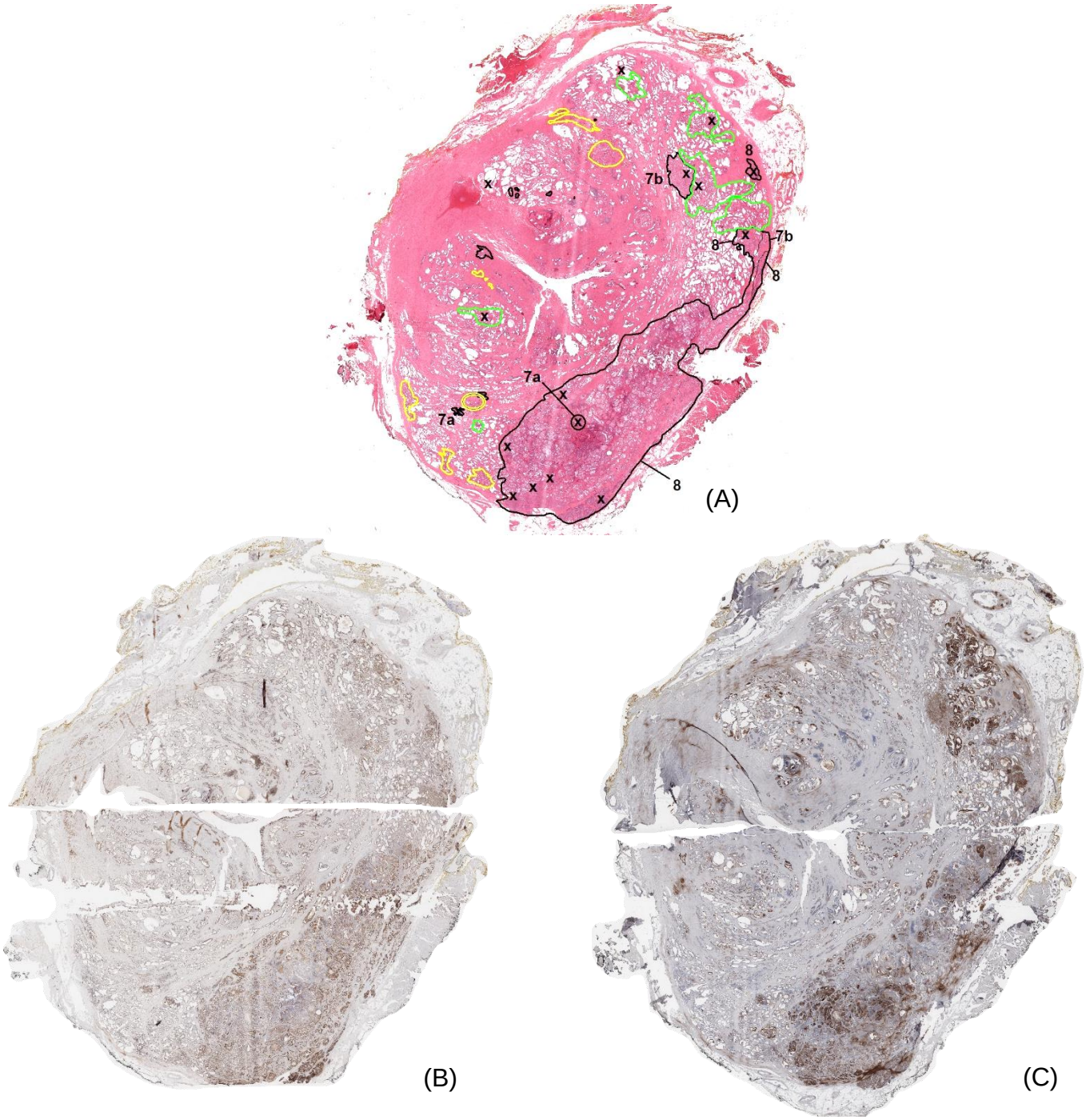

Figure 4: Example of processing of a RP specimen stained in H&E ***(A),*** *for PARP1* ***(B)*** *and for PSMA* ***(C)***

(A) *different drawn colored lines that mark certain tissues:*

Black: tumor tissue, Green: PIN, Yellow: uncertain, needs to be checked with pathologist, Black writing: Gleason score,

X: locations, where the close-ups (20x) were taken in all 3 images A-C

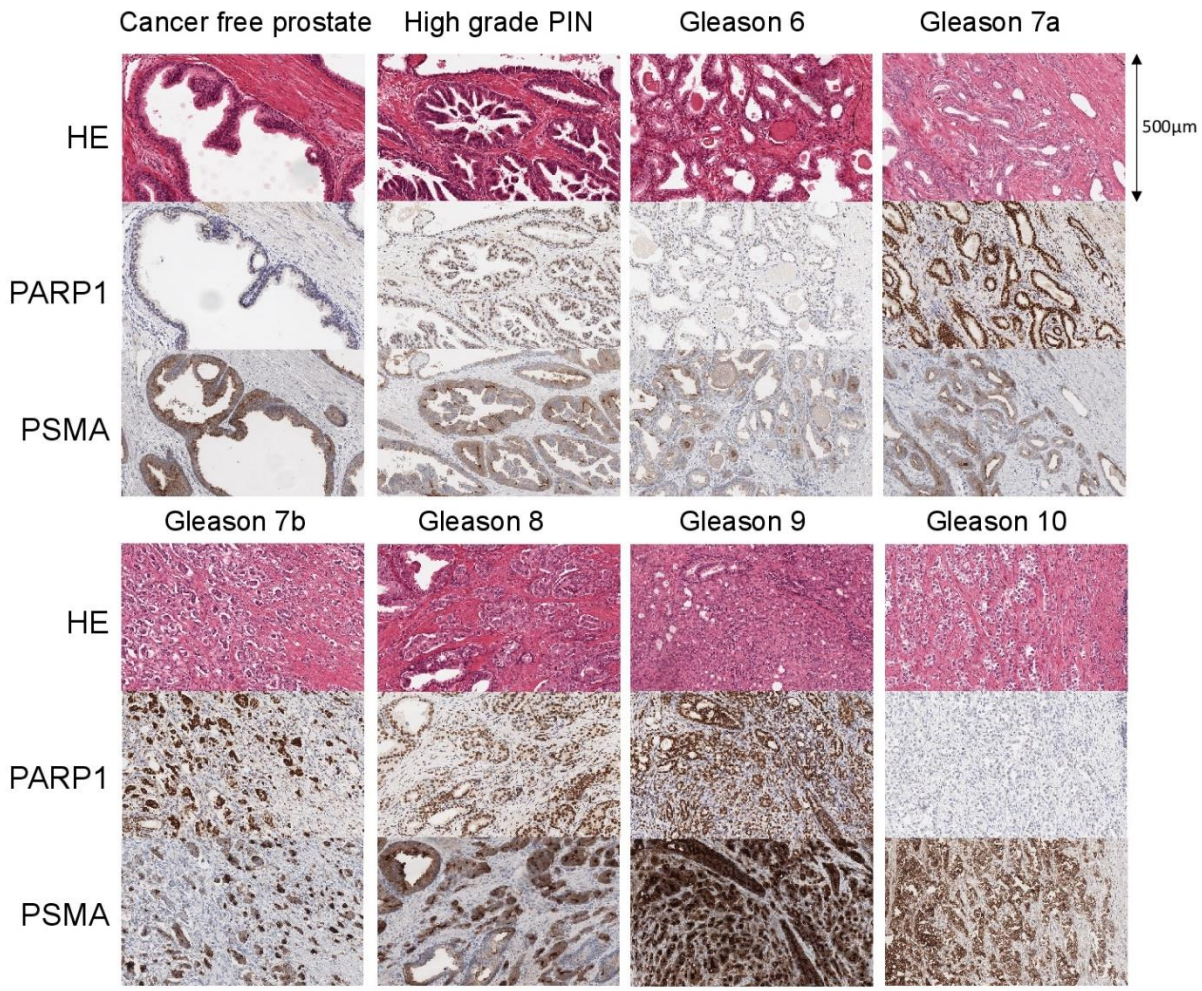

Figure 5: Examples of enlarged RP specimens in HE, PARP1, and PSMA sorted by Gleason stage, as well as High Grade PIN and cancer free prostate.

In total, there were 563 close-up images from 31 RPs. These were from two different cohorts of 18 (A) and 13 (B) patients. These two groups were first analyzed separately and then subsequently added together after data analysis. Figure 6 shows that Gleason 7b, 8 and 9 were most common and accounted for >60%. HG-PIN, Gleason 6 and 10 were very low, which can also be seen by their % of total close-ups each under 2.5% in Table 12. Cancer free prostate accounted for approximately one fifth of the values (20.43%).

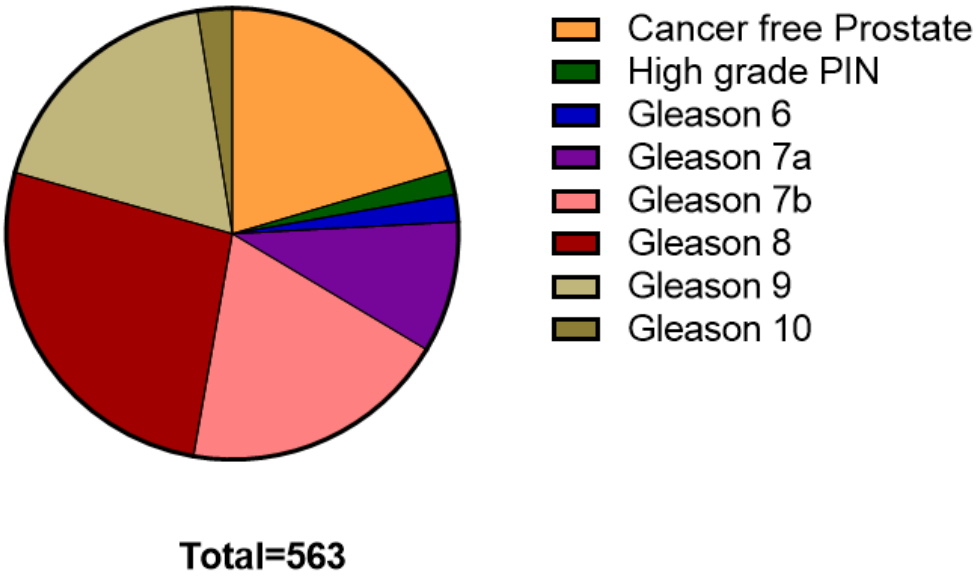

Figure 6: Distribution of the number of close-up images on tumor stage divided into the Gleason scores

Table 12: Distribution of RP close-ups by tumor stage & number of origins of specimens

	Number of close-ups	% of total close-ups	Number of RPs containing the close-ups
Cancer free prostate	115	20.43%	22
High Grade PIN	10	1.78%	1
Gleason 6	11	1.95%	5
Gleason 7a	53	9.41%	15
Gleason 7b	108	19.18%	18
Gleason 8	150	26.64%	18
Gleason 9	102	18.12%	9
Gleason 10	14	2.49%	1
Total	563	100.00%	/

6.3 Analysis of PARP1 expression in TMAs

In the second approach, 554 TMA spots from 248 patients were analyzed after IHC staining for PARP1. In the TMA method, small tissue columns were punched out of tumor tissue and transferred into a block. Here, 5 TMAs with 3 punchings/ patient of

~50 patients were available, exemplarily shown in Figure 7. Each spot was analyzed zoomed in 4x and matched to one Gleason score on the PARP staining by me and verified by an employee of the pathology department both using the Aperio ImageScope program. Spots that were not homogeneous were assigned the dominant Gleason score. Correct assignment of morphology was more difficult in PARP staining than in HE, which is why high-grade PIN does not appear as a category in the TMA analysis.

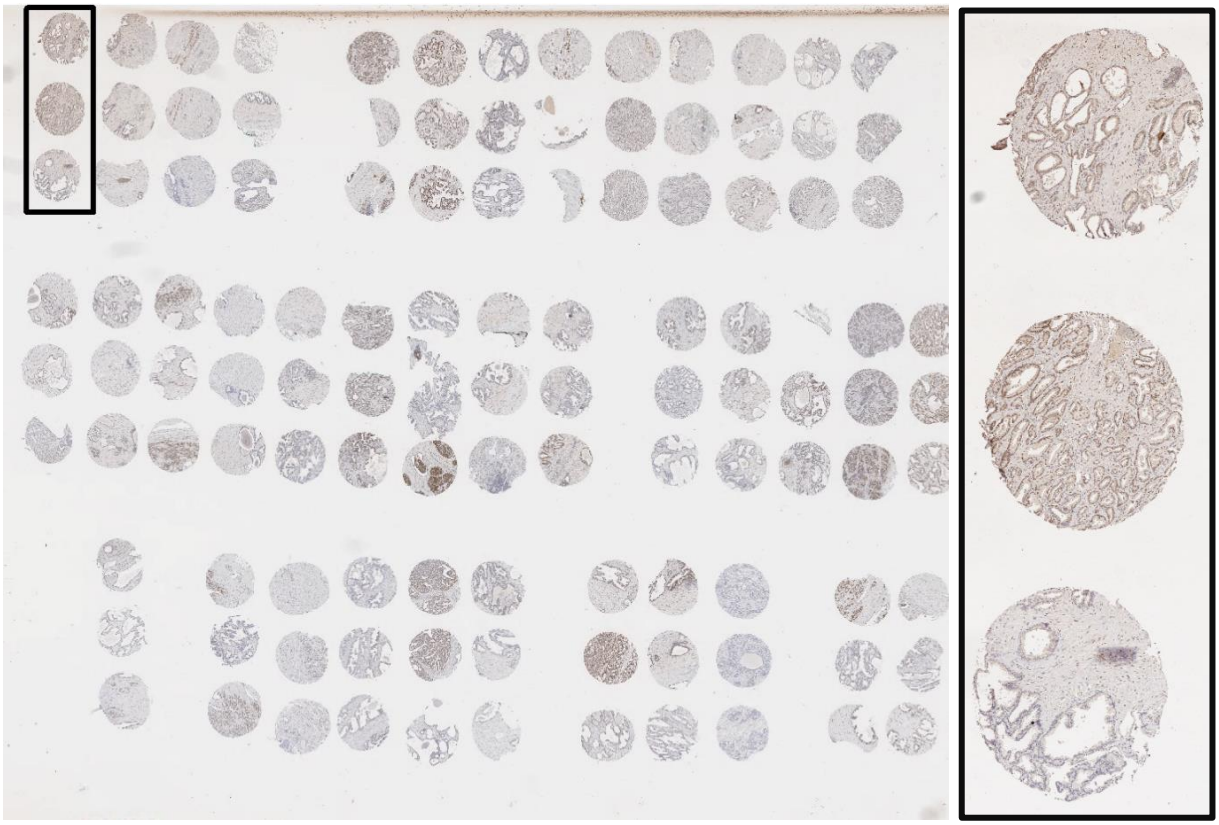

(A) (B)

*Figure 7: Example block TMA 17, 3 spots of one patient outlined in black **(A)** and zoomed in 4x **(B)***

The absolute numbers of spots assigned to a Gleason score can be found in Table 13 and graphically represented in Figure 8. Figure 8 shows that cancer free prostate was most common and accounted for >50% which is a common sampling error when attempting to punch tumor tissue. Gleason 6, 8, 9 and 10 were very low, which is displayed by their percentage of total close-ups each under 3.5% in Table 13. Gleason 7a and 7b accounted for approximately 38% of the values. Comparing both analyses, in the TMA approach the category cancer free prostate has the largest share and it tends to represent the lower tumor stages (7a, 7b), reflecting the average, unselected

patient population. In RP, on the other hand, the higher Gleason scores (7b, 8, 9) accounted for a majority (63.94%) of the preparations.

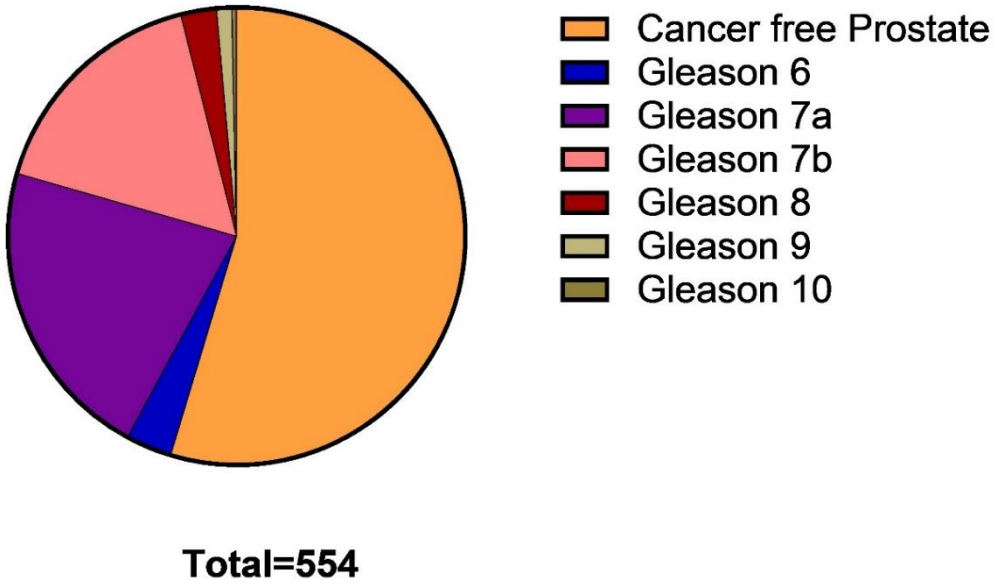

Figure 8: Distribution of TMA spots among tumor stages

Table 13: Distribution of TMA spots among tumor stages

Tumor stage	Number of TMA spots	% of total TMA spots
Cancer free prostate	303	54.69%
Gleason 6	18	3.25%
Gleason 7a	119	21.48%
Gleason 7b	92	16.61%
Gleason 8	14	2.53%
Gleason 9	6	1.08%
Gleason 10	2	0.36%
Total	554	100.00%

The TMAs were mainly spots of Gleason score 6-8 as well as tumor-free prostate. The sample size of Gleason 9 (n=6, 1,08%) and Gleason 10 (n=2, 0,36%) was too low to derive meaningful analysis. Therefore, these Gleason scores were excluded from subsequent statistical analysis.

6.4 Analysis of PARP1/ PSMA expression using Image J

To quantify PARP1 and PSMA staining, the program Image J was used. This is an image processing program used for medical and scientific image analysis. The program allows quantification of IHC staining using an automated thresholding method to calculate the % pta. This method for data collection with the use of a threshold was developed by Prof. Dr. Kossatz et all. [43, 44]. Using a macro, the image is first deconvoluted into three color images, which represent the PARP1 or PSMA staining (brown), the tissue background staining (blue) and residual signal (green) (Figure 9). A color threshold is then applied to the brown image, and the total % pta is calculated based on the percentage of the thresholded area in relation to the total area of the image frame.

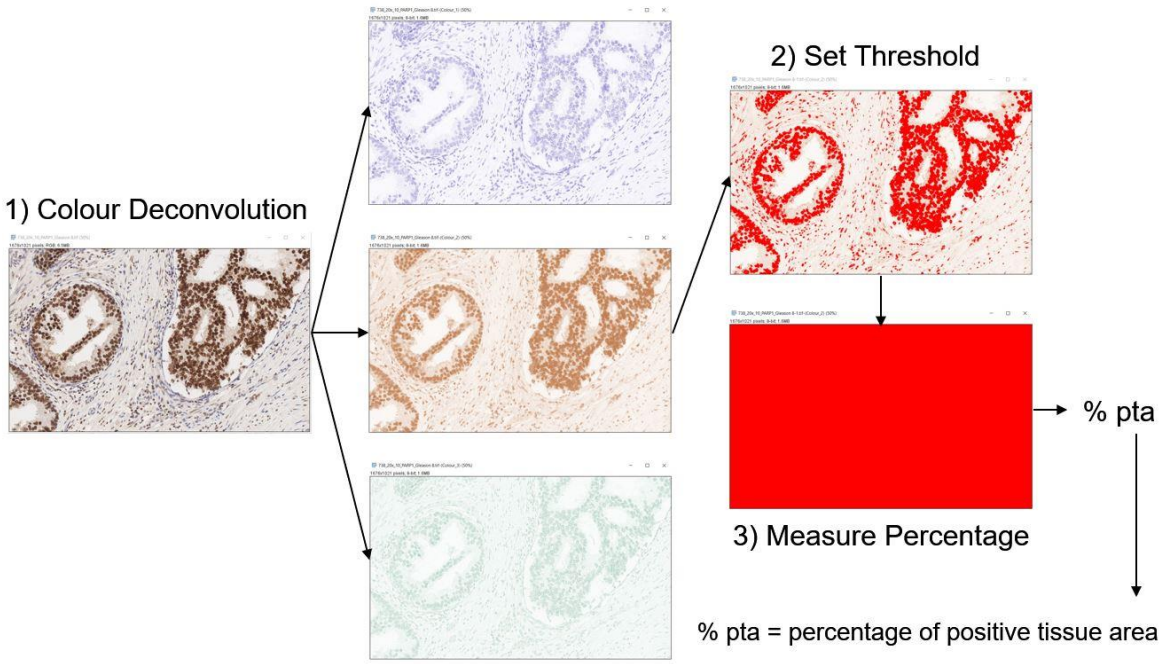

Figure 9: Representation of the analysis with Image J via an automated threshold method

We noticed that some specimens showed very weak IHC staining, which was below the threshold limit and therefore resulted in very low % pta values, although staining positivity was visible upon inspection. Therefore, all values below 0.1% pta were excluded from subsequent analyses. In this way, samples are discarded where IHC staining did not work properly, possibly due to insufficient adhesion of the antibody. IHC quantification was then correlated with the Gleason score of each close-up.

6.5 Statistical Analysis

The data in graphs and in the text are reported as mean values with standard deviations. Bar graphs usually also contain all individual data points. Statistical analysis was performed using GraphPad Prism 9. All statistical evaluations carried out with this program can be found in tabular form in the appendix in chapter 10.1. The data were analyzed using descriptive statistics. First, the normal distribution of the variables was tested using the D'Agostino & Pearson test. Since the data were not normally distributed, the Kruskal-Wallis test was used as the non-parametric equivalent of the single factor analysis of variance. For analyzing the correlation of all the values of PARP1 and PSMA expression in the RP specimens and then separately related to the Gleason scores, the Spearman correlation was used. The closer the value gets to 1, the stronger the correlation.

Furthermore, multiple comparisons were separately carried out for PARP and PSMA. For both, the values of the expression of cancer-free prostate tissue were compared with each Gleason score to find a significant difference. In the second step, the different Gleason scores were compared to each other. The results of these analyses are presented in graphs in the following chapters 6.6 and 6.7.The scheme just described was applied to all analyses of RP and TMA. Results with a $p \leq 0.05$ were considered significant. The significance level was indicated by asterisks in the graphs. The explanation of the stars can be found in Table 14.

Table 14: Meaning of significance stars in graphs

Symbol	Meaning
ns	$p > 0.05$
*	$p \leq 0.05$
**	$p \leq 0.01$
***	$p \leq 0.001$
****	$p \leq 0.0001$

6.6 PARP1 and PSMA expression in RPs

6.6.1 PARP1 expression in RPs

All patients had undergone a surgical therapy with RP, in which 30 of 31 patients were found to have tumors with a Gleason stage of at least Gleason 6. One preparation only contained low-grade PIN, a precursor lesion of PC. In the RP specimens, PARP1 expression was significantly higher in cancer (11.4% pta) than in cancer-free prostate tissue (4.6% pta; $p<0.05$). PARP1 expression increased steadily from Gleason 6 (1.9% pta) to Gleason 9 (15.4% pta). Compared to cancer-free prostate tissue, significant differences were seen at Gleason 7b (10.1% pta), 8 (13.3% pta), and 9 (16.0% pta) [$p<0.05$, Kruskal-Wallis test; (Significance level: * - ****)] (see Figure 10).

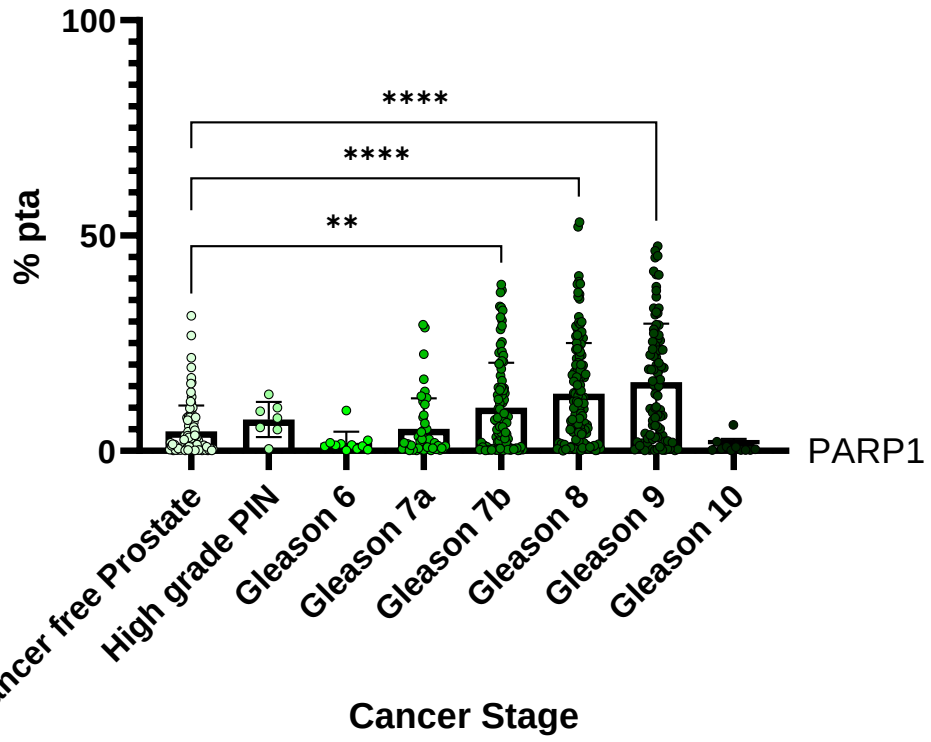

Figure 10: Quantification of PARP1 expression in all RP specimens (n=31)

From Gleason 6 (1.9% pta) to Gleason 7a (5.1% pta) a 2.7-fold increase was observed, which is clinically very relevant, since Gleason 6 is a low-risk tumor and Gleason 7a already represents a tumor with intermediate risk. The risk classification is crucial for the choice of therapy, which is why the ability to differentiate these categories would be of great importance. However, it must be added that the difference of the expression values of Gleason 6 and Gleason 7a compared to cancer free prostate were both not significant due to a too small number of samples. The detailed descriptive analysis of PARP1 in RPs can be found in Table 15.

Table 15: Descriptive analysis - PARP1 in RPs

	Descriptive statistics	A	B	C	D	E	F	G	H
		Cancer free Prostate	High grade PIN	Gleason 6	Gleason 7a	Gleason 7b	Gleason 8	Gleason 9	Gleason 10
1	Number of values	95	7	11	49	101	142	93	11
2									
3	Minimum	0.1174	0.4798	0.1024	0.1382	0.1086	0.04564	0.1249	0.1654
4	25% Percentile	0.4483	4.962	0.4740	0.5922	0.9368	3.616	3.111	0.1922
5	Median	2.314	7.612	1.254	1.887	7.215	10.47	15.08	0.3646
6	75% Percentile	6.830	10.06	1.860	7.083	14.62	20.18	25.52	0.9690
7	Maximum	31.42	13.12	9.337	29.29	38.63	53.08	47.57	6.048
8	Range	31.30	12.64	9.235	29.16	38.53	53.04	47.44	5.883
9									
10	Mean	4.578	7.264	1.905	5.135	10.07	13.26	16.00	1.075
11	Std. Deviation	5.960	4.096	2.558	7.082	10.37	11.76	13.53	1.751
12	Std. Error of Mean	0.6114	1.548	0.7713	1.012	1.032	0.9866	1.403	0.5279

Looking at the two cohorts individually in Figure 11, one sees an increase from Gleason 6 (1.9% pta) to Gleason 9 (21.6% pta) in cohort A. In contrast to that, cohort B only contained samples with Gleason 7a to 9 and cancer-free prostate. It can be noted that the expression of Gleason 7b (11.8% pta) and 8 (12.1% pta) were similar. In Gleason 9, however, there was a decrease to 8.2% pta.

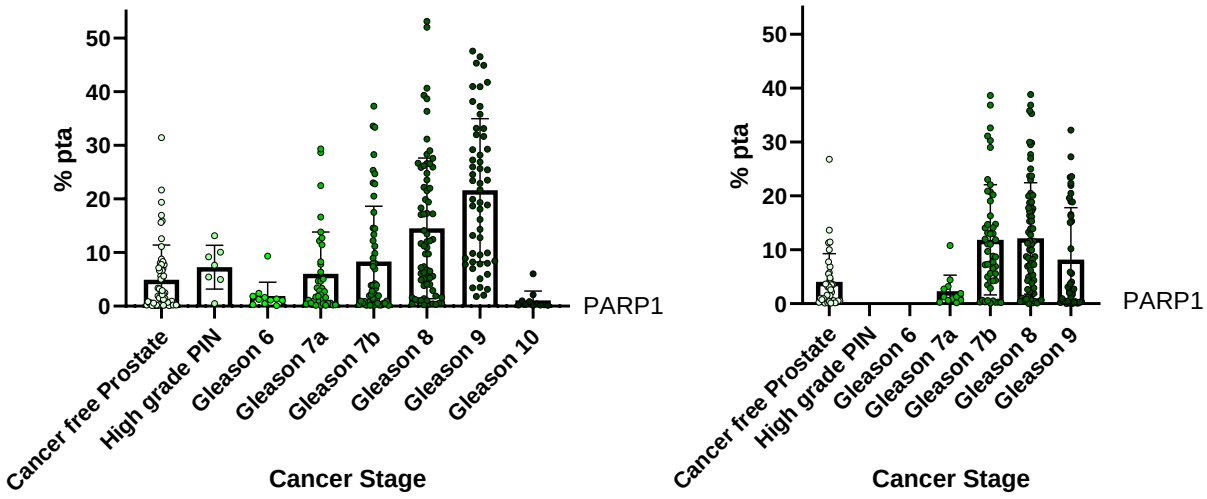

Figure 11: PARP1 expression in RPs - cohort A (left) and cohort B (right)

If comparing the results of both cohorts directly (see Figure 12), the values in cohort A were higher in all categories than in B, except Gleason 7b. It was striking that in Gleason 9 the values were even increased by a factor of 2.6. In general, both cohorts had similar means and trends. An exception was Gleason 9, where they diverged. Thus, the values in cohort A seem more plausible. The standard deviations in the

categories in which both cohorts had samples were higher in cohort A than in cohort B, if compared directly.

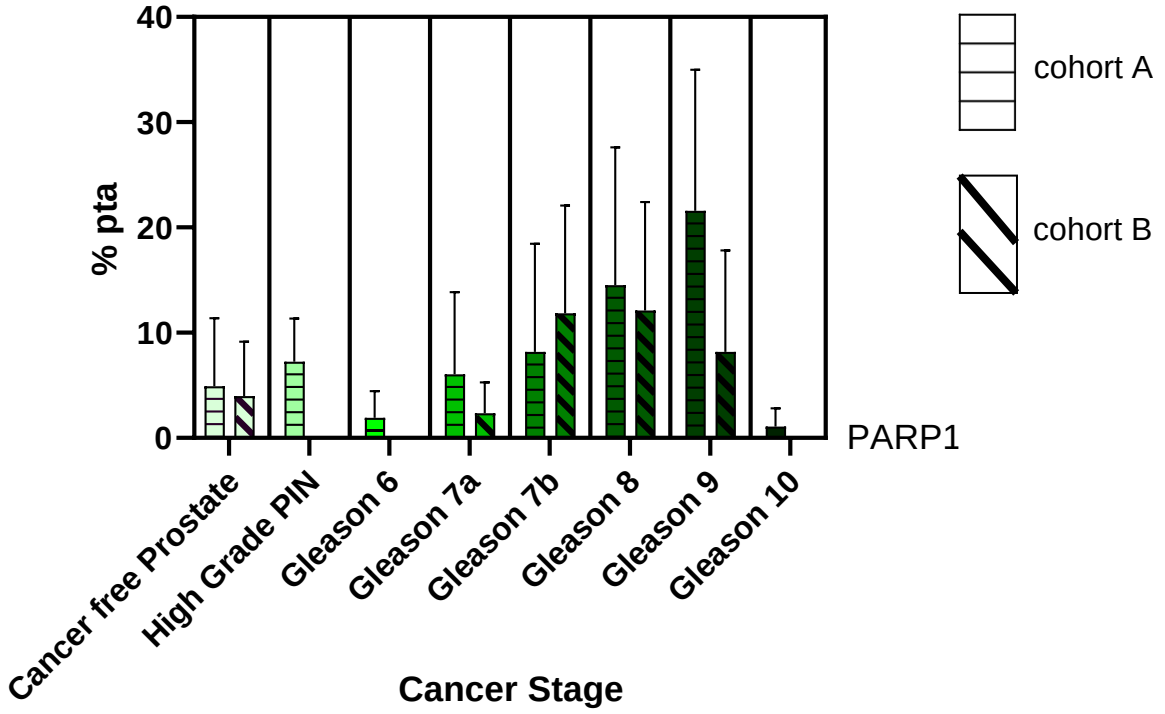

Figure 12: PARP1 expression in RPs - cohort A and B in comparison

6.6.2 PSMA expression in RPs

PSMA expression was also significantly higher in cancer (22.5% pta) than in cancer-free prostate tissue (7.7% pta; $p<0.05$). It increased from Gleason 6 (3.8% pta) to 8 (34.6% pta), while Gleason 9 (19.2% pta) and 10 (20.5% pta) were lower than Gleason 8. Compared with cancer-free prostate tissue, there were significant differences in Gleason 7b (19.1% pta), 8 (34.6% pta), and 9 (19.2% pta) [$p<0.05$, Kruskal-Wallis test; (Significance level: * - ****)] (see Figure 13). From, Gleason 6 (3.8% pta) to Gleason 7a (8.1% pta) was a 2.1-fold increase in mean % pta of PSMA.

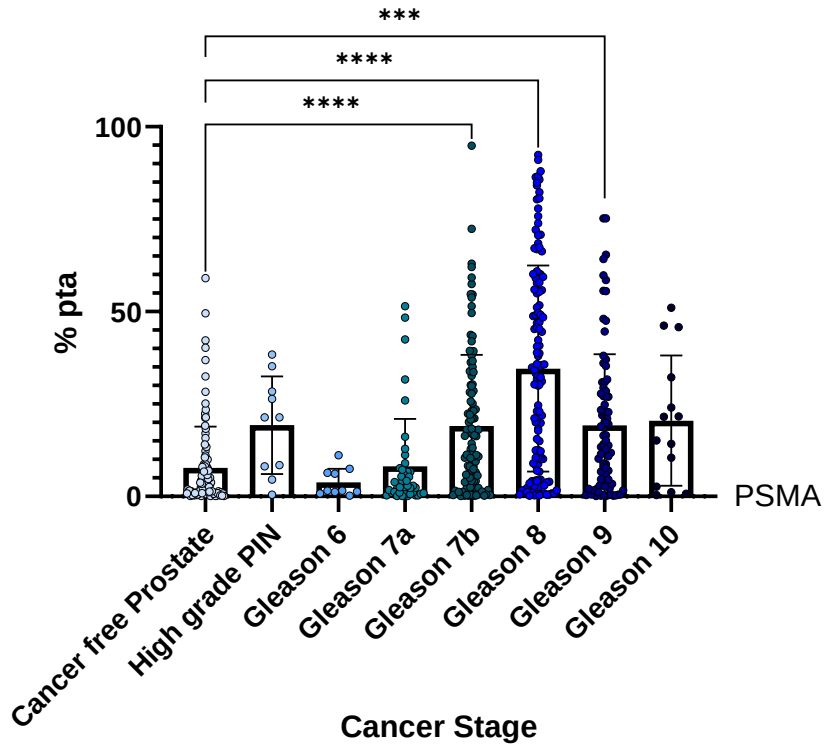

Figure 13: Quantification of PSMA expression in all RP specimens (n=31)

However, the expression values of Gleason 6 and Gleason 7a were both repeatedly not significant due to the small number of samples. The detailed descriptive analysis of PARP1 in RPs can be found in Table 16.

Table 16: Descriptive analysis - PSMA in RPs

Descriptive statistics		A	B	C	D	E	F	G	H
		Cancer free Prostate	High grade PIN	Gleason 6	Gleason 7a	Gleason 7b	Gleason 8	Gleason 9	Gleason 10
1	Number of values	102	10	10	42	106	123	83	14
2									
3	Minimum	0.1031	0.4722	0.2133	0.1037	0.1133	0.2380	0.1164	0.3976
4	25% Percentile	0.8690	7.228	1.087	0.9557	3.405	6.996	3.405	2.267
5	Median	3.341	21.37	1.533	2.839	12.18	32.62	13.63	18.32
6	75% Percentile	8.721	30.06	6.640	7.297	29.95	57.69	27.83	35.62
7	Maximum	59.01	38.38	11.14	51.43	94.85	92.35	75.23	51.00
8	Range	58.91	37.91	10.93	51.33	94.73	92.11	75.12	50.60
9									
10	Mean	7.689	19.26	3.764	8.095	19.06	34.57	19.22	20.50
11	Std. Deviation	11.16	13.22	3.721	12.86	19.22	27.87	19.20	17.64
12	Std. Error of Mean	1.105	4.179	1.177	1.985	1.867	2.513	2.108	4.714

Looking at the two cohorts individually, an increase from Gleason 6 (3.8% pta) to Gleason 8 (35.8% pta) was observed in cohort A (Figure 14). In contrast to that, in cohort B only samples with Gleason 7a to 9 and cancer-free prostate could be found. The expression of Gleason 7a (14.7% pta), 7b (14.3% pta) and 9 (14.8% pta) were of

similar value. In Gleason 8, however, there was an increase to 34.0% pta, which was 2.3 times higher than the average of Gleason 7a, 7b and 9.

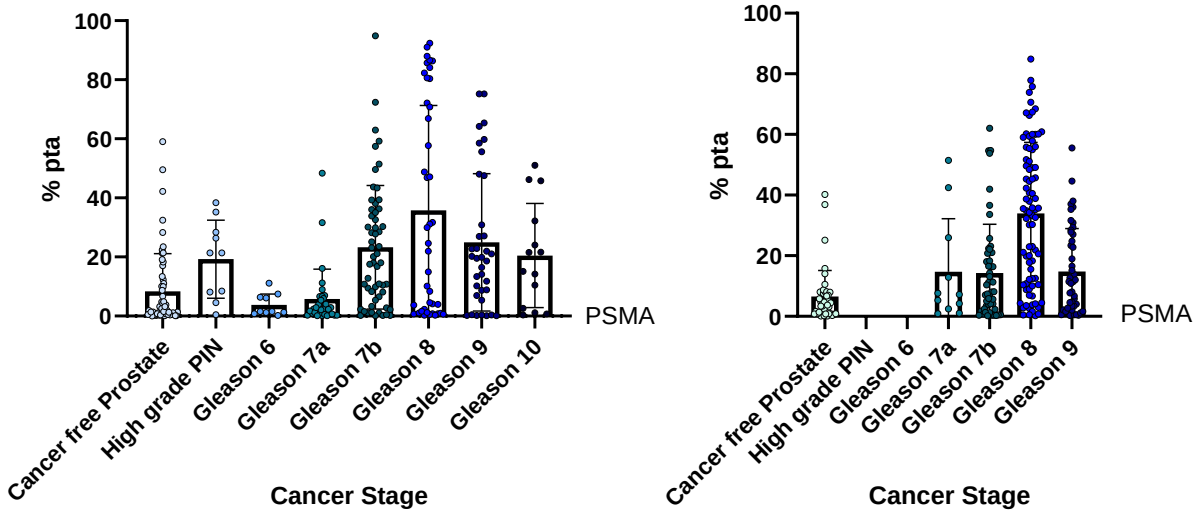

Figure 14: PSMA expression in RPs - cohort A (left) and cohort B (right)

Comparing both cohorts with each other (see Figure 15), cohort A had slightly higher values in all categories except in Gleason 7a. The standard deviations in both cohorts also followed this pattern in cancer free prostate, Gleason 7b, 8 and 9.

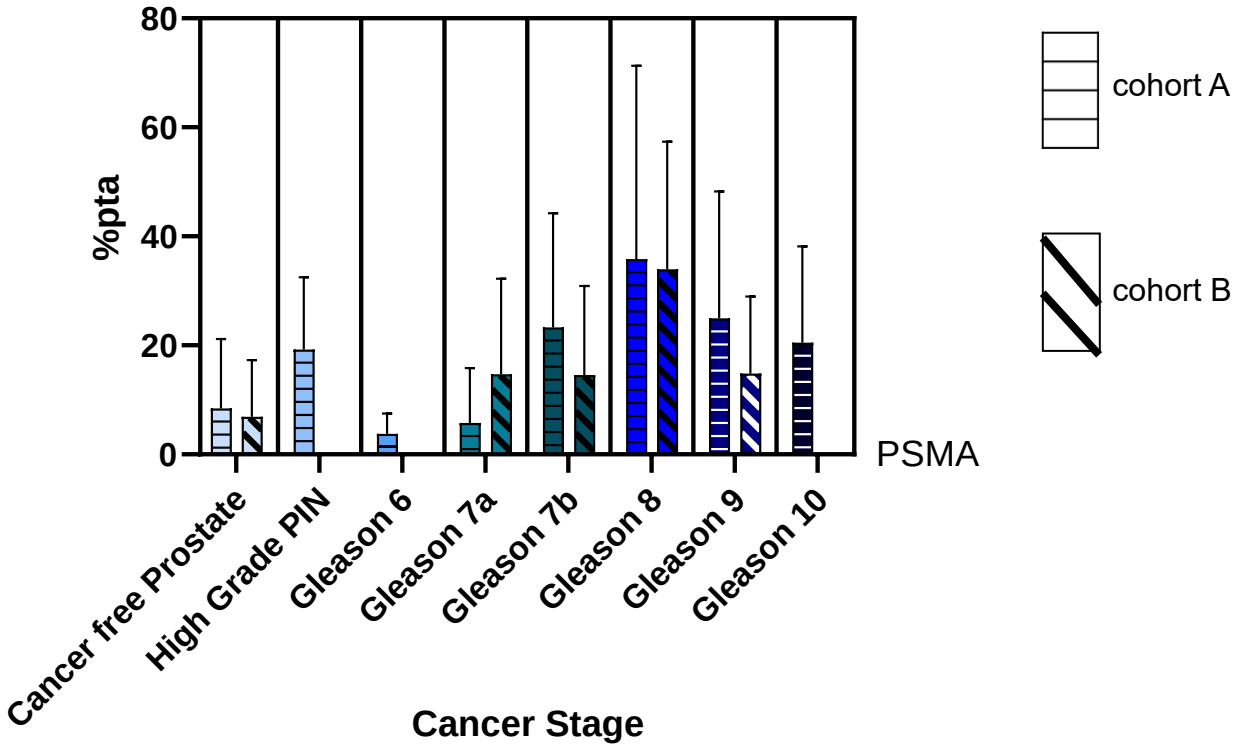

Figure 15: PSMA expression in RPs - cohort A and B in comparison

6.6.3 Comparison of PARP1- and PSMA expression in RPs

In the final comparison of both biomarkers, cohorts A and B were analyzed in combination. PARP1 expression was compared with PSMA expression [p<0.05, Kruskal-Wallis test; (Significance level: * - ****)] (see Figure 16). PARP1 showed a 3-fold increase from Gleason 6 to Gleason 9. Gleason 10 was not considered here due to the small specimen number. In PSMA was a 9-fold increase from Gleason 6 to Gleason 8, with a drop in values at Gleason 9, although Gleason 9 values being significant. PARP expression showed a more linear increase as PSMA (see Figure 17). PSMA expression was 2,92-fold higher in cancer (22.5% pta) than in cancer-free prostate tissue (7.7% pta; p<0.05) and PARP1 expression was 2,47-fold higher in cancer (11.4% pta) than in cancer-free prostate tissue (4.6% pta; p<0.05). This showed that for both markers cancer free prostate was lower than the mean value of cancer tissue (Gleason 6-10). For PARP1, High grade PIN (HG-Pin) (7,3%) was 3,8-fold higher than Gleason 6 (1,9%) and 1,4-fold higher than Gleason 7a (5,1%). For PSMA, HG-PIN (19,3%) was 5,1-fold higher than Gleason 6 (3,8%) and 2,4-fold higher than Gleason 7a (8,1%). To summarize, in both graphs HG-PIN was considerably higher than Gleason 6 and 7a. However, this is only partially meaningful because HG-PIN results were not statistically significant due to the low number of specimens.

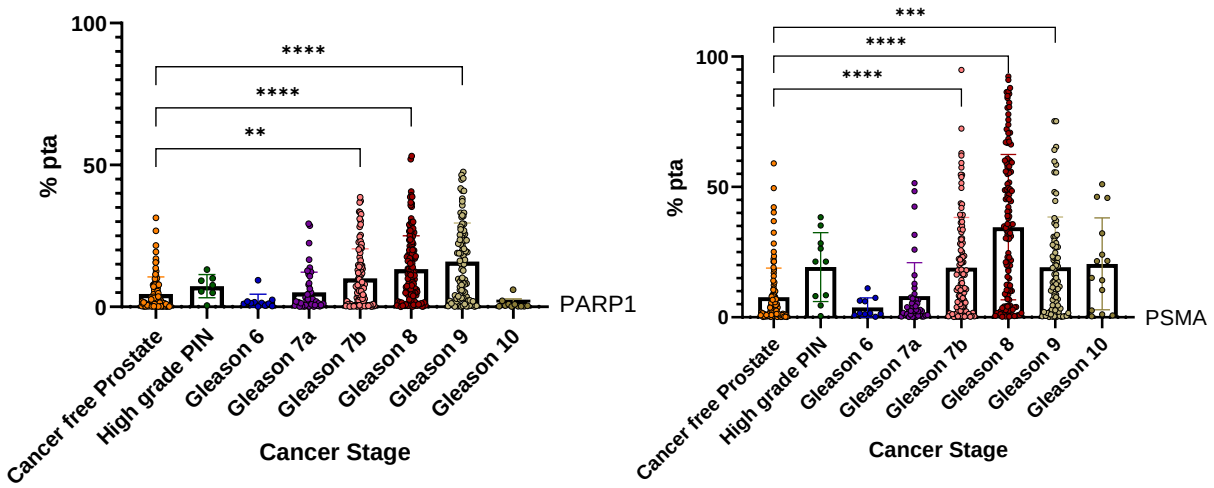

Figure 16: Comparison of PARP1 (left) and PSMA (right) expression in RPs

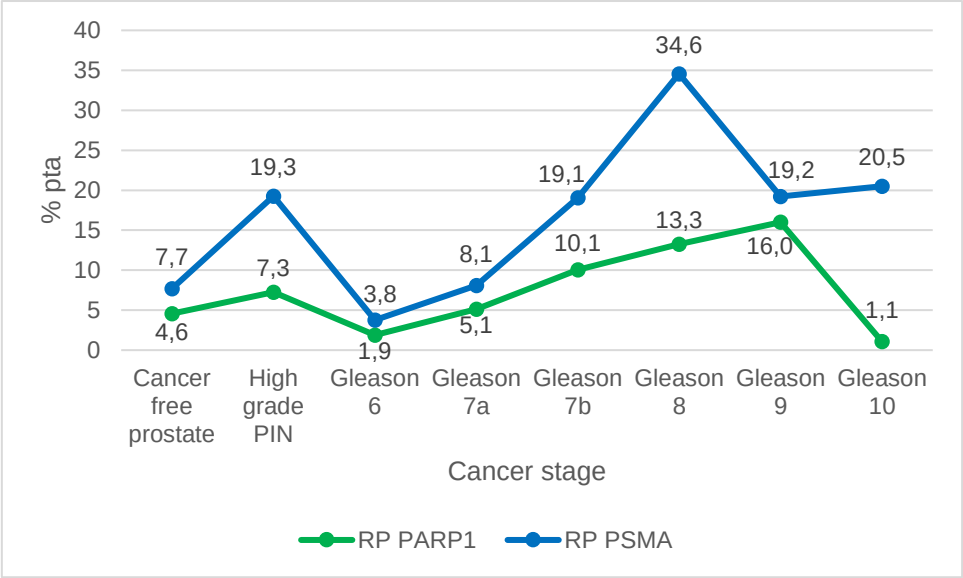

Figure 17: RP comparison PARP1 (green) & PSMA (blue)

The values of PSMA in % pta were higher than those of PARP1. However, one cannot compare this directly, as there were different antibodies used. Much more relevant than the absolute values were the relative ones, thus the progress of the increase.

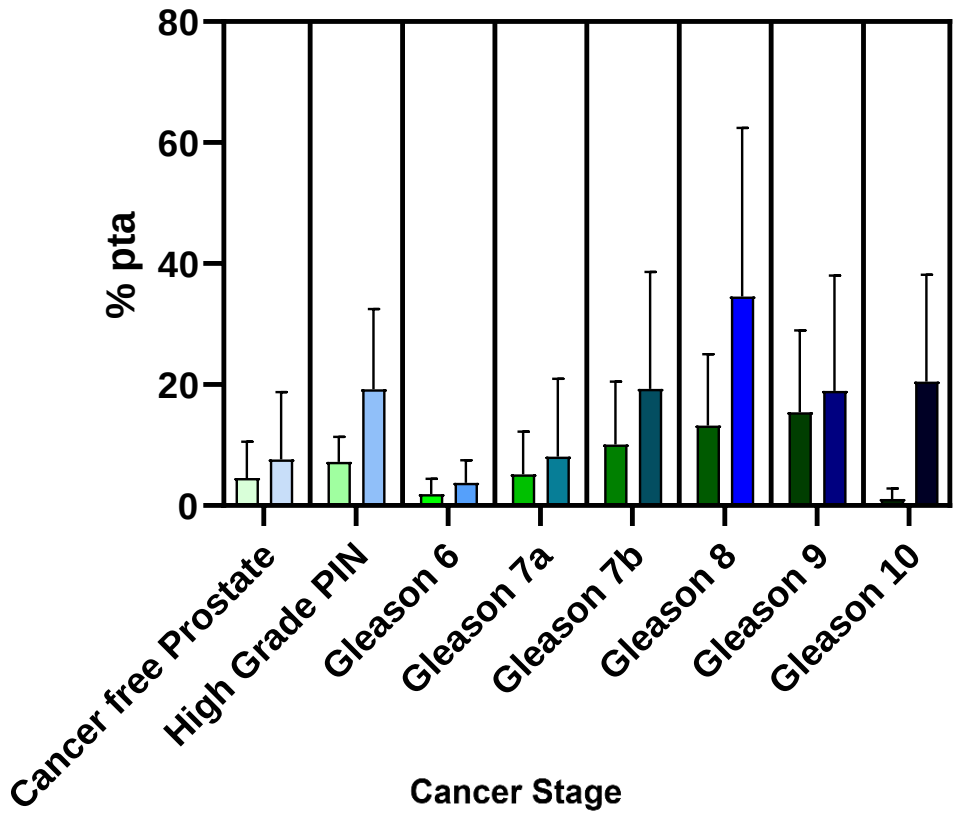

Figure 18: PARP1 (green) and PSMA (blue) expression in RPs in comparison

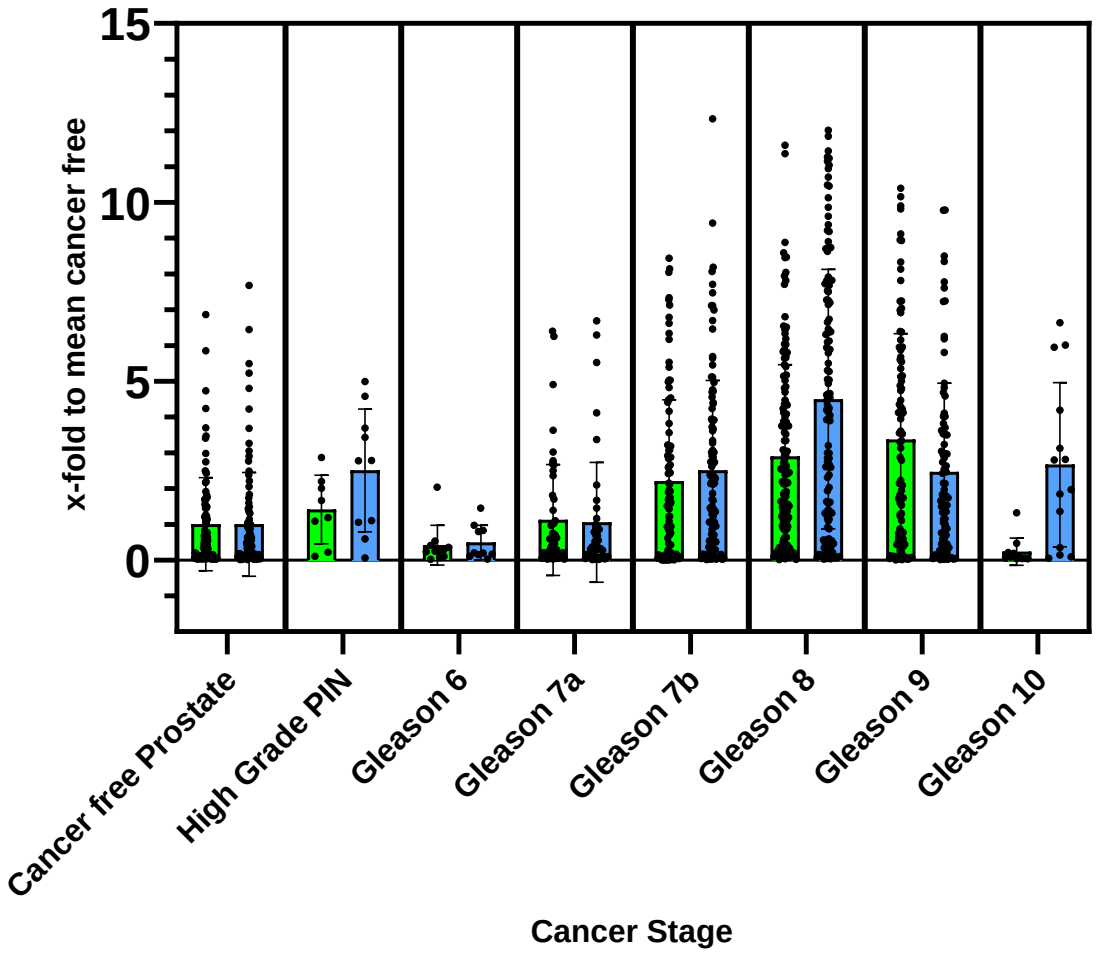

Figure 19: PARP1 (green) and PSMA (blue) in comparison normed to mean cancer free prostate

Gleason 6 was lower than cancer free prostate for both biomarkers. Comparing all values relative to the mean cancer free value of the respective biomarker (see Figure 19), PARP1 had a higher expression in Gleason 9 than PSMA. In contrast, in Gleason 7b, 8 and 10 the expression in PSMA was higher than in PARP1. In general, both biomarkers did not strike properly until Gleason 7b. According to these results, PARP1 appears to be an equally good biomarker for PC, more suitable in Gleason 9, but there was no significant result for Gleason 10. Importantly, PARP1 increased from Gleason 7a to Gleason 9 and thus also elevated with progressing cancer stage. This is an important property for the use of PARP1 as a biomarker.

6.6.4 Correlation PARP1 and PSMA expression

In the following section, it will be reviewed whether the expression of both biomarkers is positively or negatively correlated This will help concluding whether they are more likely to be targeted in combination or complementary. Comparing all values of PARP1 and PSMA expression, they showed a weak but significant positive correlation with an r-value of 0.37 displayed in Figure 20. Analyzing the correlations related to Gleason scores, significant results were found for cancer free prostate (r: 0.50***), Gleason 8 (r: 0.21*) and Gleason 9 (r: 0.48***). Thereby, especially cancer free prostate and Gleason 9 have a positive medium-grade correlation. HG-PIN, Gleason 6, 7a, 7b and 10 did not show significant results (see Figure 21). HG-PIN and Gleason 6 showed negative values and Gleason 7a (r: 0.16) and 7b (r: 0.08) very low positive values.

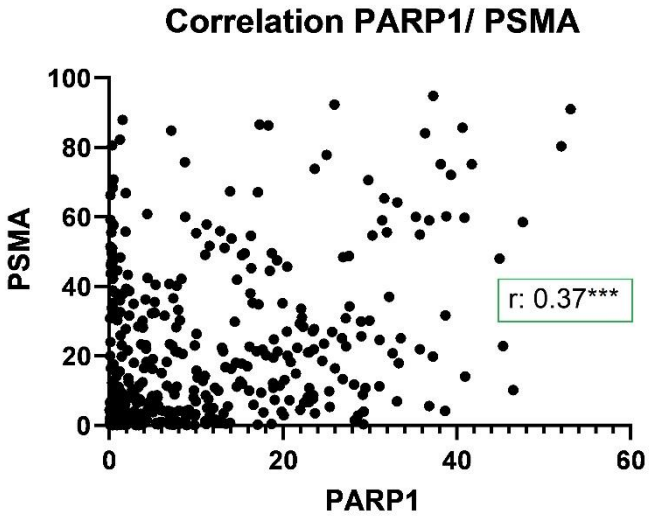

Figure 20: Correlation of PARP1 and PSMA expression using all available data points across all Gleason scores

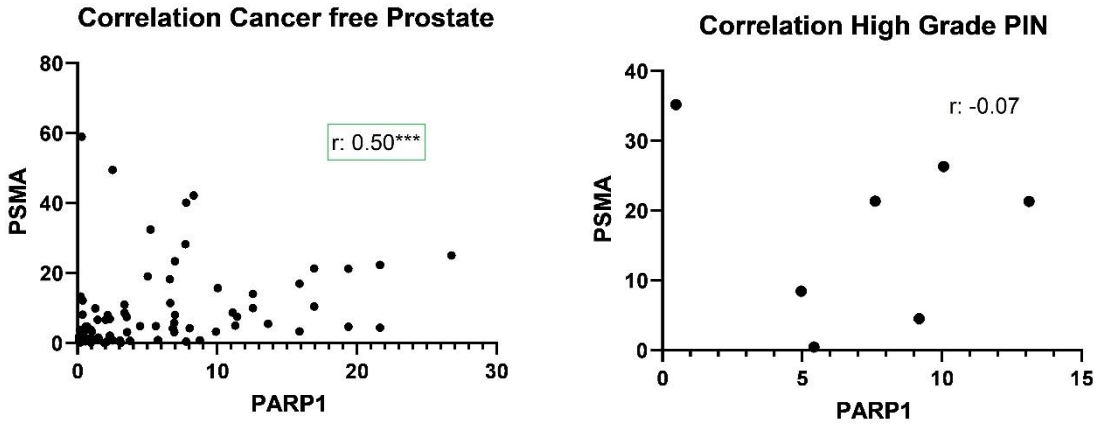

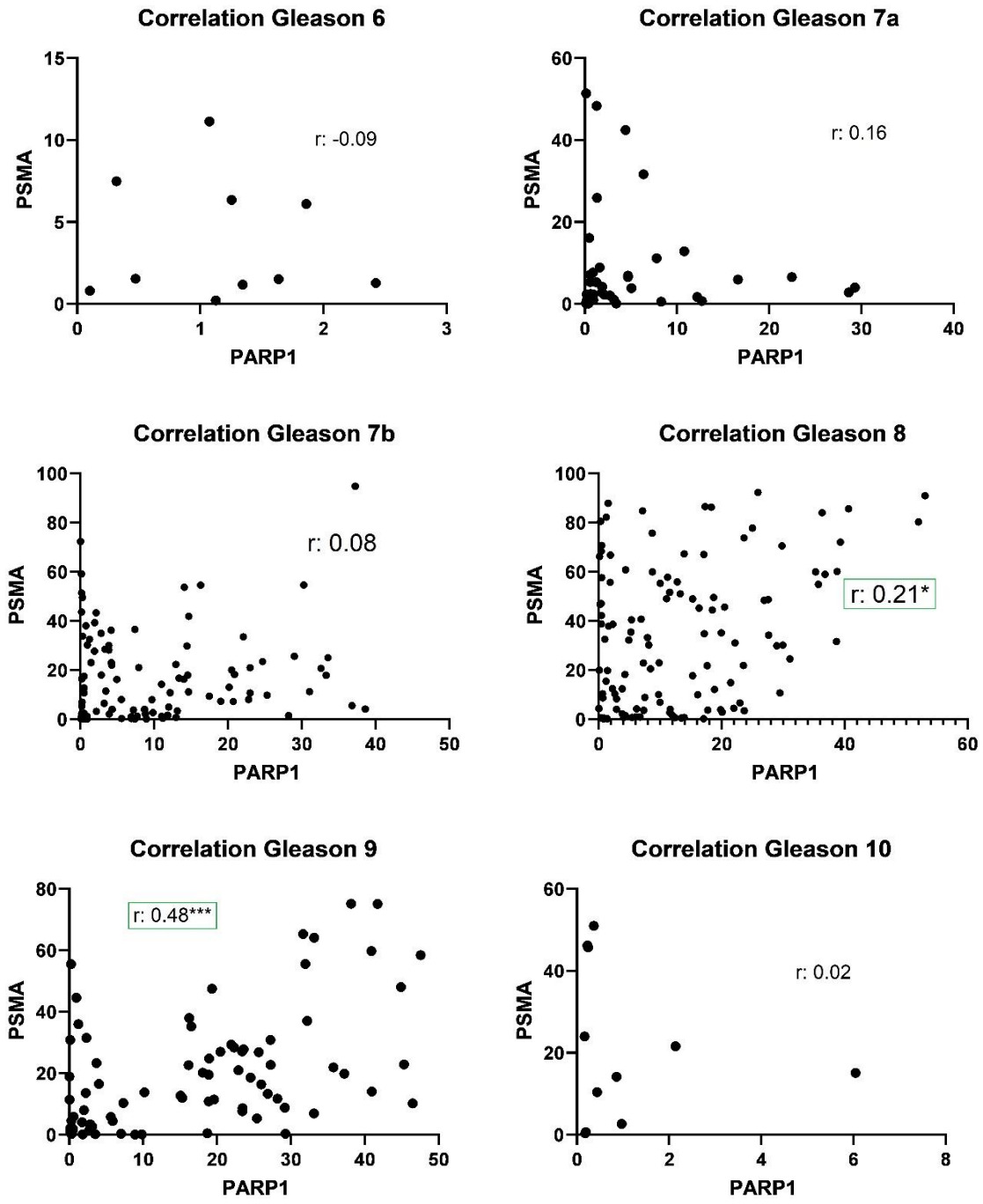

Figure 21: Correlation cancer free prostate, High Grade PIN and Gleason 6 to Gleason 10

The two biomarkers correlated positively in cancer free, Gleason 8 and Gleason 9, thus could be used for tumor free and advanced tumors for complementary targeting. It does not correlate relevantly in the subgroups Gleason 6, 7a, 7b and 10 and therefore no statement can be made to what extent PSMA and PARP could be used in these tumor stages.

6.7 PARP1 expression in TMAs

In the TMA cohort, PARP1 expression increased from Gleason 7a (3.4% pta) to Gleason 9 (7.2% pta), compared to 1.7% pta in cancer free prostate [p<0.05, Kruskal-Wallis test; (Significance level: * - ****)] (see Figure 22). From cancer free prostate to Gleason 7a the value doubled, which is important because from this stage on, it is categorized as cancer with intermediate risk.

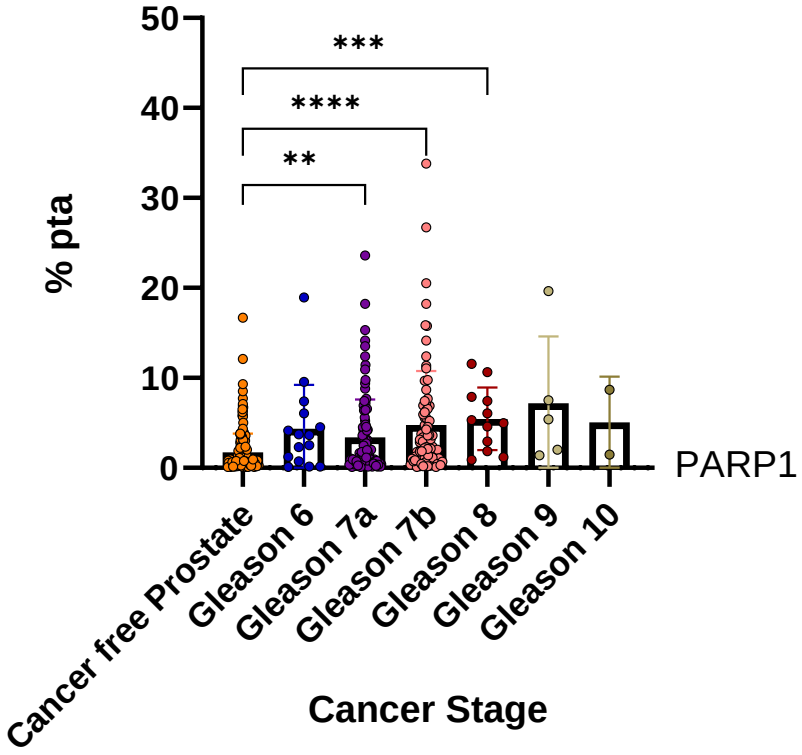

Figure 22: PARP1 expression in TMAs

The detailed descriptive analysis of PARP1 in TMAs can be found in Table 17.

Table 17: Descriptive analysis - PARP1 in TMAs

Descriptive statistics		A	B	C	D	E	F	G
		Cancer free Prostate	Gleason 6	Gleason 7a	Gleason 7b	Gleason 8	Gleason 9	Gleason 10
1	Number of values	246	15	111	84	12	5	2
2								
3	Minimum	0.04660	0.1098	0.1015	0.1154	0.9019	1.387	1.459
4	Maximum	16.67	18.94	23.62	33.81	11.58	19.64	8.668
5	Range	16.63	18.83	23.52	33.69	10.67	18.25	7.209
6								
7	Mean	1.723	4.340	3.376	4.778	5.451	7.188	5.064
8	Std. Deviation	2.104	4.907	4.218	5.980	3.489	7.396	5.097
9	Std. Error of Mean	0.1342	1.267	0.4003	0.6525	1.007	3.307	3.604

6.8 Comparison of PARP1 expression in RPs and TMA

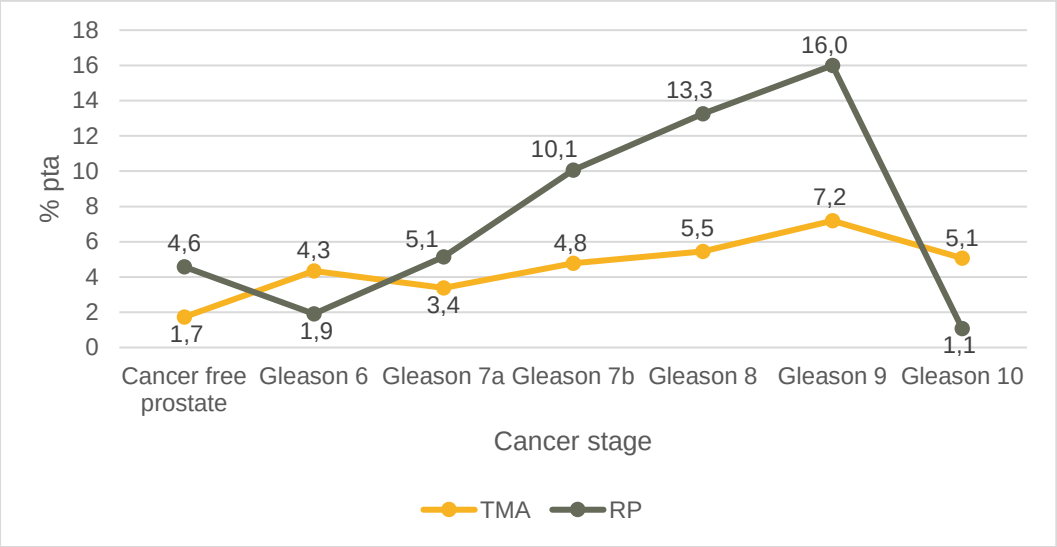

Figure 23: PARP1 results of TMA (yellow) and RP (gray) in comparison

For this comparison, all categories except HG-PIN were included, as there was no value for it in the TMA analysis due to the grading process on PARP staining. The TMA-derived values were overall lower than the RPs besides in Gleason 6 and 10. Too much importance should not be attached to this result since there were few specimens in both categories and therefore the results were not significant. Looking at the mean values the largest difference was in cancer free prostate, where RP was 2.6 times higher than TMA. The values were most similar in Gleason 7a in which case RP was only 1,5 times higher than TMA. The biggest difference could be found in Gleason 10 with a 4.7 times higher TMA mean than in RP. Comparing the mean values over increasing cancer stage (see Figure 23), a steeper increase from Gleason 7a to Gleason 9 for RP than for TMA could be seen. This was likely the result of weaker IHC staining due to prolonged storage of the TMAs.

7 Discussion

As a result, it was discovered that PARP1 was expressed in almost all patients to varying degrees. Furthermore, a steadily increasing expression from Gleason 6 (1.9% pta) to Gleason 9 (15.4% pta) was detected. When comparing these results to cancer-free prostate tissue, a significant divergence at Gleason 7b (10.1% pta), 8 (13.3% pta), and 9 (16.0% pta) becomes apparent.

To achieve a higher level of significance, in a second step, a larger cohort in the form of TMAs was analyzed. This resulted in PARP1 expression increasing from Gleason 7a (3.4% pta) to Gleason 9 (7.2% pta), compared to 1.7% pta in cancer free prostate, confirming the finding in RPs that PARP1 expression elevated with increasing cancer stage. However, by directly comparing the percentages, overall lower TMA-derived values than RP values were perceived. An exception to this observation can be found in Gleason 6 and 10, in which only few specimens were used in both categories. The mean values of cancer free prostate showed a 2.6 times higher value in RP than TMA, which can be explained with a weaker IHC staining due to prolonged storage of the TMAs.

Regarding the genetics of the patient cohort studied in this work, it was not screened for BRCA mutations. Nonetheless, the literature shows that 14%-16% with CRPC have a BRCA mutation [45], leading to the assumption that many patients in our study expressed PARP1 without having a BRCA mutation. In Germany the use of PARPi monotherapy is limited to patients with mCRPC and a BRCA1/2 mutation [33], indicating that patients without this mutation would benefit from monotherapy as well. Many studies are currently screening patients for other DDR genes in order to significantly increase the percentage of patients who could benefit from PARP inhibitor therapies and PARP inhibitor combination therapies [46].

Wichmann et al. addressed the expansion of the therapeutic spectrum of PARPi beyond BRCA1 deficiency and/ or overcoming PARPi resistance [47]. To this end, the therapeutic effect of novel triazene derivatives, including the compound CT913 and its metabolite CT913-M1, on ovarian cancer cells was investigated and their interaction with the PARPi olaparib was described. CT913 showed a synergistic interaction with olaparib, independent of BRCA1 mutation status [47]. Therefore, the new triazene drug CT913 is proposed as an enhancer drug to expand the therapeutic spectrum of PARPi.

Dehdashti et al. created a prospective pilot study, in which a screening of patients with HRR mutations was done to investigate the feasibility of imaging PARP1 expression with FTT-PET/CT in cancer patients [48]. For that a comparison of PARP-1 expression in PC patients with and without HRR genomic alternations was done using [18F]FluorThanatrace (FTT), an analogue of the PARPi rucaparib, as a a novel PARP-based imaging agent. During the study, significantly higher maximum standardized uptake values (SUVs) ($p = 0.0379$) with HRR mutations than patients with non-HRR mutations were observed. The study showed that FTT-PET/CT may serve as an alternate biomarker for PARP1 expression and a potential method for PARPi treatment selection [48].

Another promising approach in PC is the use of PARP inhibitors as radiosensitizers [49]. For this, PARP inhibitors would be combined with radiotherapy. The preclinical data suggest a similar cytotoxic effect with half the radiation dose under the effect of olaparib or rucaparib irrespective of HRR status [49]. And by being independent of germinal or somatic molecular alterations, this could find application in the majority of patients [49]. The randomized phase II trial of niraparib with a standard combination of radiotherapy and androgen deprivation therapy (ADT) in high-risk PC (NCT04037254) [50] is a currently enrolling study addressing this topic. There will be an estimated 180 participants with histologically confirmed prostatic adenocarcinoma at high risk for recurrence in the study with the primary measured outcome being the maintenance of disease-free state.

Zhang et al. addressed PARP expression in PC with the attempt to measure a significant increase in localization of the PARP imaging tracer in tumors treated with targeted α therapy [51]. For this purpose, [18F]-PARPZ was used as a positron-emitting PARP1 tracer, thus investigating its utility in a PC mouse model. [18F]-PARPZ uptake was quantitatively discriminated in tumors treated with 225Ac-PSMA-617, an α-emitting targeted radiotherapy [51]. The study aimed to validate PARP-1 expression for potential clinical use and to assist in the selection and dosing of clinically approved PARP inhibitors. A significant increase in the localization of the PARP imaging tracer in tumors treated with α-therapy could be measured. The improved imaging properties and stability of [18F]-PARPZ combined with the implementation of [18F]-FTT may provide the basis for future initiation of clinical trials for imaging of the DNA damage response in patients treated with both approved (radium-223 dichloride) and alpha particle radiotherapy. [51].

Looking now at PSMA expression to better understand the differences between the two biomarkers, an increase in expression was seen from Gleason 6 (3.8% pta) to 8 (34.6% pta), while Gleason 9 (19.2% pta) and 10 (20.5% pta) were lower than Gleason 8. Significant differences were found in Gleason 7b (19.1% pta), 8 (34.6% pta), and 9 (19.2% pta), when compared with cancer-free prostate tissue. Figure 19 pointed out that PSMA, when normed to mean cancer-free prostate, was similarly high in HG-PIN, Gleason 7b, Gleason 9, and Gleason 10 in contrast to PARP1, which increased gradually in advanced stages up to Gleason 9. In summary these results show that the biomarkers have a different behavior of expression, which could be used complementary. These findings accentuate the future potential of PARP1 as a progression parameter to track the increment of cancer stage non-invasively and PSMA as a linking biomarker for radioactive substances.

The comparison of PARP1 and PSMA expression showed a weak but significant positive correlation with an r value of 0.37. The analysis of correlations in relation to Gleason scores revealed significant results for cancer-free prostate (r: 0.50***), Gleason 8 (r: 0.21*), and Gleason 9 (r: 0.48***). The indication that many patients express both biomarkers could be used for combination therapies with PSMA-Targeted Radionuclide Therapy (TRT) and PARPi. There is a preclinical assessment that deals with this combination for PC treatment [52]. In this approach, three classes of PARPi were combined with PSMA-TRT in preclinical PCa models. In vitro viability and survival assays were performed with two PSMA-expressing PCa cell lines to evaluate the effect of increasing concentrations of the PARPi veliparib, olaparib, or talazoparib in combination with PSMA-TRT compared with PARPi treatment alone [52]. Finally, the potential of the combination treatments was evaluated in vivo in mice with PC3-PIP xenografts. The results of the study showed that the combination of PSMA-TRT with PARPi had no synergistic effects on clonogenic survival or cell viability in vitro. Furthermore, PSMA-TRT with PARPi treatment did not improve tumor control compared with PSMA-TRT monotherapy [52]. Unfortunately, the data presented do not support the assumption that the combination of PSMA-TRT with PARPi leads to a synergistic antitumor effect in PCa. Promising results were also shown with the combination of PSMA-TRT in neuroendocrine tumor cells, which is why the approach should be pursued further in studies [53].

In the future, there will be more and more studies combining RLT and PARPi to enhance Double-strand breaks (DSBs) and increase cancer cell lethality [54]. Two

trials of RLT and PARPi are currently recruiting mCRPC patients who have not been selected for HRR alterations: LuPARP (NCT03874884) [55] and COMRADE (NCT03317392) [56], evaluating [177Lu]Lu-PSMA-617 and olaparib and radium-223 and olaparib, respectively [57]. NiraRad (NCT03076203), a phase Ib trial of radium-223 and niraparib, recently completed recruiting and enrolled 30 patients across three PARPi dose cohorts with the result that whilst toxicity was manageable, responses were modest, with PSA50 at 12 weeks in 10/30 patients [36].

In the following section, the limiting aspects of the project are examined in more detail. In the analyses of the RPs, some Gleason scores are underrepresented. Therefore, the results of this section are not significant, making it impossible to assess all cancer stages equally well. Furthermore, the antibodies for PARP1 and PSMA show different color intensities with respect to the brown color, which makes the comparison of the absolute values more complex than the analysis of their progression. To optimize this, an analysis was performed in which the values were normed to the average of the cancer free prostate values (see Figure 19).

Another aspect influencing the results is the duration of storage before staining, as the TMA preparation were years older than to the RPs. This was also reflected in the intensity of the staining. There are advantages and drawbacks to the threshold method being observer-independent when it comes to determining a value. On the one hand this allows for objectiveness, while on the other hand this might lead to deficient values due to improper staining or the inaccurate analysis of artifacts with larger accumulation of the antibody. Additionally, the threshold was made a fixed value in order to enable standardized comparison. This allowed for the average of the preparations to be captured precisely, whereas lighter and darker brown specimens suffered from it. Regarding the TMAs, it should be noted that a circular template was placed over all samples to calculate the coloration of the punchings. However, since not all samples were exactly circular, a certain range must be considered when interpreting the results. A common problem in the evaluation of histopathological specimens is that the classification of Gleason scores is subjective, as there are no fixed definable categories, but rather a scale. To make this as accurate as possible, all assignments were reviewed by an employee of the pathology department. Another consideration is the varying size of tumor. In larger tumors, more close ups could be taken, making the expression more representative than in the very small tumors. In our project, RPs were used to draw conclusions about PARP1 expression. To use this for diagnostic

purposes, instead of removing the whole prostate, one would need to perform a similar analysis using transrectal ultrasound-guided systematic biopsy to then see if the expression of PARP1 is similarly conclusive. To improve the project, in a second step, instead of using an overview of the largest cross section of the prostate, several layers from different areas of the RP specimen could be used, thereby making three-dimensional analysis possible. This would increase the significance and ensure that no tumor is missed.

8 Conclusion

We found a widespread and consistent expression of PARP1 in PC in a total of 31 RP specimens and 5 TMAs. The increasing expression of PARP1 with the progressing tumor stage in the specimens indicates that PARP1 is a promising biomarker for emerging imaging and therapeutic applications in PC, in addition to PARP inhibitor therapy. Interestingly, PARP1 and PSMA overexpression in PC was not strongly correlated, which could indicate a complementary value. [50]

9 Bibliography

1. Ferlay, J., et al., *Cancer incidence and mortality patterns in Europe: estimates for 40 countries in 2012.* Eur J Cancer, 2013. **49**(6): p. 1374-403.
2. Ghafoor, S., I.A. Burger, and A.H. Vargas, *Multimodality Imaging of Prostate Cancer.* J Nucl Med, 2019. **60**(10): p. 1350-1358.
3. National Cancer Institute, S., Epidemiology, and End Results Program. *Cancer Stat Facts: Prostate Cancer: Survival Statistics*. 2022 28.03.2024]; Available from: https://seer.cancer.gov/statfacts/html/prost.html.
4. Edited by James D. Brierley, Mary K. Gospodarowicz, and C. Wittekind, *TNM classification of malignant tumours*. 8th ed. 2016, Union for International Cancer Control: John Wiley & Sons, Ltd.
5. Bostwick, D.G., et al., *Prognostic factors in prostate cancer. College of American Pathologists Consensus Statement 1999.* Arch Pathol Lab Med, 2000. **124**(7): p. 995-1000.
6. Cancer Research UK. *TNM Staging*. 15.07.2019 08.01.2022]; Available from: https://www.cancerresearchuk.org/about-cancer/prostate-cancer/stages/tnm-staging.
7. N. Mottet, J.B., E. Briers, R.C.N. van den Bergh,, et al., *Guidelines on Prostate Cancer.* European Association of Urology (EAU), 2015.
8. Cancer Research UK. *The Gleason score and Grade Groups*. 31.05.2019 08.01.2022].
9. Grunert, M., et al., *Nuklearmedizinische Diagnostik und Therapie des Prostatakarzinoms.* Journal für Urologie und Urogynäkologie/Österreich, 2021. **28**(2): p. 58-72.
10. Ghosh, A. and W.D.W. Heston, *Tumor target prostate specific membrane antigen (PSMA) and its regulation in prostate cancer*, in *Journal of Cellular Biochemistry*. 2004. p. 528-539.
11. Minner, S., et al., *High level PSMA expression is associated with early psa recurrence in surgically treated prostate cancer.* The Prostate, 2011. **71**(3): p. 281-288.
12. Yunusa, G.H., A.U. Kaoje, and A.T. Orunmuyi, *Comparison of 99mTc-PSMA SPECT/CT and 68Ga-PSMA PET/CT in patients with prostate cancer: a protocol for systematic review and meta-analysis*. 2021: SpringerOpen.

13. Neels, O.C., et al., *Radiolabeled PSMA Inhibitors.* Cancers (Basel), 2021. **13**(24).
14. European Medicines Agency, *Locametz (gozetotide) - Medicine Overview*. 2022: https://www.ema.europa.eu/en/medicines/human.
15. U.S. Food and Drug Administration *FDA approves second PSMA-targeted PET imaging drug for men with prostate cancer*. 2021.
16. Keam, S.J., *Piflufolastat F 18: Diagnostic First Approval.* Mol Diagn Ther, 2021. **25**(5): p. 647-656.
17. Werner, P., et al., *[(99cm)Tc]Tc-PSMA-I&S-SPECT/CT: experience in prostate cancer imaging in an outpatient center.* EJNMMI Res, 2020. **10**(1): p. 45.
18. Fendler, W.P., et al., *(177)Lu-PSMA Radioligand Therapy for Prostate Cancer.* J Nucl Med, 2017. **58**(8): p. 1196-1200.
19. U.S. Food and Drug Administration, *FDA approves Pluvicto for metastatic castration-resistant prostate cancer*. 2022: https://www.fda.gov/drugs/resources-information-approved-drugs.
20. European Medicines Agency, *Pluvicto : EPAR - Medicine overview*. 2022: https://www.ema.europa.eu/en/medicines/human.
21. Hennrich, U. and M. Eder, *[(177)Lu]Lu-PSMA-617 (Pluvicto(TM)): The First FDA-Approved Radiotherapeutical for Treatment of Prostate Cancer.* Pharmaceuticals (Basel), 2022. **15**(10).
22. Ahmadzadehfar, H., et al., *Prior therapies as prognostic factors of overall survival in metastatic castration-resistant prostate cancer patients treated with [(177)Lu]Lu-PSMA-617. A WARMTH multicenter study (the 617 trial).* Eur J Nucl Med Mol Imaging, 2021. **48**(1): p. 113-122.
23. National Library of Medicine, *PSMAfore: A Phase III, Open-label, Multi-Center, Randomized Study Comparing 177Lu-PSMA-617 vs. a Change of Androgen Receptor-directed Therapy in the Treatment of Taxane Naïve Men With Progressive Metastatic Castrate Resistant Prostate Cancer*.
24. Hofman, M.S., et al., *TheraP: a randomized phase 2 trial of (177) Lu-PSMA-617 theranostic treatment vs cabazitaxel in progressive metastatic castration-resistant prostate cancer (Clinical Trial Protocol ANZUP 1603).* BJU Int, 2019. **124 Suppl 1**: p. 5-13.
25. Antonarakis, E.S., L.G. Gomella, and D.P. Petrylak, *When and How to Use PARP Inhibitors in Prostate Cancer: A Systematic Review of the Literature with*

an Update on On-Going Trials. European Urology Oncology, 2020. **3**(5): p. 594-611.

26. Javle, M. and N.J. Curtin, *The role of PARP in DNA repair and its therapeutic exploitation.* Br J Cancer, 2011. **105**(8): p. 1114-22.
27. Lord, C.J. and A. Ashworth, *The DNA damage response and cancer therapy.* Nature, 2012. **481**(7381): p. 287-94.
28. Clovis Oncology, I. and M. Foundation, *A Study of Rucaparib in Patients With Metastatic Castration-resistant Prostate Cancer and Homologous Recombination Gene Deficiency*. 2021.
29. Abida, W., et al., *Rucaparib in Men With Metastatic Castration-Resistant Prostate Cancer Harboring a BRCA1 or BRCA2 Gene Alteration.* J Clin Oncol, 2020. **38**(32): p. 3763-3772.
30. Abida, W., et al., *Non-BRCA DNA Damage Repair Gene Alterations and Response to the PARP Inhibitor Rucaparib in Metastatic Castration-Resistant Prostate Cancer: Analysis From the Phase II TRITON2 Study.* Clin Cancer Res, 2020. **26**(11): p. 2487-2496.
31. AstraZeneca, et al., *Study of Olaparib (Lynparza™) Versus Enzalutamide or Abiraterone Acetate in Men With Metastatic Castration-Resistant Prostate Cancer (PROfound Study)*. 2019.
32. de Bono, J., et al., *Olaparib for Metastatic Castration-Resistant Prostate Cancer.* N Engl J Med, 2020. **382**(22): p. 2091-2102.
33. Leitlinienprogramm Onkologie, *S3-Leitlinie Prostatakarzinom.* 2021. **6.2**.
34. Messina, C., et al., *BRCA Mutations in Prostate Cancer: Prognostic and Predictive Implications.* J Oncol, 2020. **2020**: p. 4986365.
35. Lang, S.H., et al., *A systematic review of the prevalence of DNA damage response gene mutations in prostate cancer.* Int J Oncol, 2019. **55**(3): p. 597-616.
36. Inderjeeth, A.J., et al., *Clinical Application of Poly(ADP-ribose) Polymerase (PARP) Inhibitors in Prostate Cancer.* Cancers (Basel), 2022. **14**(23).
37. Clarke, N.W., et al., *Abiraterone and Olaparib for Metastatic Castration-Resistant Prostate Cancer.* NEJM Evidence, 2022. **1**(9).
38. Sato, H., et al., *DNA double-strand break repair pathway regulates PD-L1 expression in cancer cells.* Nature Communications, 2017. **8**(1).

39. Karzai, F., et al., *Activity of durvalumab plus olaparib in metastatic castration-resistant prostate cancer in men with and without DNA damage repair mutations.* J Immunother Cancer, 2018. **6**(1): p. 141.
40. European Medicines Agency, *Lynparza - Medicine overview*. 2023: https://www.ema.europa.eu/en/medicines/human.
41. IQWIG. *[A22-117] Olaparib (Ovarialkarzinom) - Nutzenbewertung gemäß § 35a SGB V*. [Report] 2023 01.02.2023 [cited 2023 10.03.2023]; 1.0:[Available from: https://www.iqwig.de/projekte/a22-117.html.
42. Ambur Sankaranarayanan, R., et al., *Advancements in PARP1 Targeted Nuclear Imaging and Theranostic Probes.* J Clin Med, 2020. **9**(7).
43. Kossatz, S., et al., *Detection and delineation of oral cancer with a PARP1 targeted optical imaging agent.* Sci Rep, 2016. **6**: p. 21371.
44. Kossatz, S., et al., *Validation of the use of a fluorescent PARP1 inhibitor for the detection of oral, oropharyngeal and oesophageal epithelial cancers.* Nat Biomed Eng, 2020. **4**(3): p. 272-285.
45. Fujimoto, N., et al., *Treatment of Metastatic Castration-resistant Prostate Cancer: Are PARP Inhibitors Shifting the Paradigm?* Anticancer Res, 2021. **41**(10): p. 4687-4695.
46. Risdon, E.N., et al., *PARP Inhibitors and Prostate Cancer: To Infinity and Beyond BRCA.* Oncologist, 2021. **26**(1): p. e115-e129.
47. Wichmann, C., et al., *The effect of the triazene compound CT913 on ovarian cancer cells in vitro and its synergistic interaction with the PARP-inhibitor olaparib.* Gynecol Oncol, 2020. **159**(3): p. 850-859.
48. Dehdashti, F., et al., *Pilot Study: PARP1 Imaging in Advanced Prostate Cancer.* Mol Imaging Biol, 2022. **24**(6): p. 853-861.
49. Angel, M., M. Zarba, and J.P. Sade, *PARP inhibitors as a radiosensitizer: a future promising approach in prostate cancer?* Ecancermedicalscience, 2021. **15**: p. ed118.
50. Oncology, N.R.G. and I. National Cancer, *Niraparib With Standard Combination Radiation Therapy and Androgen Deprivation Therapy in Treating Patients With High Risk Prostate Cancer*. 2023.
51. Zhang, H., et al., *[(18)F]-Labeled PARP-1 PET imaging of PSMA targeted alpha particle radiotherapy response.* Sci Rep, 2022. **12**(1): p. 13034.

52. Ruigrok, E.A.M., et al., *Preclinical Assessment of the Combination of PSMA-Targeting Radionuclide Therapy with PARP Inhibitors for Prostate Cancer Treatment.* Int J Mol Sci, 2022. **23**(14).
53. Purohit, N.K., et al., *Potentiation of (177)Lu-octreotate peptide receptor radionuclide therapy of human neuroendocrine tumor cells by PARP inhibitor.* Oncotarget, 2018. **9**(37): p. 24693-24706.
54. Marchetti, A., et al., *PARP Inhibitors and Radiometabolic Approaches in Metastatic Castration-Resistant Prostate Cancer: What's Now, What's New, and What's Coming?* Cancers (Basel), 2022. **14**(4).
55. Peter MacCallum Cancer Centre, A., *177Lu-PSMA-617 Therapy and Olaparib in Patients With Metastatic Castration Resistant Prostate Cancer*. 2023.
56. National Cancer, I., *Testing the Safety of Different Doses of Olaparib Given Radium-223 for Men With Advanced Prostate Cancer With Bone Metastasis*. 2023.
57. Shaya, J., et al., *A phase I/II study of combination olaparib and radium-223 in men with metastatic castration-resistant prostate cancer with bone metastases (COMRADE): A trial in progress.* Journal of Clinical Oncology, 2021. **39**(6_suppl): p. TPS182-TPS182.

10 Appendices

10.1 Analysis results from GraphPad Prism

10.1.1 Analysis of PARP1 – RPs

10.1.1.1 Normality and Lognormality Tests

Normality and Lognormality Tests Tabular results	A	B	C	D	E	F	G	H
	Cancer free Prostate	High grade PIN	Gleason 6	Gleason 7a	Gleason 7b	Gleason 8	Gleason 9	Gleason 10
1 **Test for normal distribution**								
2 **D'Agostino & Pearson test**								
3 K2	57.69	N too small	25.92	31.30	16.89	20.46	8.476	23.43
4 P value	<0.0001		<0.0001	<0.0001	0.0002	<0.0001	0.0144	<0.0001
5 Passed normality test (alpha=0.05)?	No		No	No	No	No	No	No
6 P value summary	****		****	****	***	****	*	****
7								
8 **Shapiro-Wilk test**								
9 W	0.7399	0.9841	0.6026	0.7074	0.8550	0.9029	0.9169	0.5822
10 P value	<0.0001	0.9771	<0.0001	<0.0001	<0.0001	<0.0001	<0.0001	<0.0001
11 Passed normality test (alpha=0.05)?	No	Yes	No	No	No	No	No	No
12 P value summary	****	ns	****	****	****	****	****	****
13								
14 **Number of values**	95	7	11	49	101	142	93	11

10.1.1.2 Kruskal-Wallis test – ANOVA results

Kruskal-Wallis test ANOVA results	
1 Table Analyzed	PARP1_all values_percentage_both projects added up
2	
3 **Kruskal-Wallis test**	
4 P value	<0.0001
5 Exact or approximate P value?	Approximate
6 P value summary	****
7 Do the medians vary signif. (P < 0.05)?	Yes
8 Number of groups	8
9 Kruskal-Wallis statistic	90.48
10	
11 **Data summary**	
12 Number of treatments (columns)	8
13 Number of values (total)	509

10.1.1.3 Comparison Cancer free prostate with cancer

10.1.1.3.1 Descriptive statistics

Descriptive statistics		A	B
		Cancer free Prostate	Cancer
1	Number of values	95	415
2			
3	Minimum	0.1174	0.04260
4	Maximum	31.42	53.08
5	Range	31.30	53.04
6			
7	Mean	4.578	11.38
8	Std. Deviation	5.960	11.70
9	Std. Error of Mean	0.6114	0.5742

10.1.1.3.2 Mann-Whitney test

Mann-Whitney test		
1	Table Analyzed	PARP1_percentage_both projects added up_comparison Cancer free- Cancer
2		
3	Column B	Cancer
4	vs.	vs.
5	Column A	Cancer free Prostate
6		
7	**Mann Whitney test**	
8	P value	<0.0001
9	Exact or approximate P value?	Exact
10	P value summary	****
11	Significantly different (P < 0.05)?	Yes
12	One- or two-tailed P value?	Two-tailed
13	Sum of ranks in column A,B	17193 , 113112
14	Mann-Whitney U	12633
15		
16	**Difference between medians**	
17	Median of column A	2.314, n=95
18	Median of column B	7.391, n=415
19	Difference: Actual	5.077
20	Difference: Hodges-Lehmann	3.653

10.1.2 Analysis of PSMA – RPs

10.1.2.1 Normality and Lognormality Tests

Normality and Lognormality Tests Tabular results		A	B	C	D	E	F	G	H
		Cancer free Prostate	High grade PIN	Gleason 6	Gleason 7a	Gleason 7b	Gleason 8	Gleason 9	Gleason 10
1	**Test for normal distribution**								
2	**D'Agostino & Pearson test**								
3	K2	68.57	1.621	2.020	33.88	28.45	28.83	18.65	1.618
4	P value	<0.0001	0.4446	0.3642	<0.0001	<0.0001	<0.0001	<0.0001	0.4453
5	Passed normality test (alpha=0.05)?	No	Yes	Yes	No	No	No	No	Yes
6	P value summary	****	ns	ns	****	****	****	****	ns
7									
8	**Shapiro-Wilk test**								
9	W	0.6762	0.9366	0.8299	0.6209	0.8619	0.9206	0.8595	0.9012
10	P value	<0.0001	0.5162	0.0334	<0.0001	<0.0001	<0.0001	<0.0001	0.1174
11	Passed normality test (alpha=0.05)?	No	Yes	No	No	No	No	No	Yes
12	P value summary	****	ns	*	****	****	****	****	ns
13									
14	**Number of values**	102	10	10	42	106	123	83	14

10.1.2.2 Kruskal-Wallis test – ANOVA results

Kruskal-Wallis test ANOVA results		
1	Table Analyzed	PSMA_all values_percentage_both projects added up
2		
3	**Kruskal-Wallis test**	
4	P value	<0.0001
5	Exact or approximate P value?	Approximate
6	P value summary	****
7	Do the medians vary signif. (P < 0.05)?	Yes
8	Number of groups	8
9	Kruskal-Wallis statistic	92.42
10		
11	**Data summary**	
12	Number of treatments (columns)	8
13	Number of values (total)	490

10.1.2.3 Comparison Cancer free prostate with cancer

10.1.2.3.1 Descriptive statistics

Descriptive statistics		A	B
		Cancer free Prostate	Cancer
1	Number of values	102	388
2			
3	Minimum	0.1031	0.1037
4	Maximum	59.01	94.85
5	Range	58.91	94.74
6			
7	Mean	7.689	22.49
8	Std. Deviation	11.16	23.23
9	Std. Error of Mean	1.105	1.179

10.1.2.3.2 Mann-Whitney test

Mann-Whitney test		
1	Table Analyzed	PSMA_all values_percentage_both projects added up_Comparison Cancer free-tumor
2		
3	Column B	Cancer
4	vs.	vs.
5	Column A	Cancer free Prostate
6		
7	**Mann Whitney test**	
8	P value	<0.0001
9	Exact or approximate P value?	Approximate
10	P value summary	****
11	Significantly different (P < 0.05)?	Yes
12	One- or two-tailed P value?	Two-tailed
13	Sum of ranks in column A,B	16963 , 103332
14	Mann-Whitney U	11710
15		
16	**Difference between medians**	
17	Median of column A	3.341, n=102
18	Median of column B	13.72, n=388
19	Difference: Actual	10.38
20	Difference: Hodges-Lehmann	7.969

10.1.3 Correlation of PARP1 & PSMA in RPs

Correlation	PARP1 vs. PSMA								
Cancer Stage	Cancer free	HG-PIN	Gleason 6	Gleason 7a	Gleason 7b	Gleason 8	Gleason 9	Gleason 10	all
Spearman r									
r	0,4963	-0,07143	-0,09091	0,1557	0,07587	0,2067	0,4817	0,01818	0,3662
95% confidence interval	0,3109 to 0,6453			-0,1821 to 0,4606	-0,1313 to 0,2767	0,01902 to 0,3803	0,2870 to 0,6382	-0,6013 to 0,6241	0,2797 to 0,4468
P value									
P (two-tailed)	<,001	0,906	0,811	0,351	0,46	0,027	<,001	0,967	<,001
P value summary	***	ns	ns	ns	ns	*	***	ns	***
Exact or approximate P value?	Approx.	Exact	Exact	Approx.	Approx.	Approx.	Approx.	Exact	Approx.
Significant? (alpha = 0.05)	Yes	No	No	No	No	Yes	Yes	No	Yes
Number of XY Pairs	85	7	10	38	97	115	80	11	439

10.1.4 Analysis of PARP1 – TMAs

10.1.4.1 Normality and Lognormality Tests

	Normality and Lognormality Tests Tabular results	A Cancer free Prostate	B Gleason 6
1	**Test for normal distribution**		
2	**D'Agostino & Pearson test**		
3	K2	181.2	17.56
4	P value	<0.0001	0.0002
5	Passed normality test (alpha=0.05)?	No	No
6	P value summary	****	***
7			
8	**Shapiro-Wilk test**		
9	W	0.7038	0.7866
10	P value	<0.0001	0.0025
11	Passed normality test (alpha=0.05)?	No	No
12	P value summary	****	**
13			
14	**Number of values**	246	15

10.1.4.2 Kruskal-Wallis test – ANOVA results

	Kruskal-Wallis test ANOVA results	
1	Table Analyzed	PARP1_TMA12, 13, 17, 18, 20_%pos. area
2		
3	**Kruskal-Wallis test**	
4	P value	<0.0001
5	Exact or approximate P value?	Approximate
6	P value summary	****
7	Do the medians vary signif. (P < 0.05)?	Yes
8	Number of groups	7
9	Kruskal-Wallis statistic	53.93
10		
11	**Data summary**	
12	Number of treatments (columns)	7
13	Number of values (total)	475

10.2 Overview illustrations of the RP specimen

stained in H&E (A) stained for PARP1 (B) and for PSMA (C)

Patient N.1 (ID: 738)

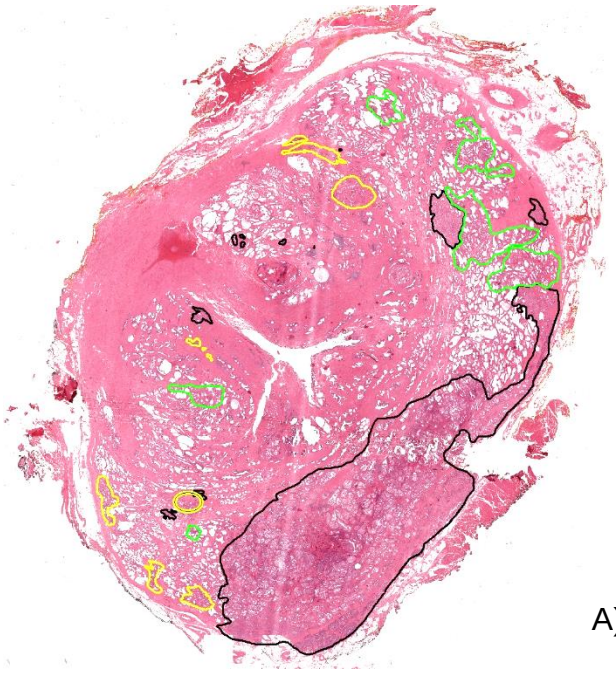

A)

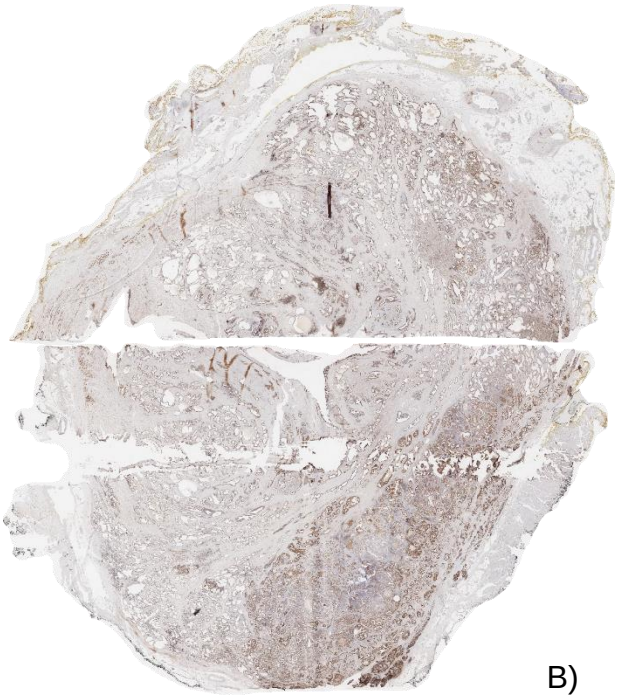

B)

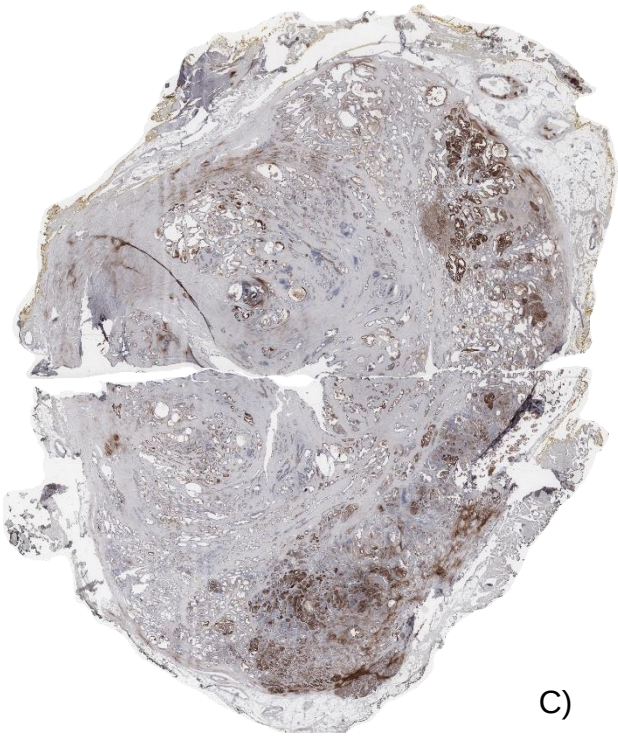

C)

Patient N.2 (ID: 1049)

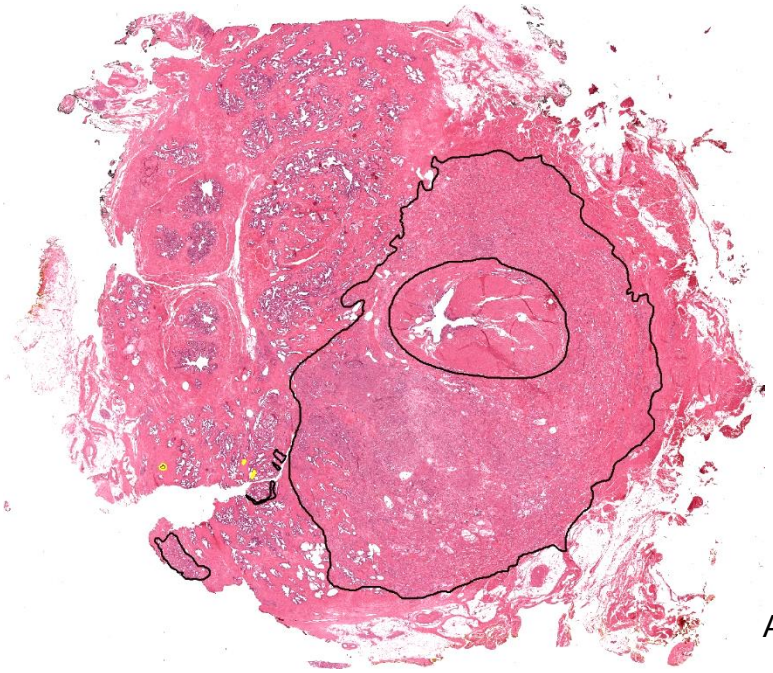

A)

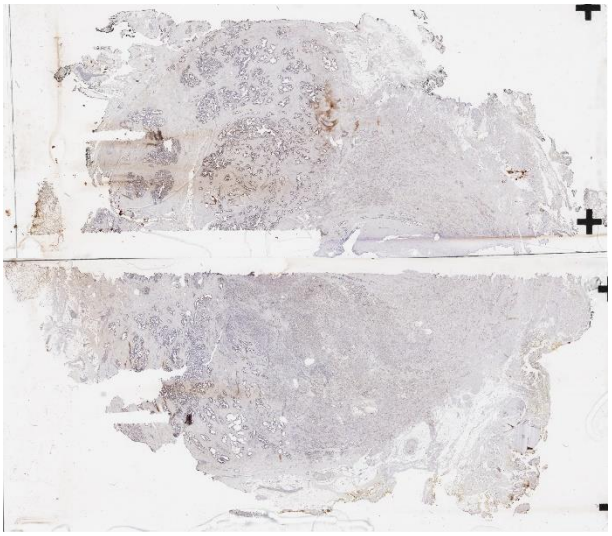

B)

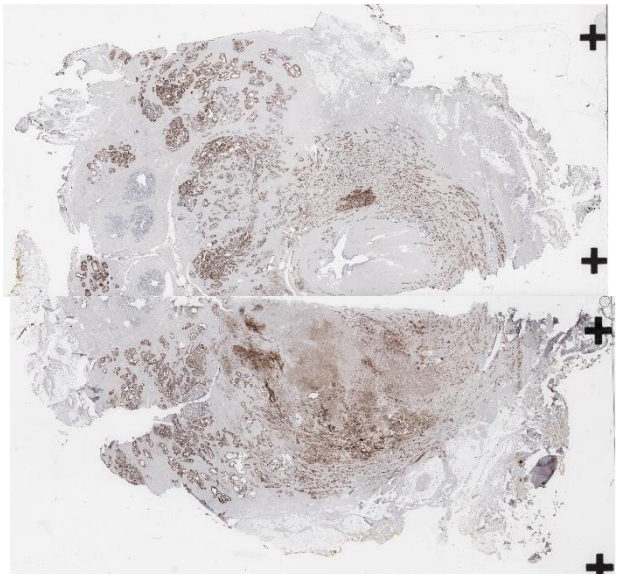

C)

Patient N.3 (ID: 1137)

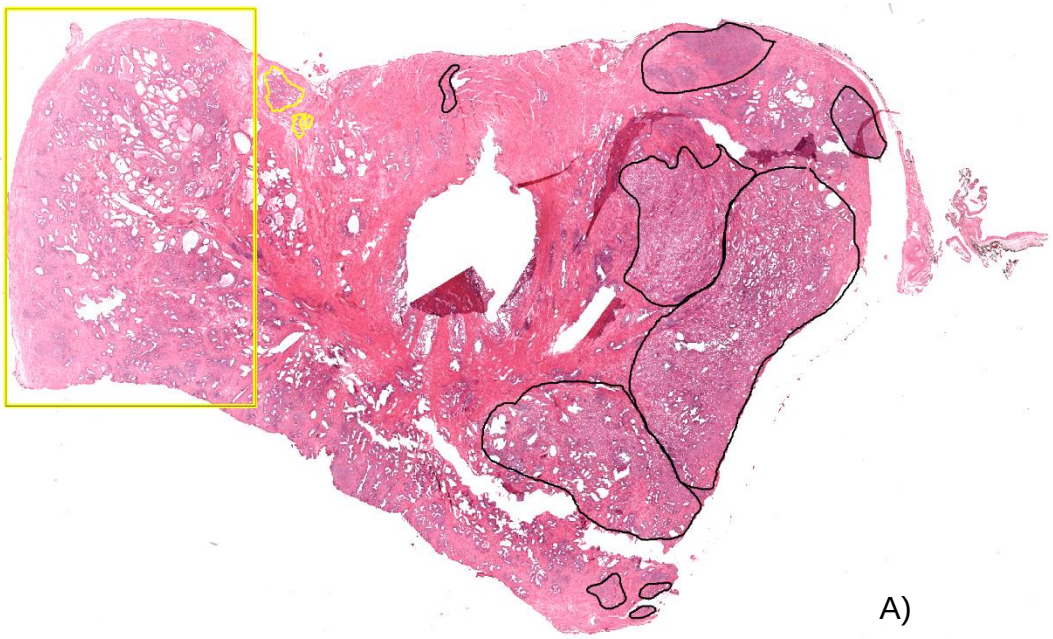

A)

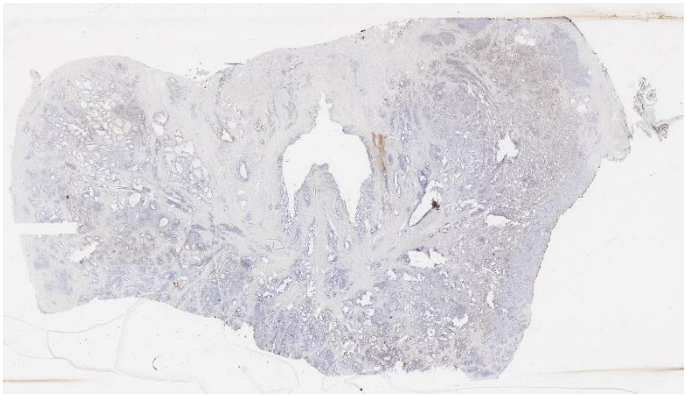

B)

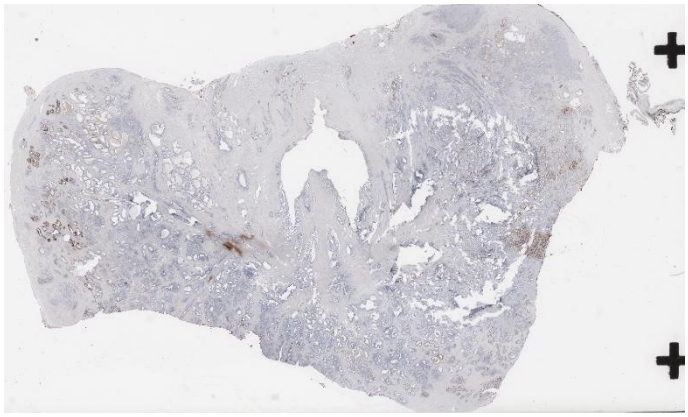

C)

Patient N.4 (ID: 1211)

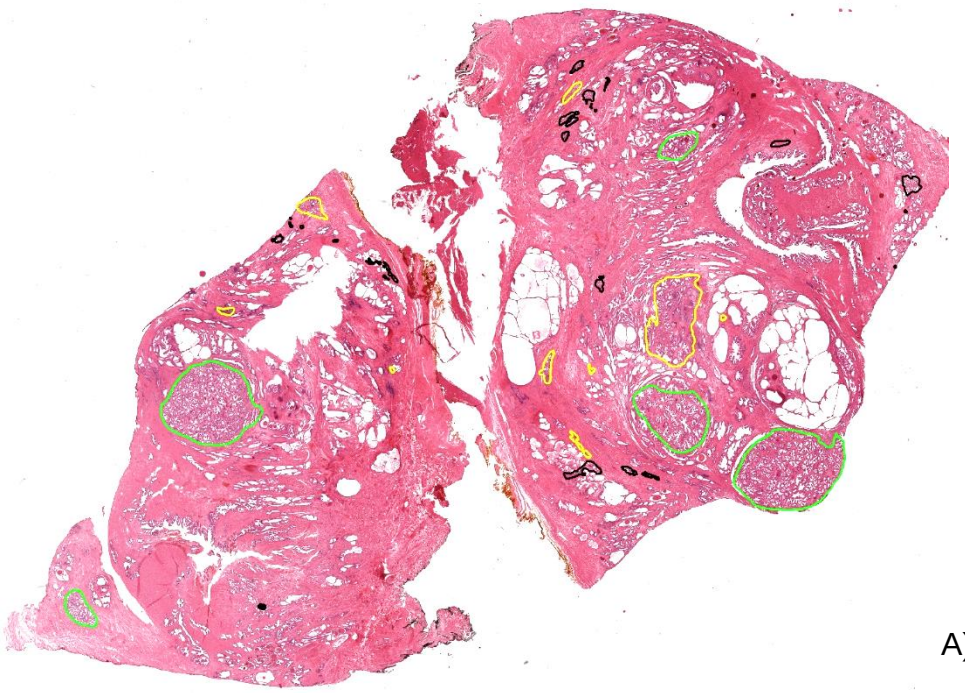

A)

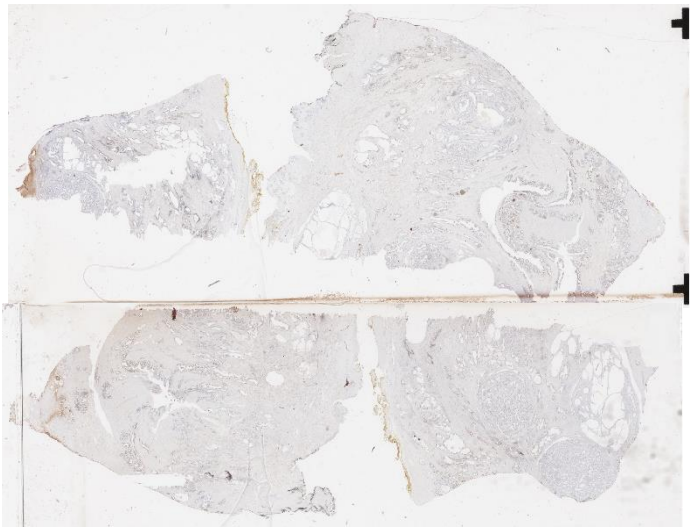

B)

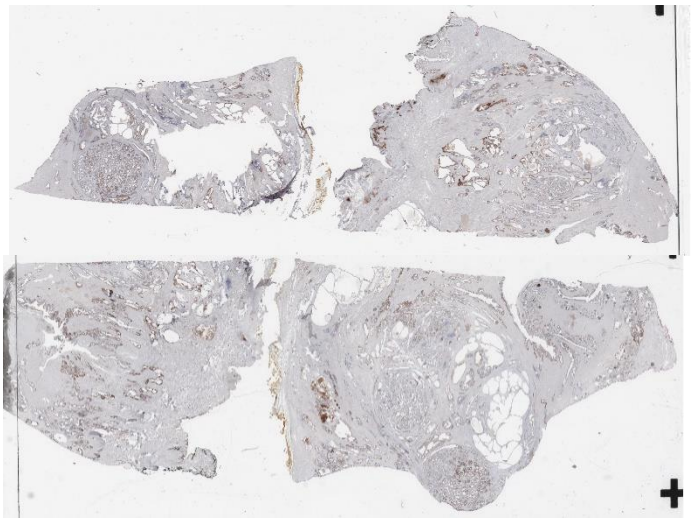

C)

Patient N.5 (ID: 1356)

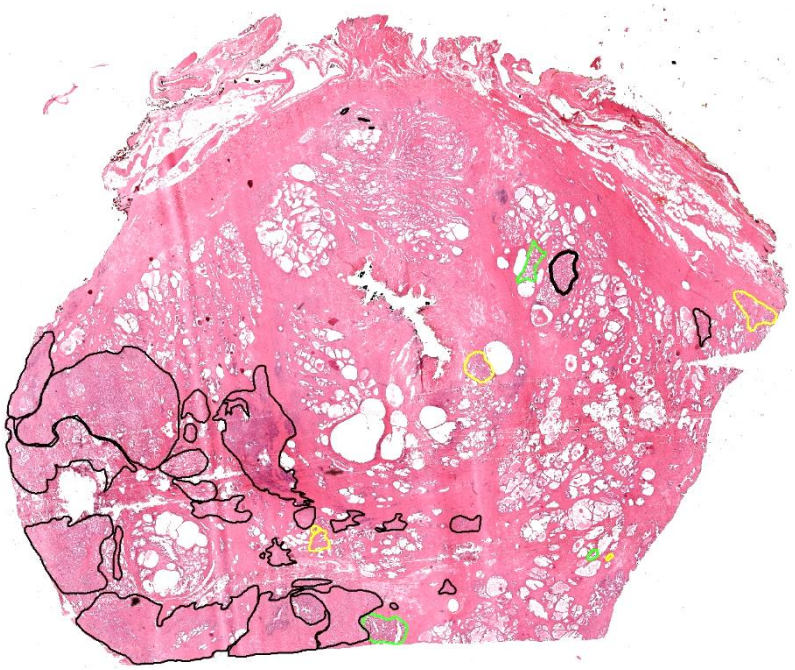

A)

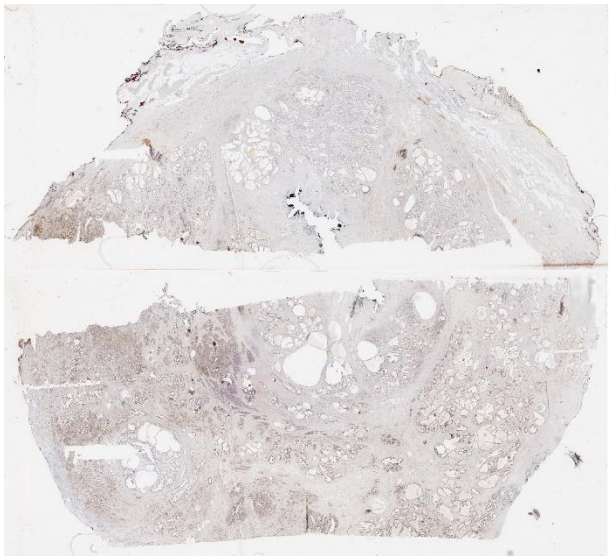

B)

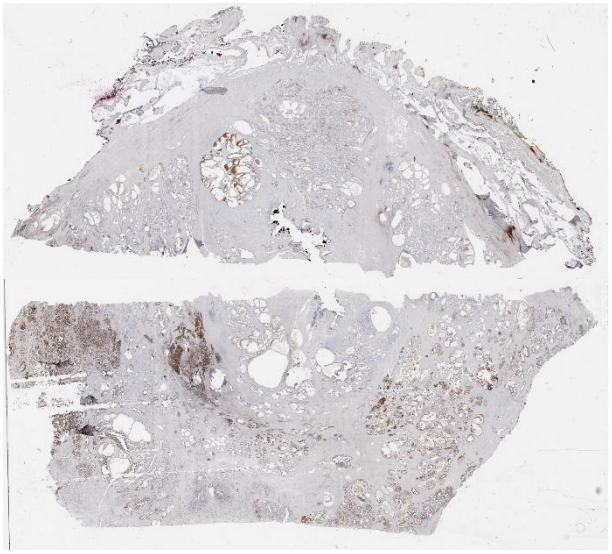

C)

Patient N.6 (ID: 1544)

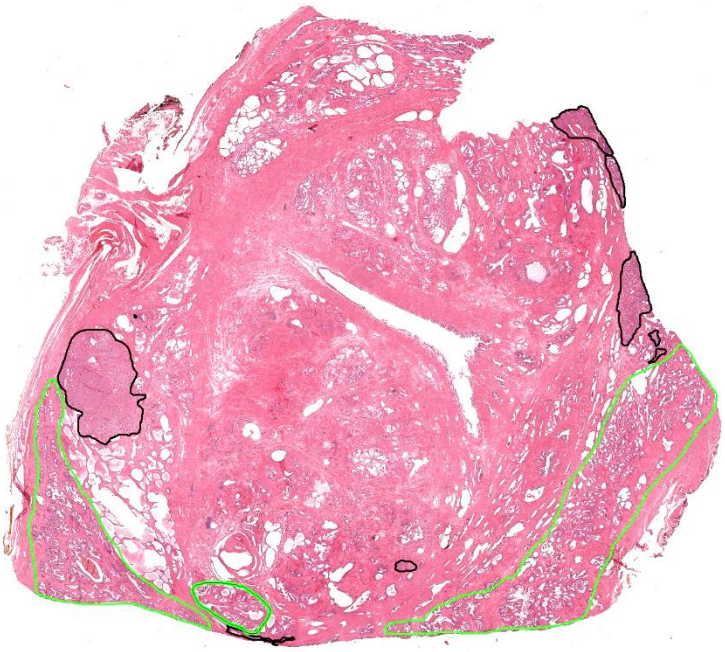

A)

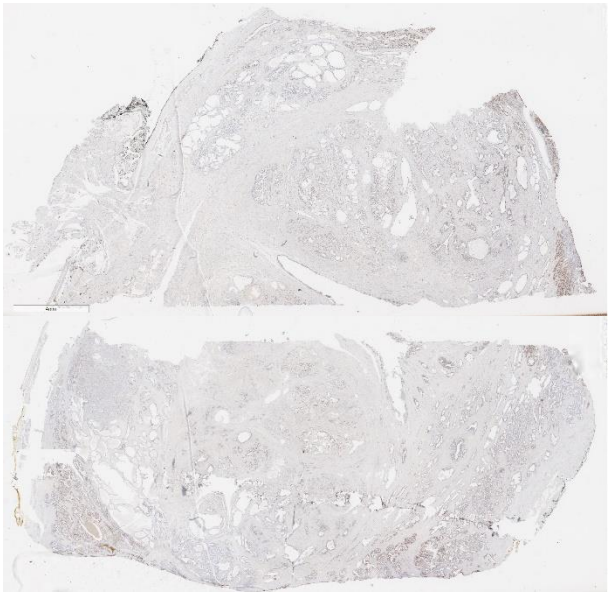

B)

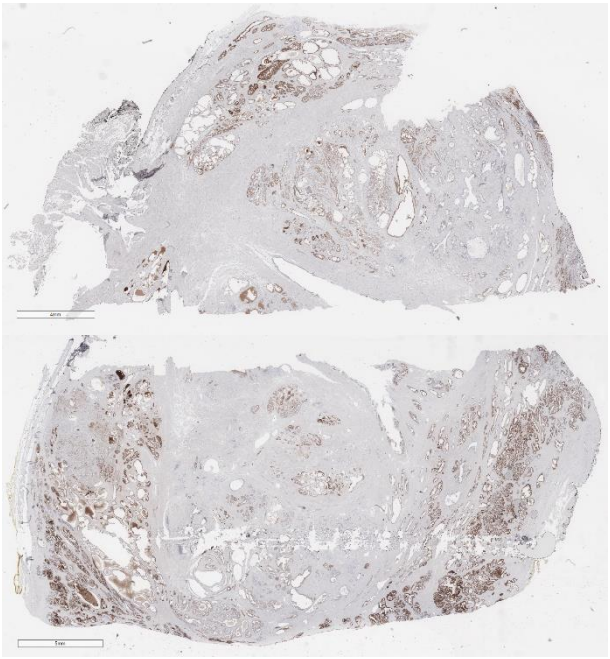

C)

Patient N.7 (ID: 1705)

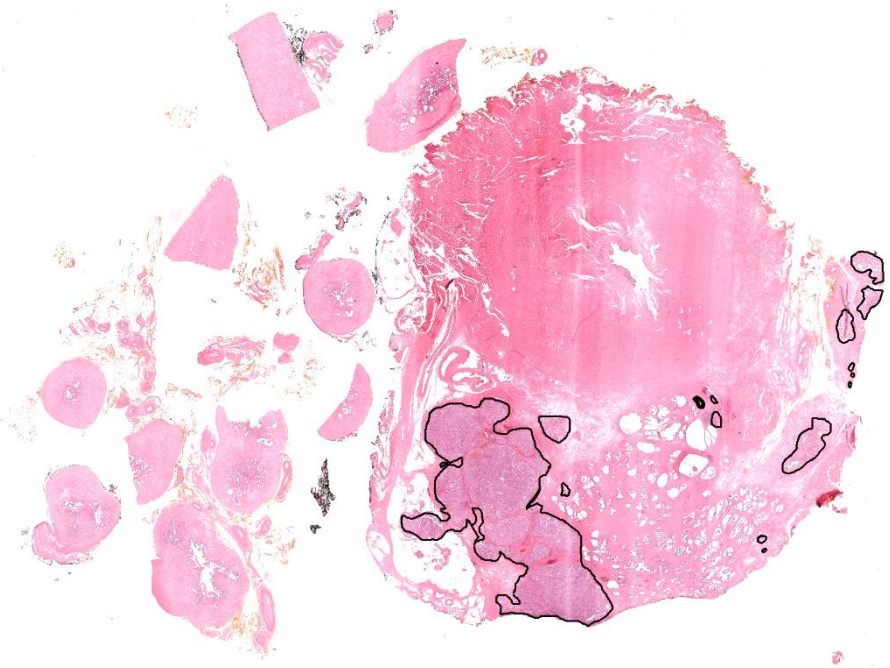

A)

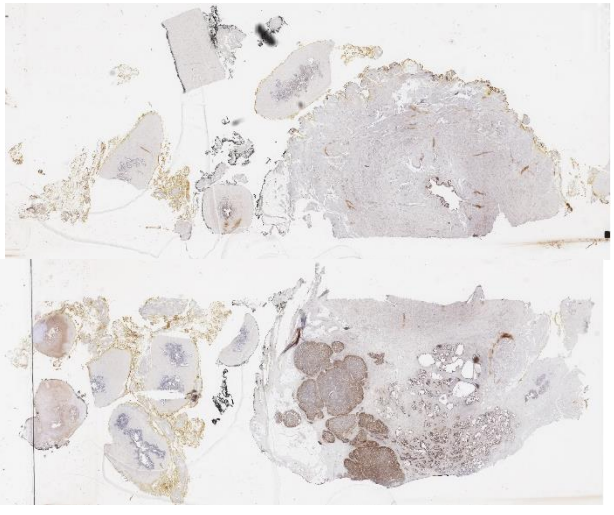

B)

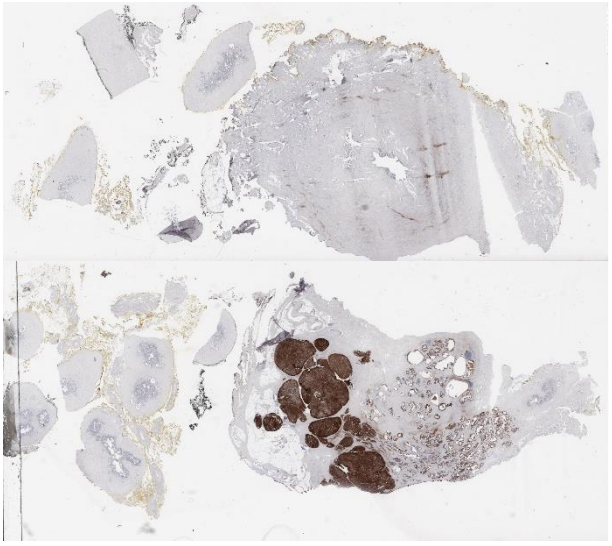

C)

Patient N.8 (ID: 1912)

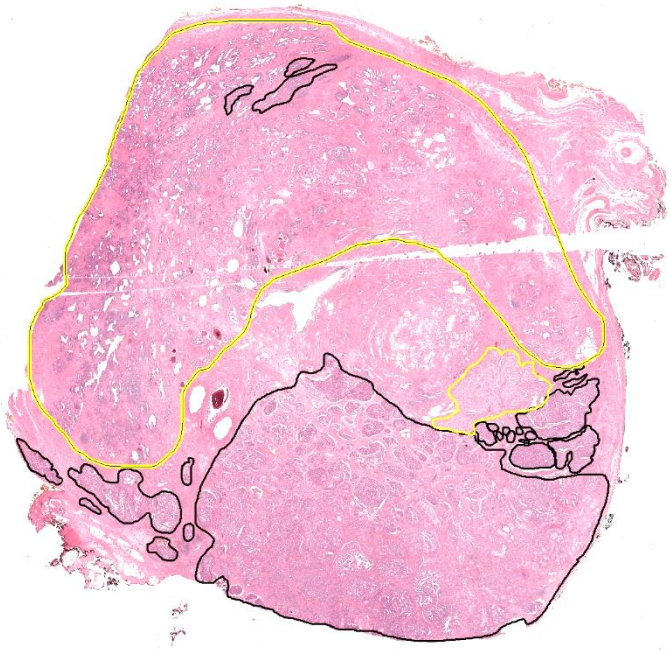

A)

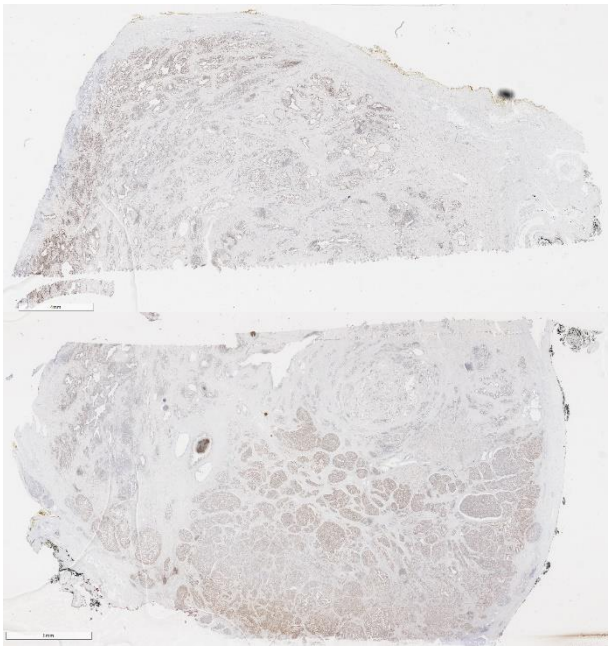

B)

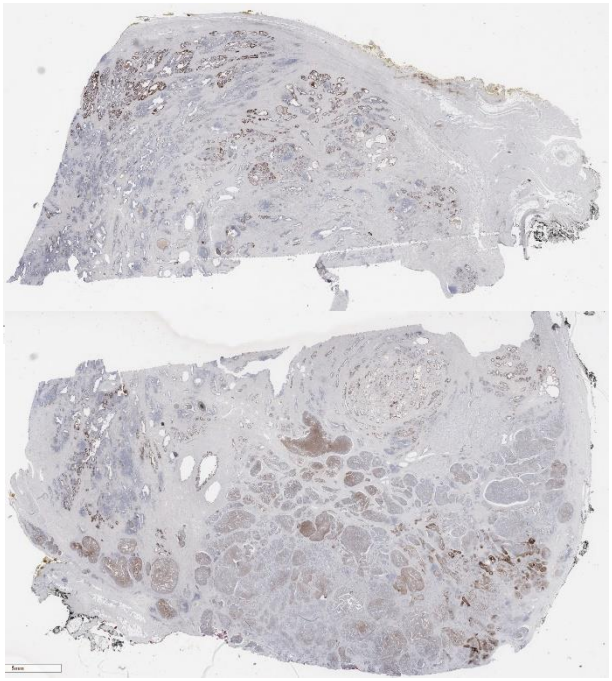

C)

Patient N.9 (ID: 2040)

A)

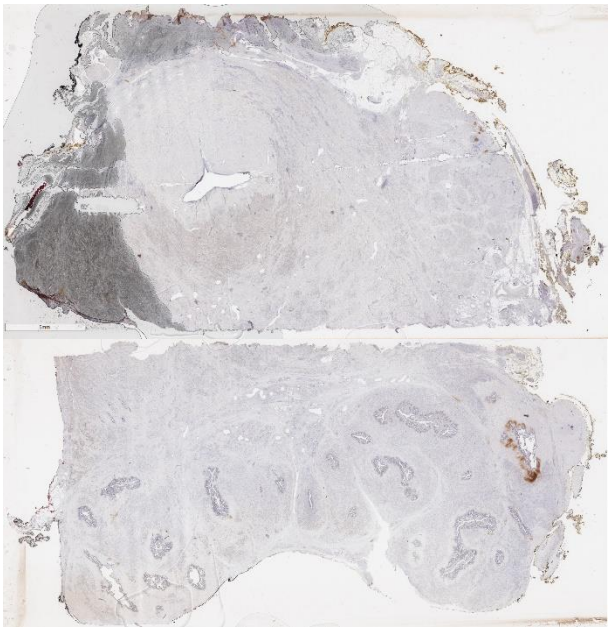

B)

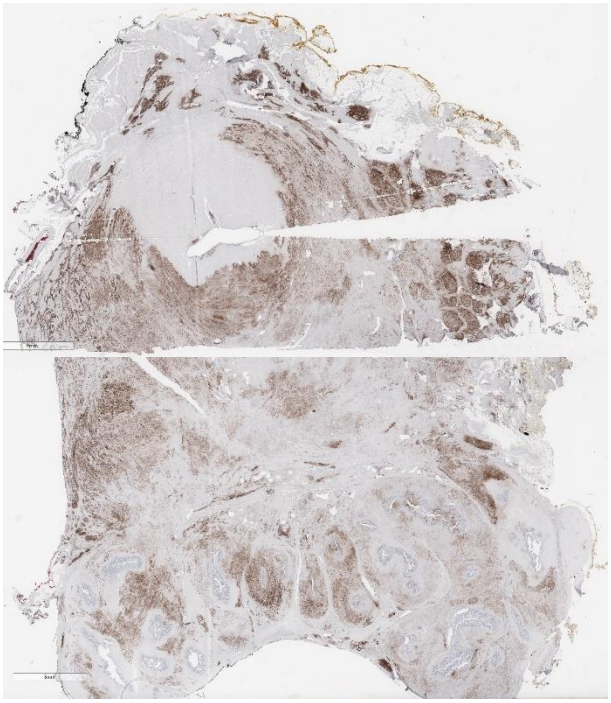

C)

Patient N.10 (ID: 2300)

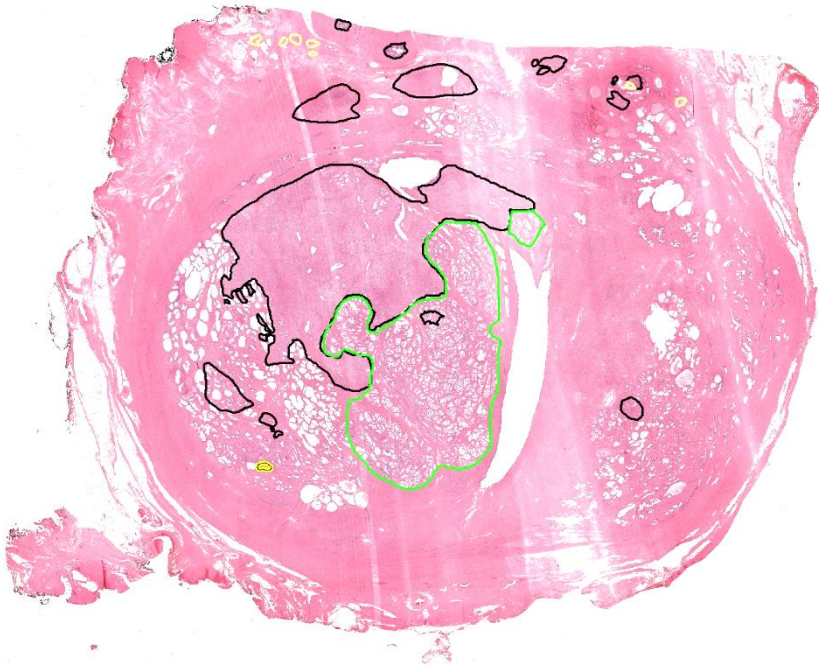

A)

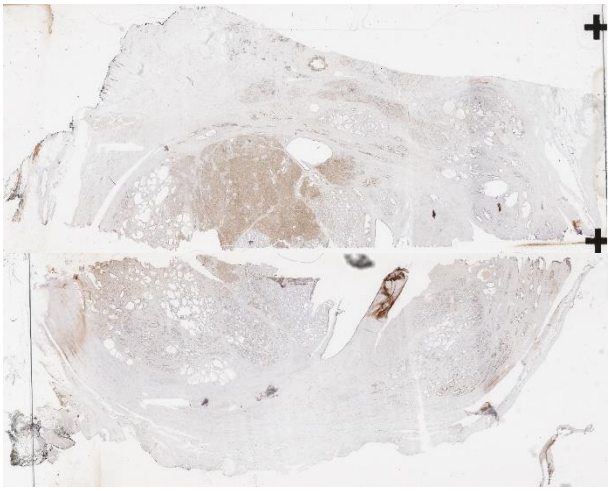

B)

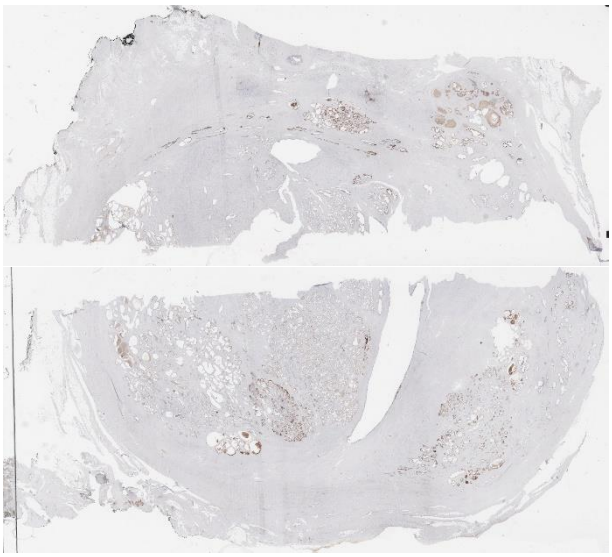

C)

Patient N.11 (ID: 2359)

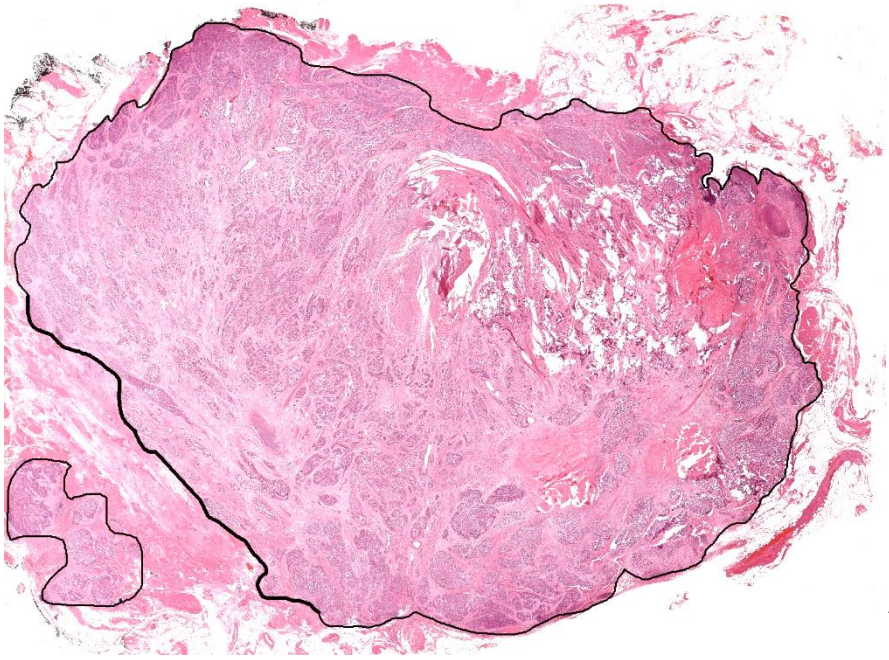

A)

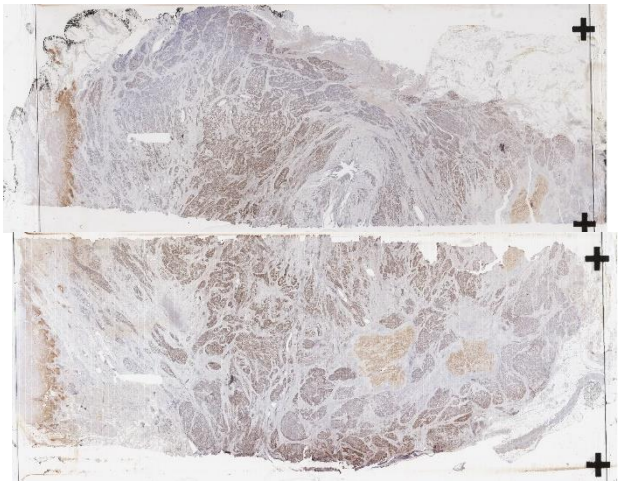

B)

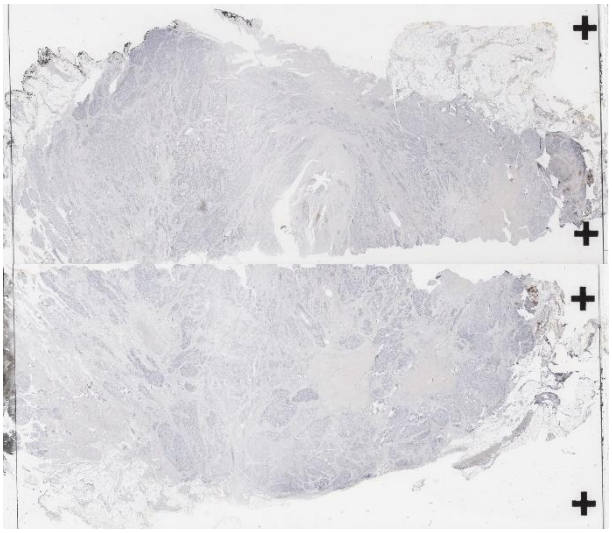

C)

Patient N.12 (ID: 2498)

A)

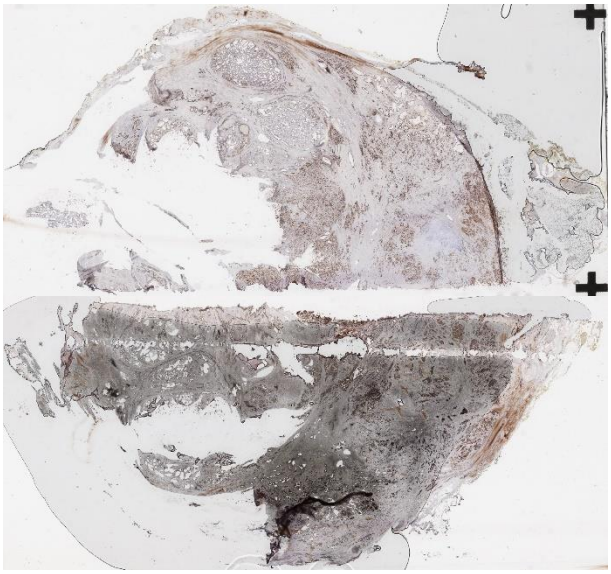

B)

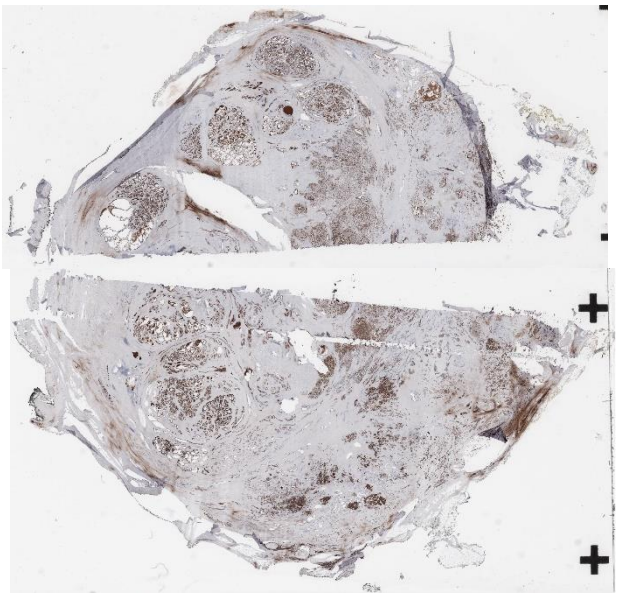

C)

Patient N.13 (ID: 2675)

A)

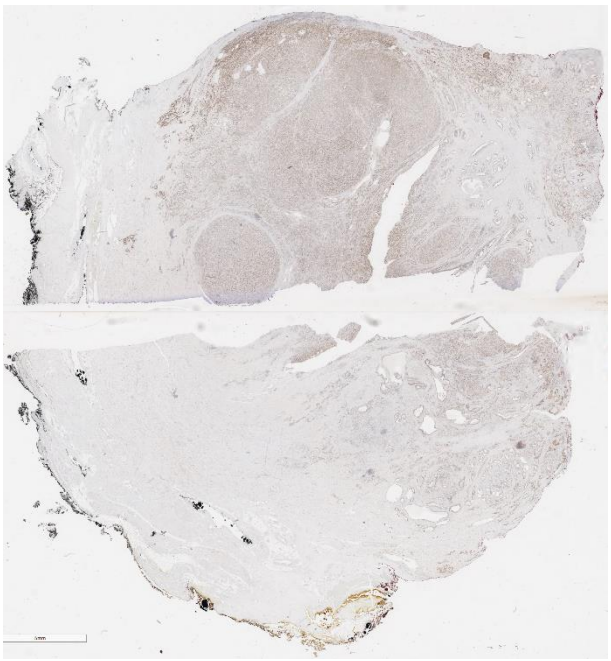

B)

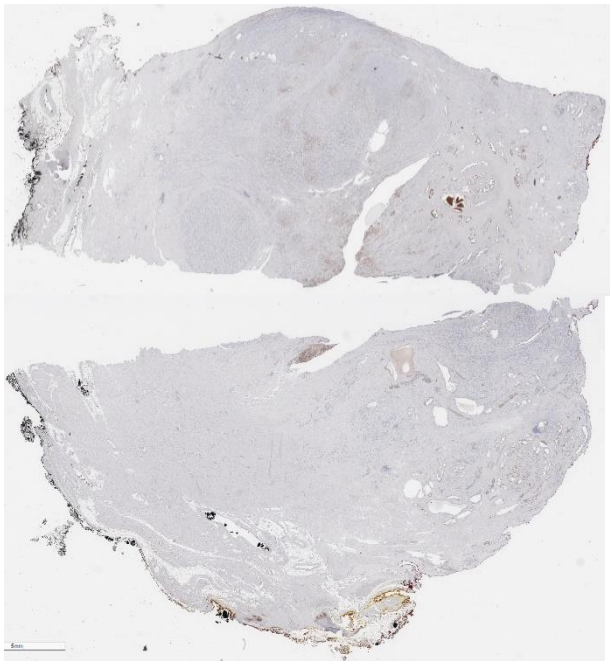

C)

Patient N.14 (ID: 3171)

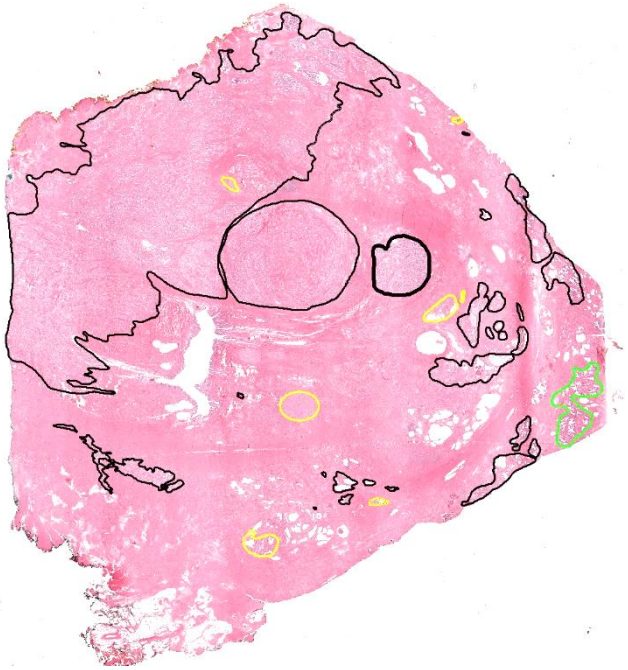

A)

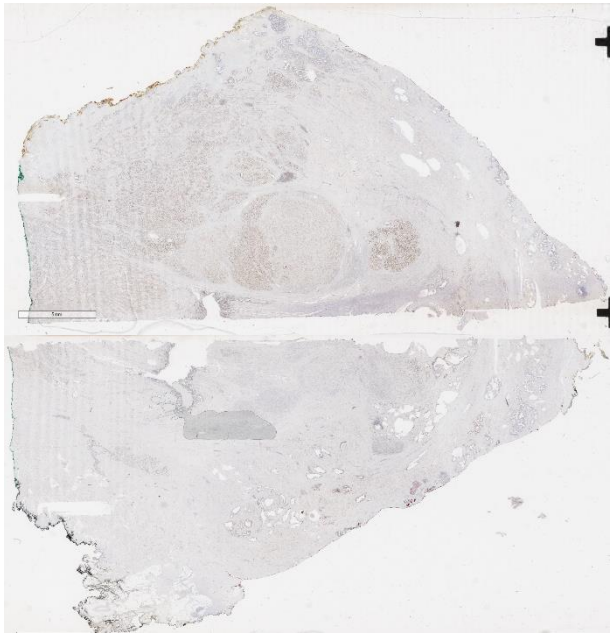

B)

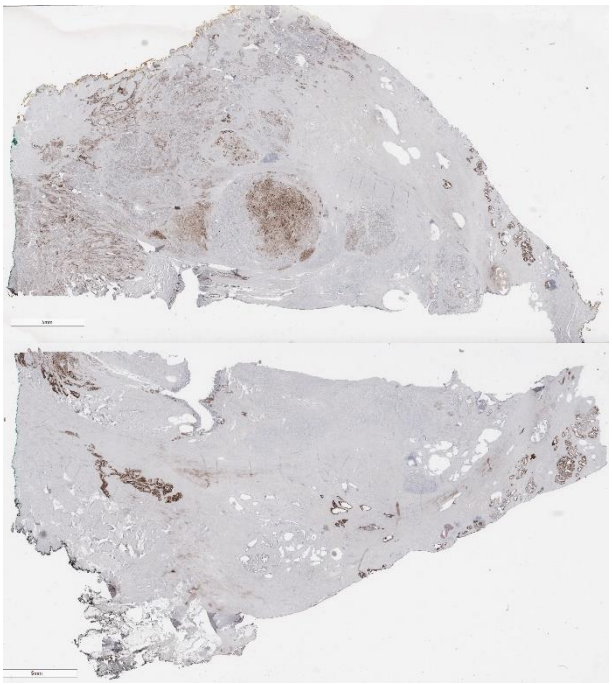

C)

Patient N.15 (ID: 3876)

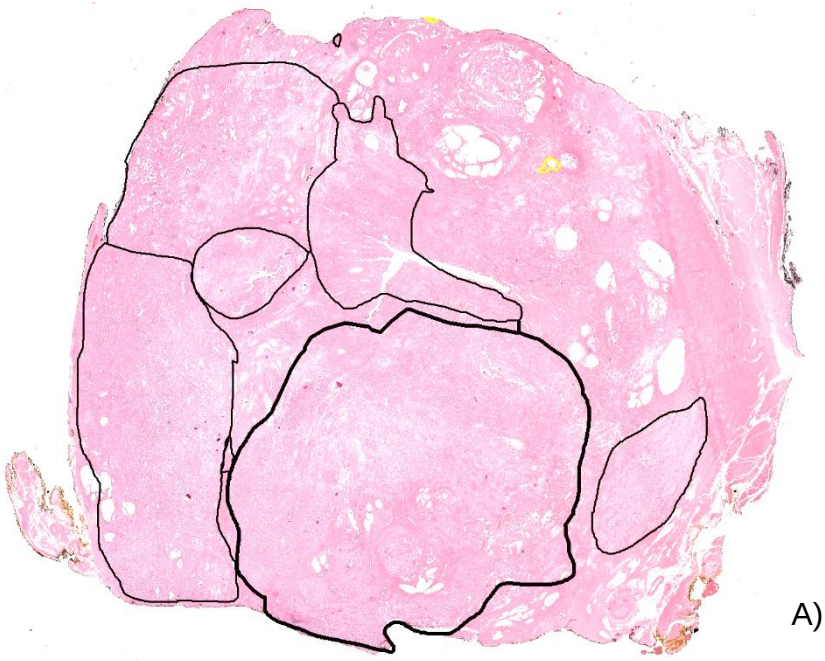

A)

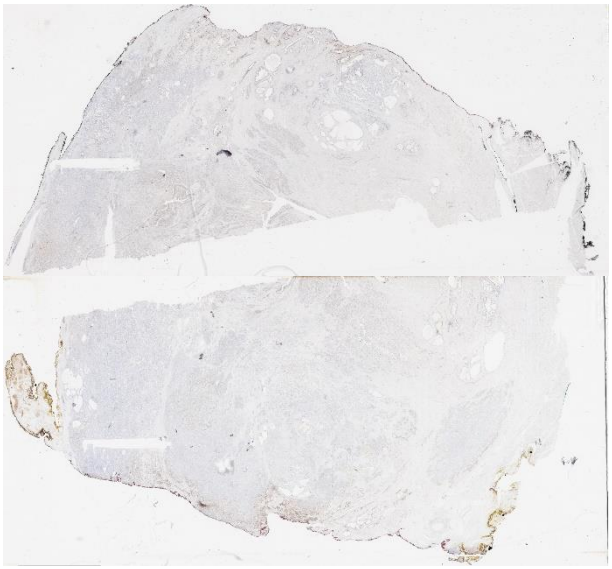

B)

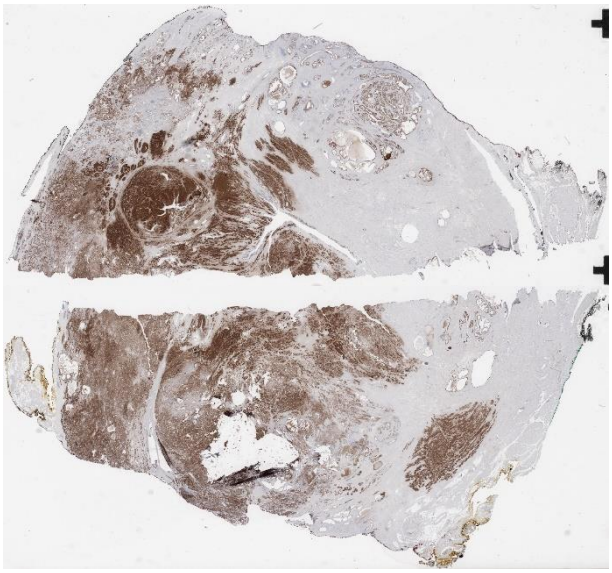

C)

Patient N.16 (ID: 4386)

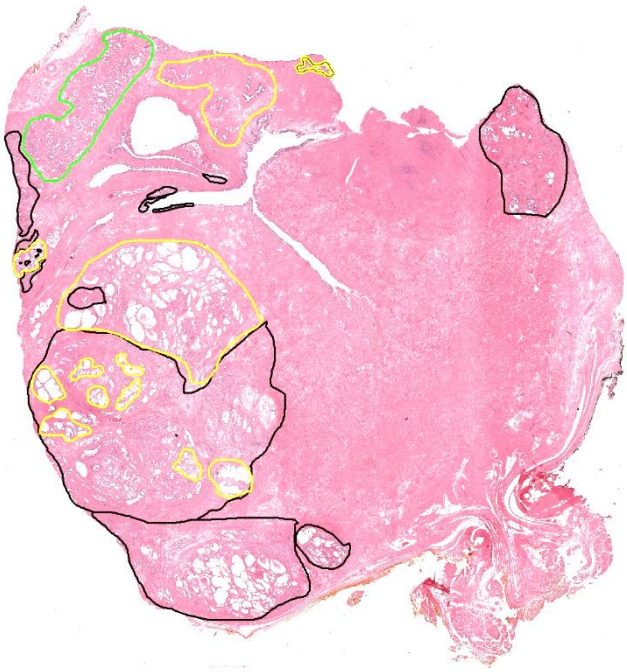

A)

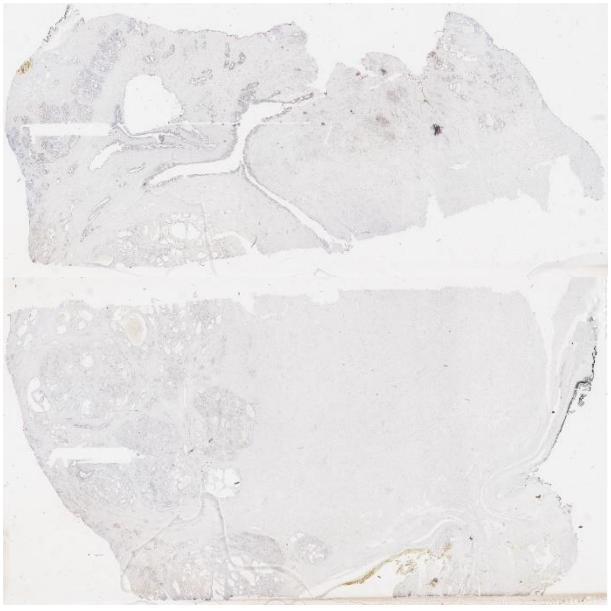

B)

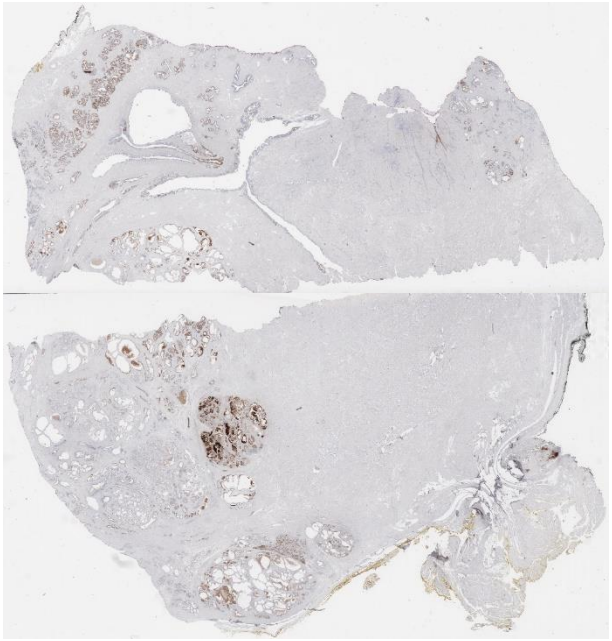

C)

Patient N.17 (ID: 4596)

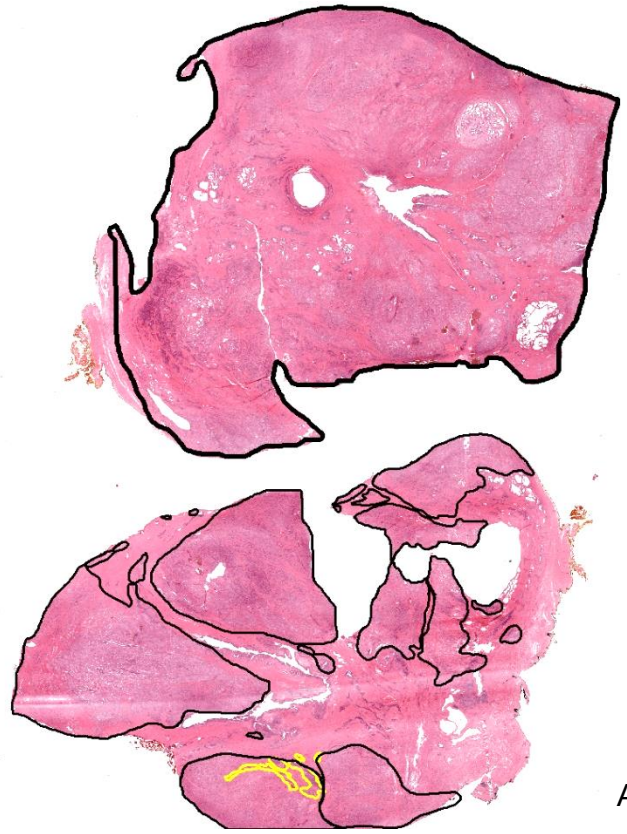

A)

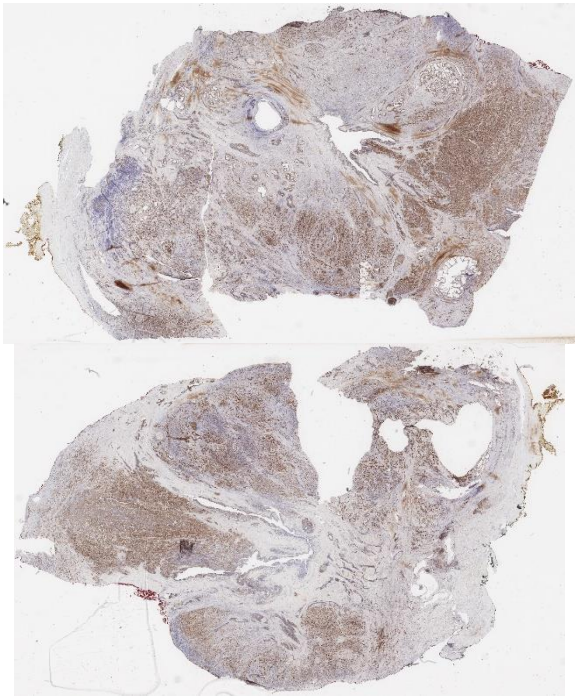

B)

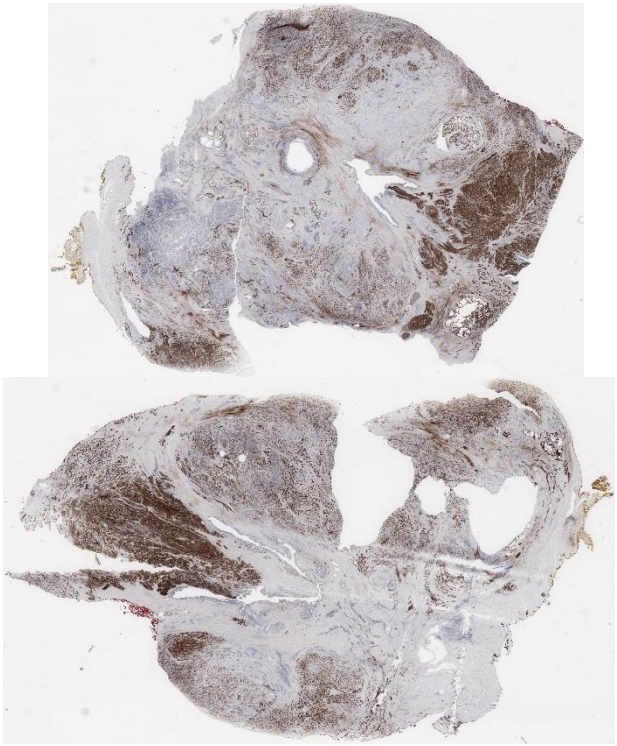

C)

Patient N.18 (ID: 4909)

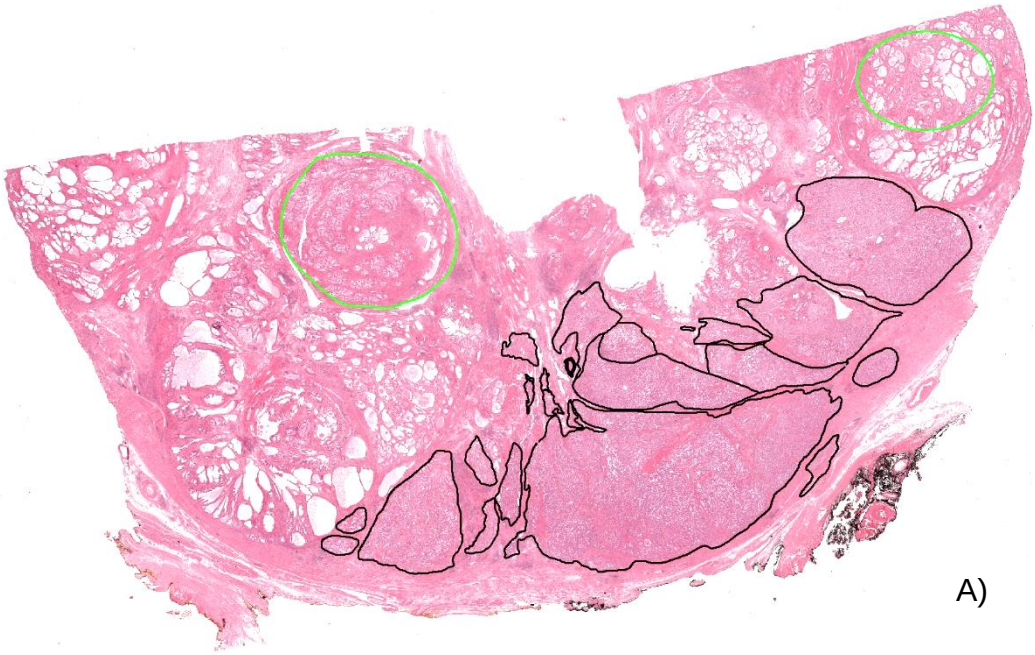

A)

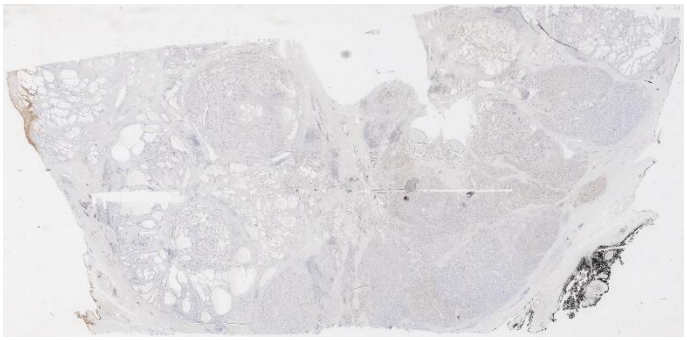

B)

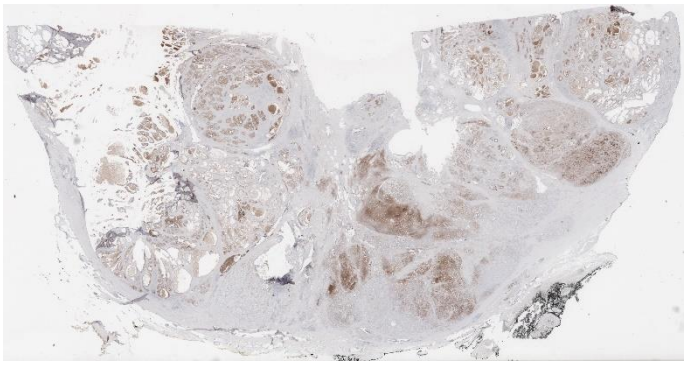

C)

Patient N.19 (ID: 3C)

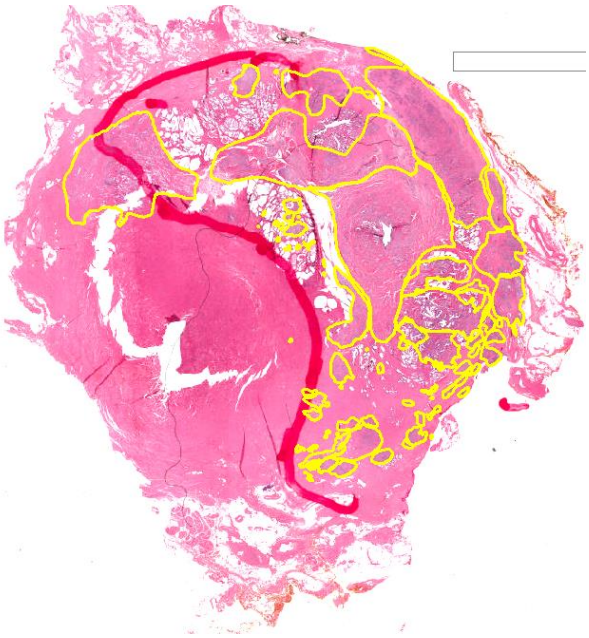

A)

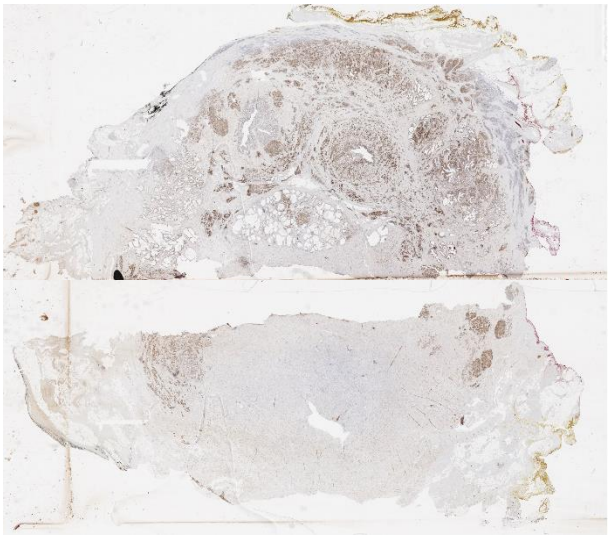

B)

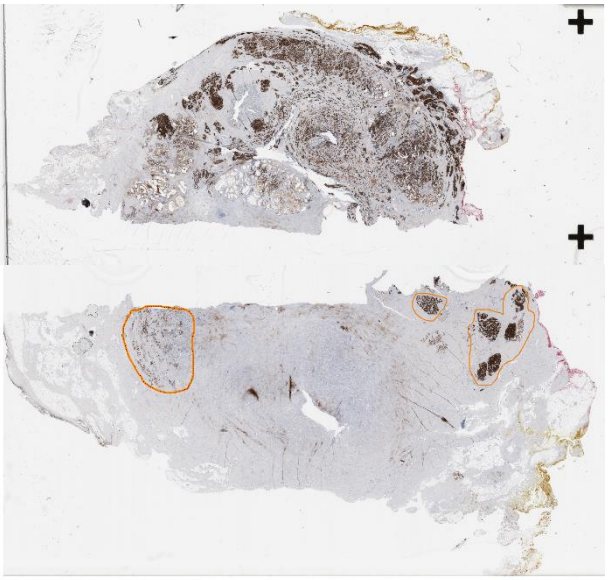

C)

Patient N.20 (ID: 4E)

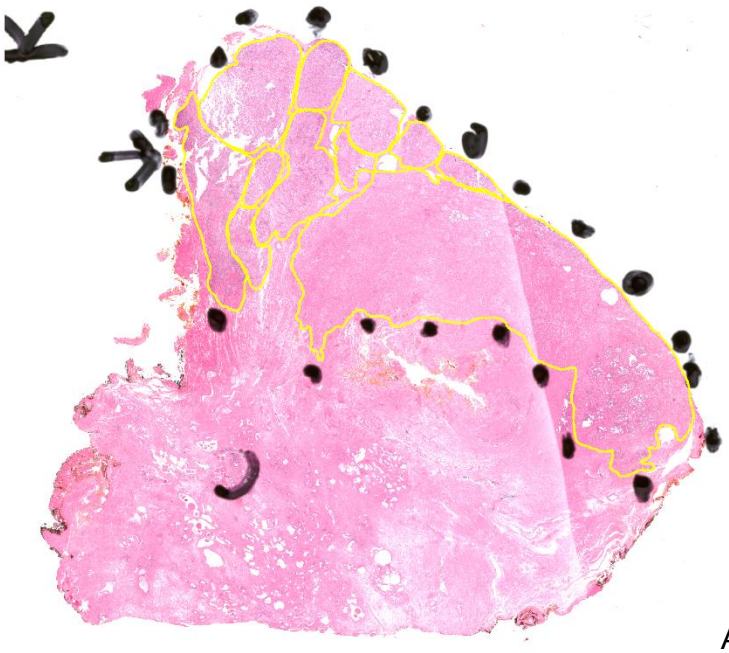

A)

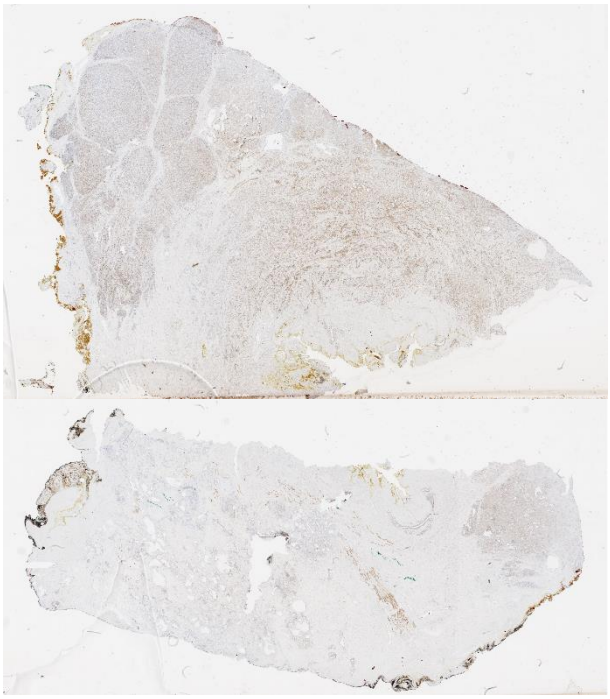

B)

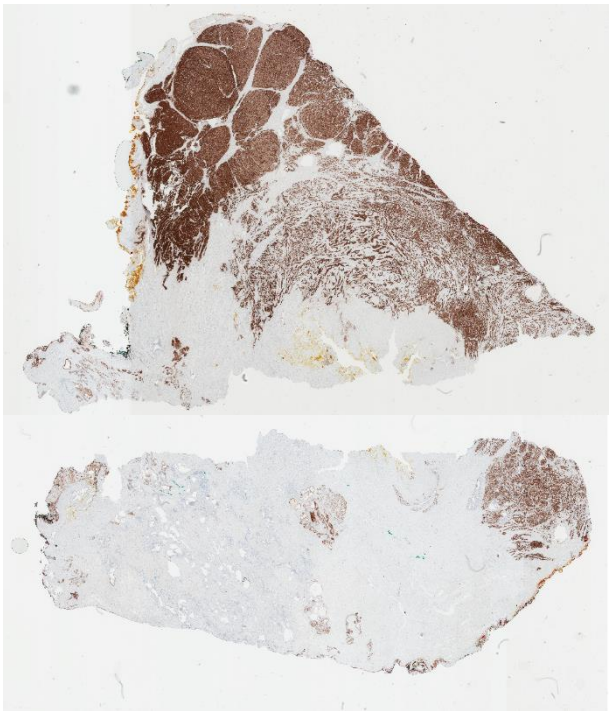

C)

Patient N.21 (ID: 5C)

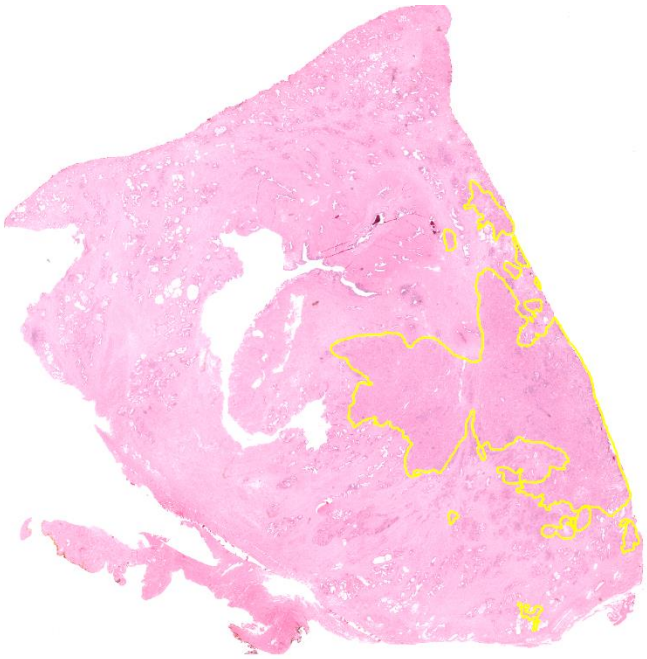

A)

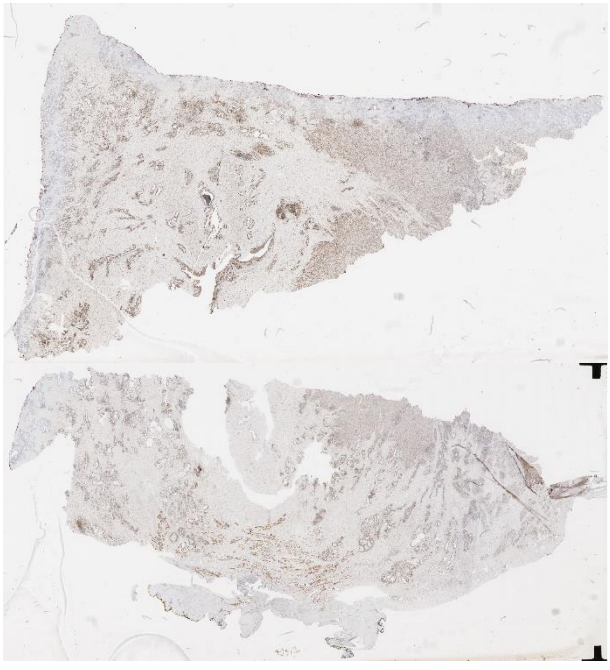

B)

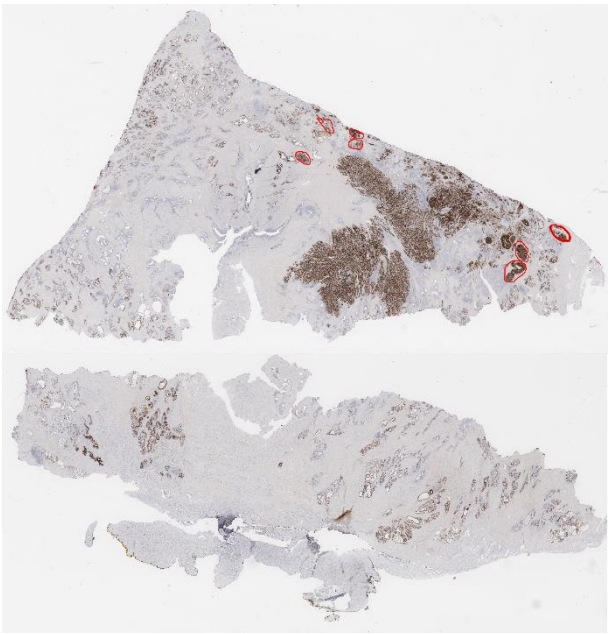

C)

Patient N.22 (ID: 6D)

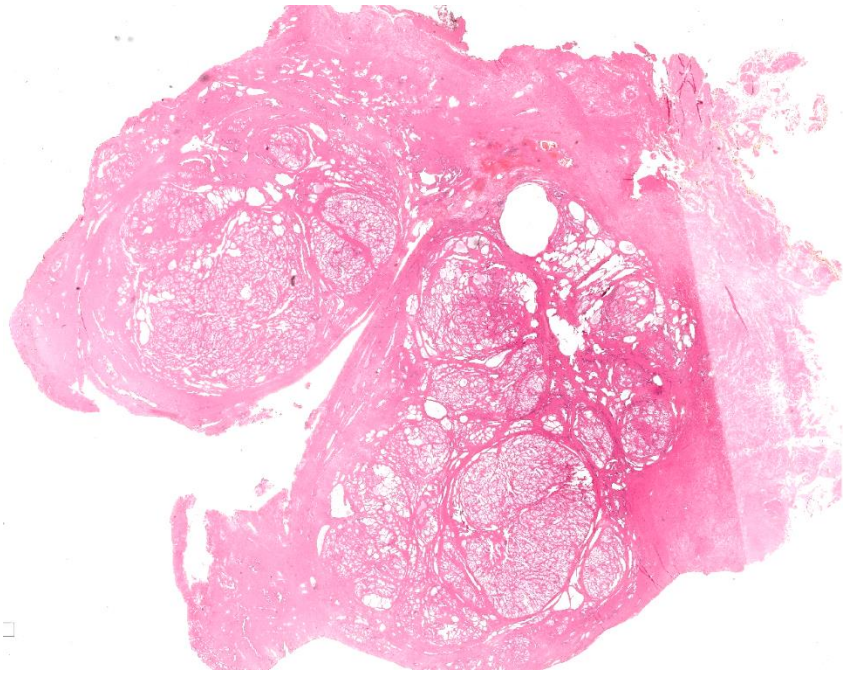

A)

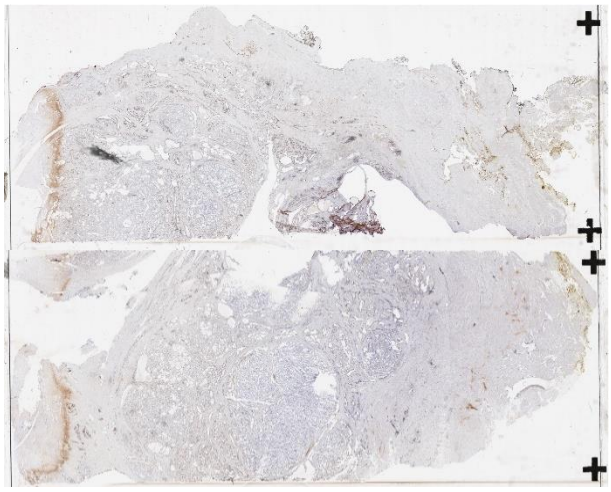

B)

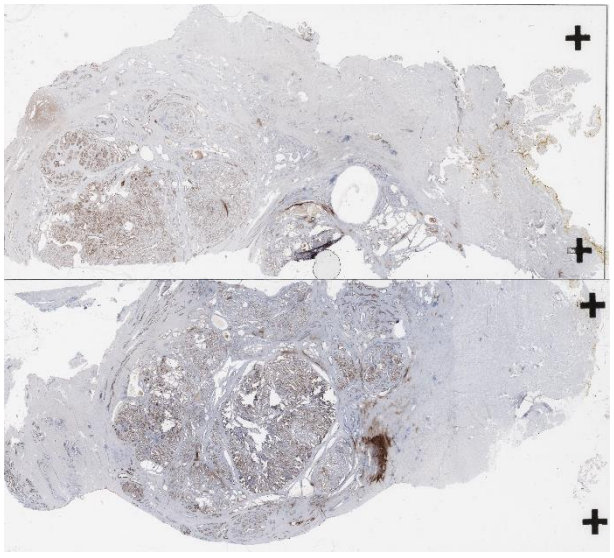

C)

Patient N.23 (ID: 7D)

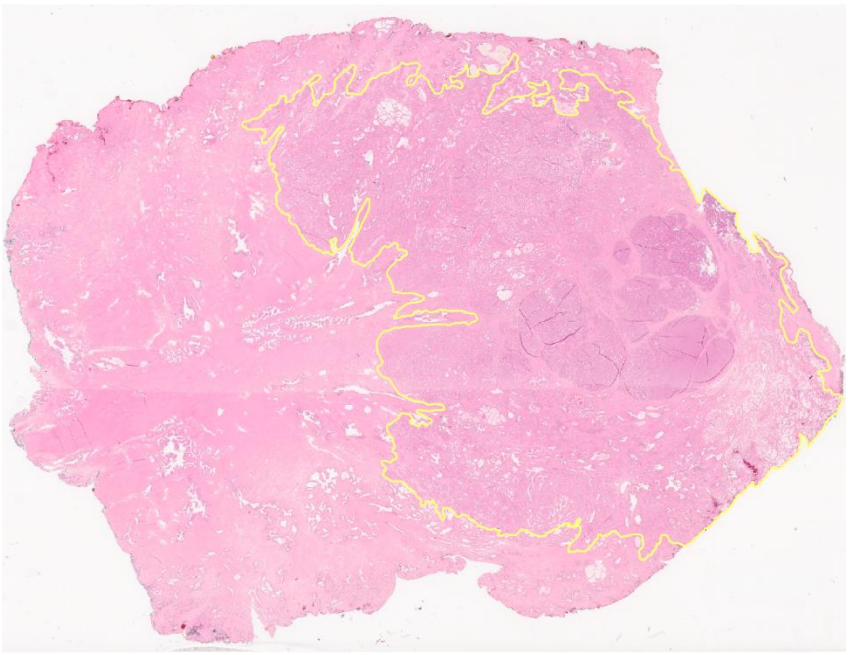

A)

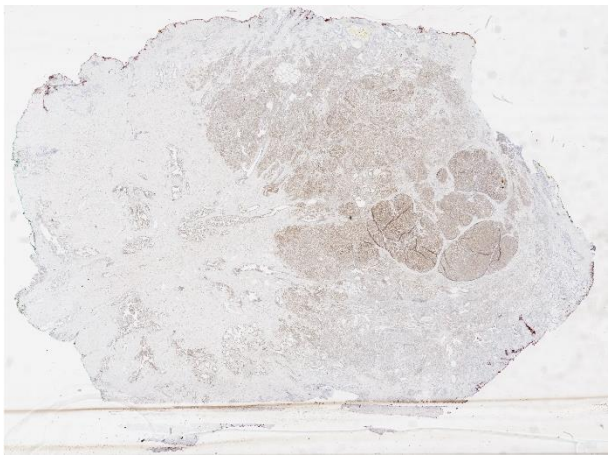

B)

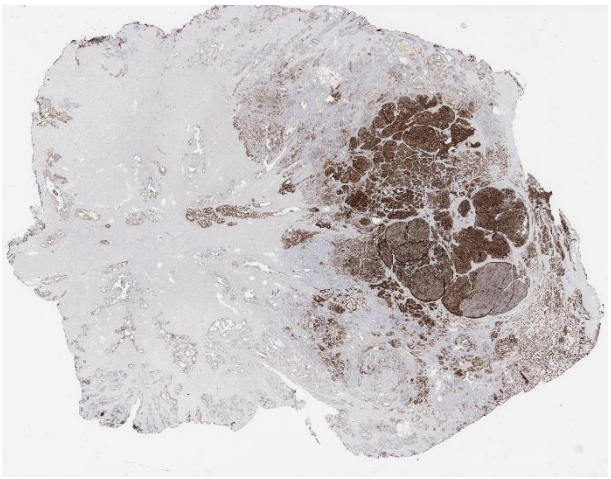

C)

Patient N.24 (ID: 8B)

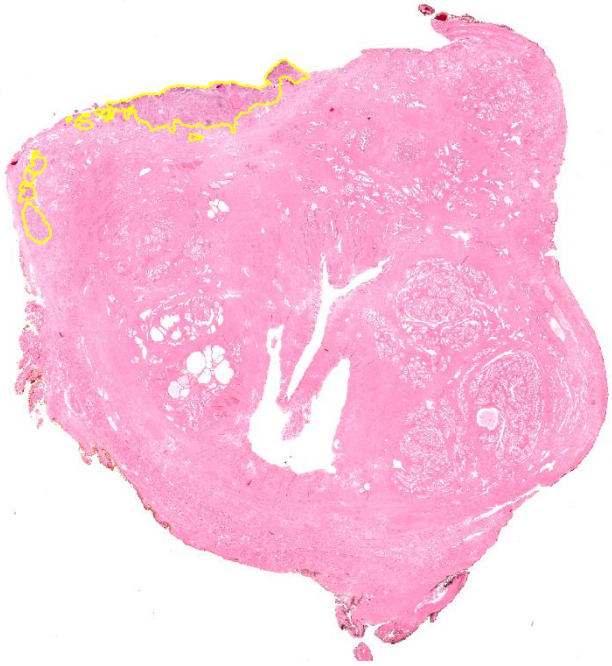

A)

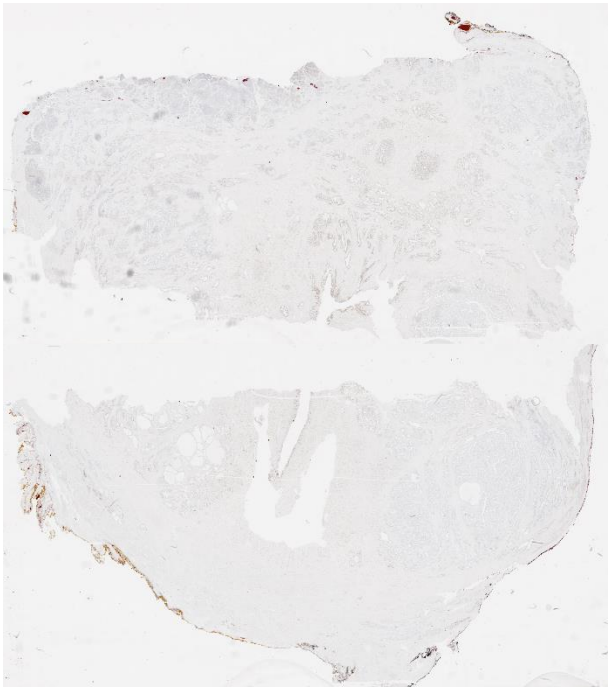

B)

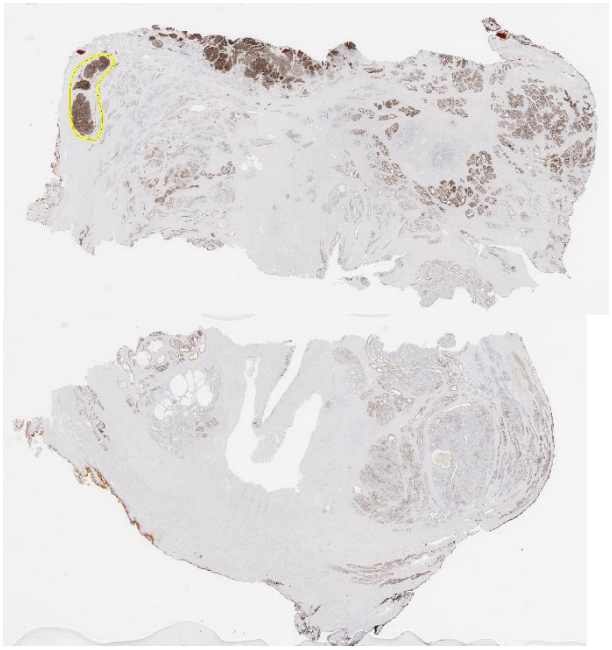

C)

Patient N.25 (ID: 9C)

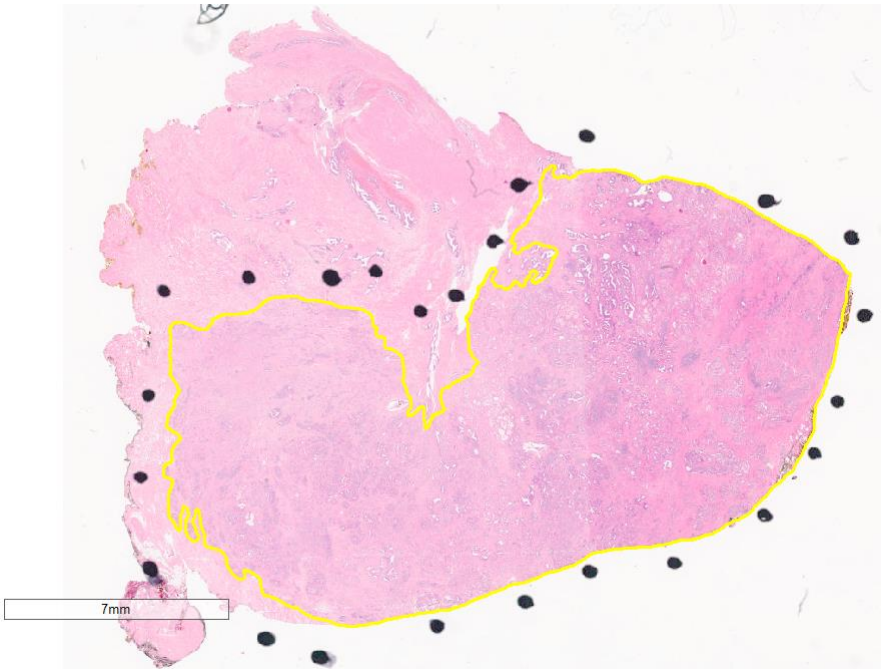

A)

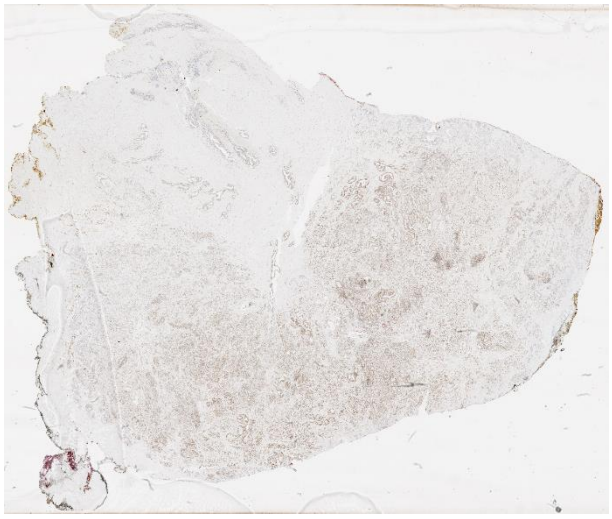

B)

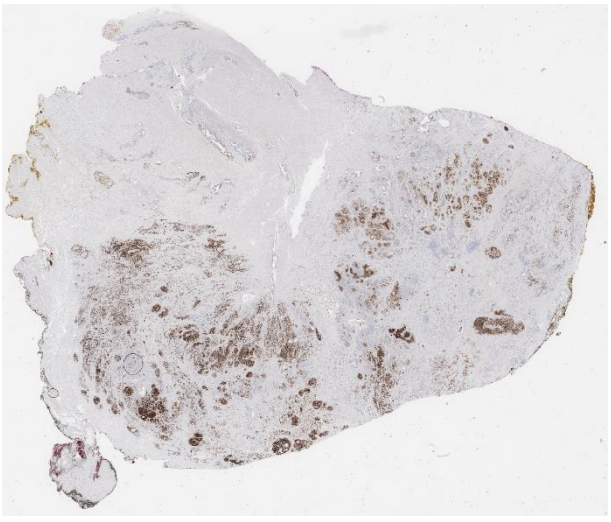

C)

Patient N.26 (ID: 11C)

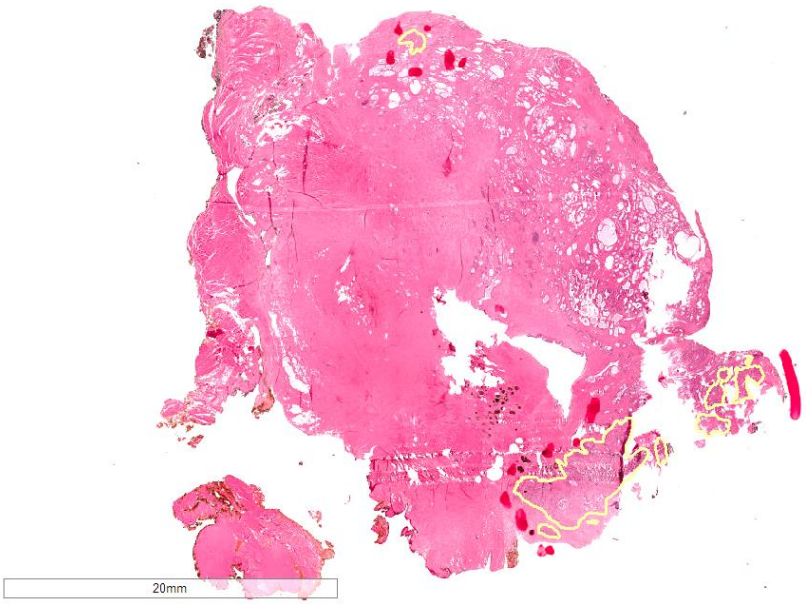

A)

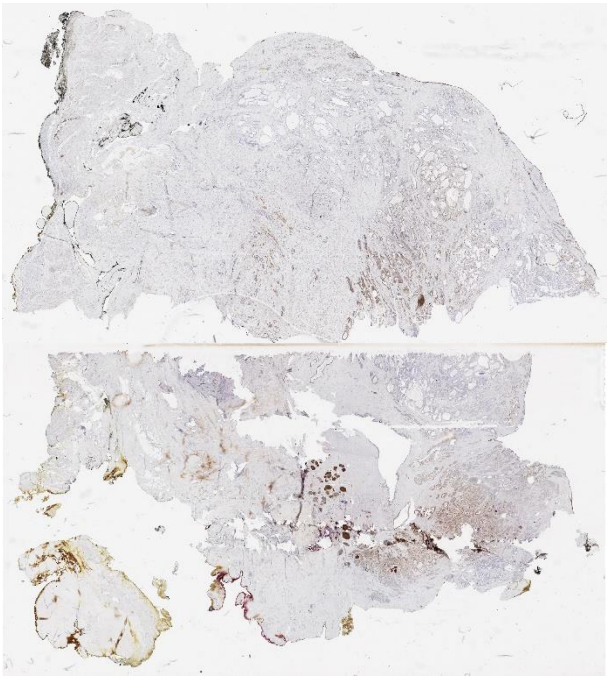

B)

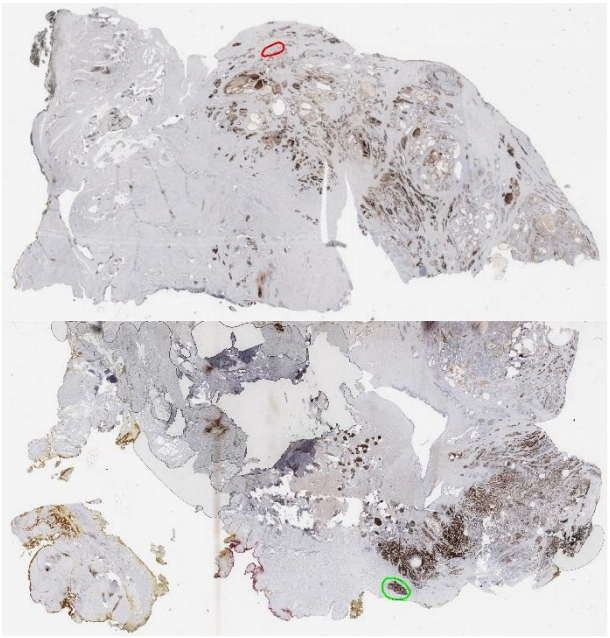

C)

Patient N.27 (ID: 12C)

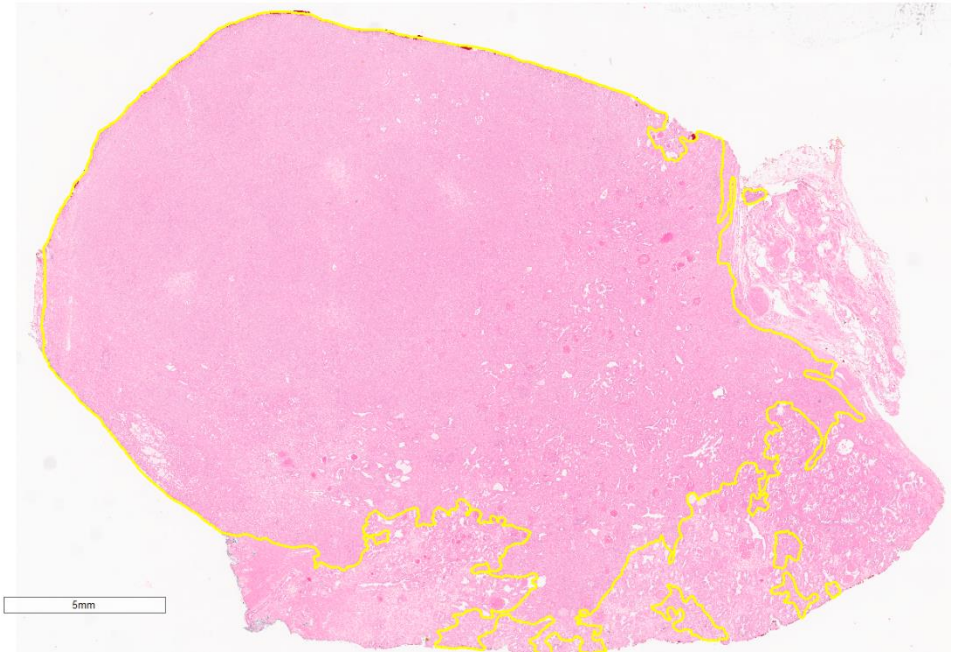

A)

B)

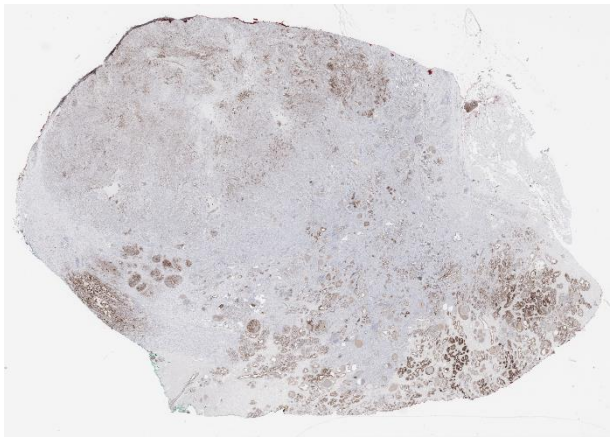

C)

Patient N.28 (ID: 13B)

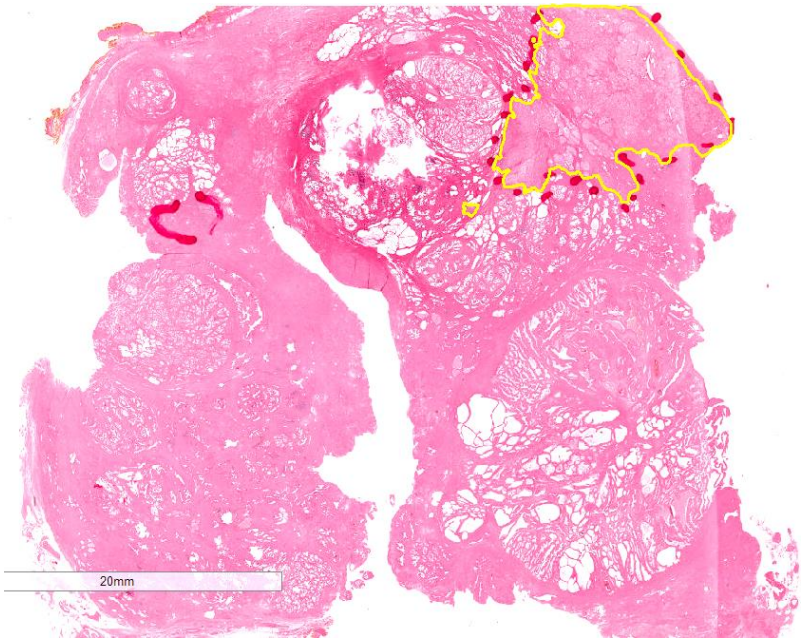

A)

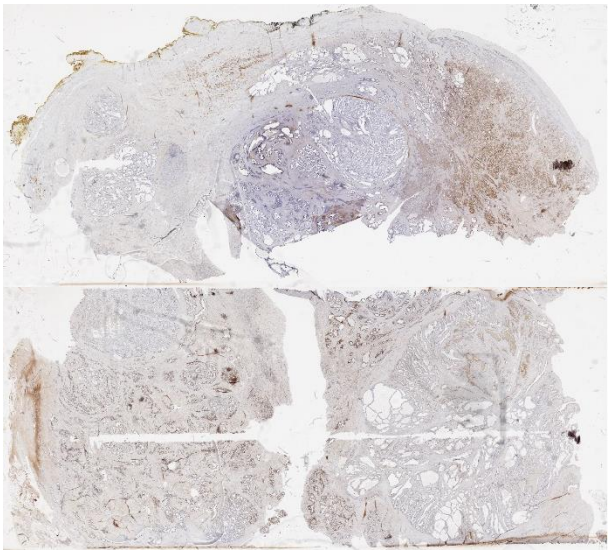

B)

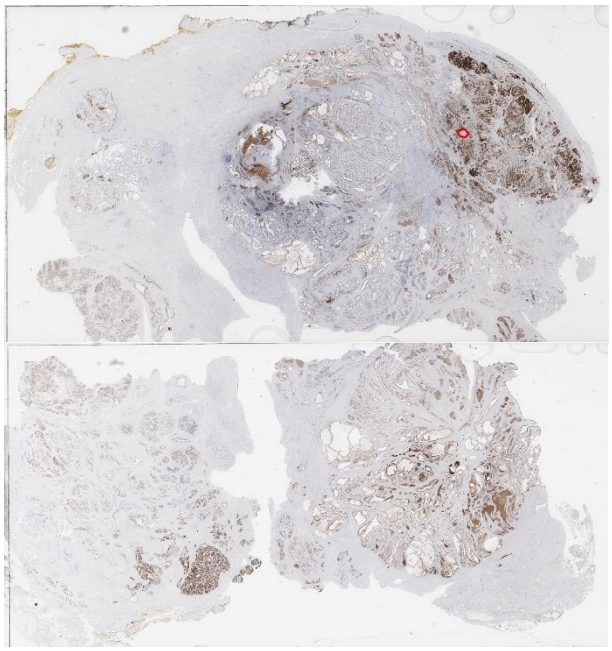

C)

Patient N.29 (ID: 15A)

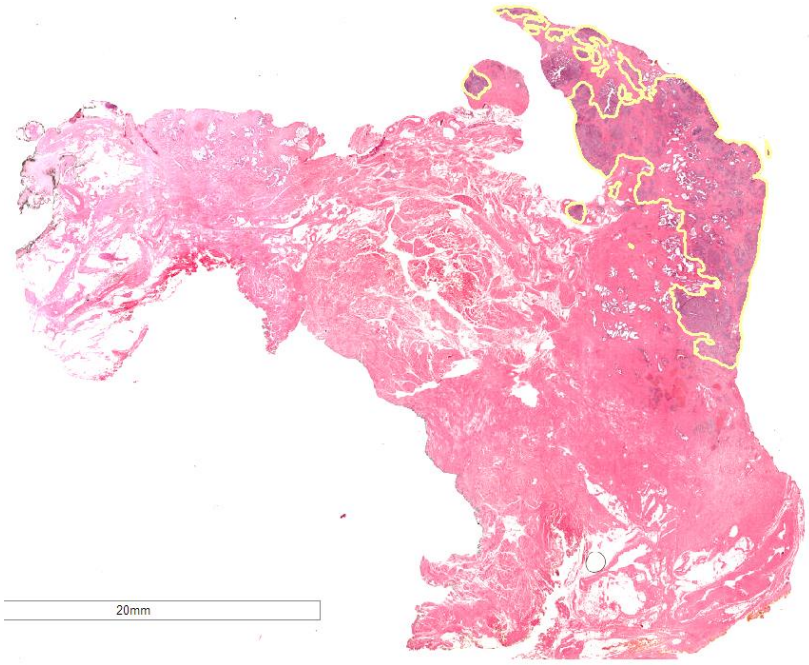

A)

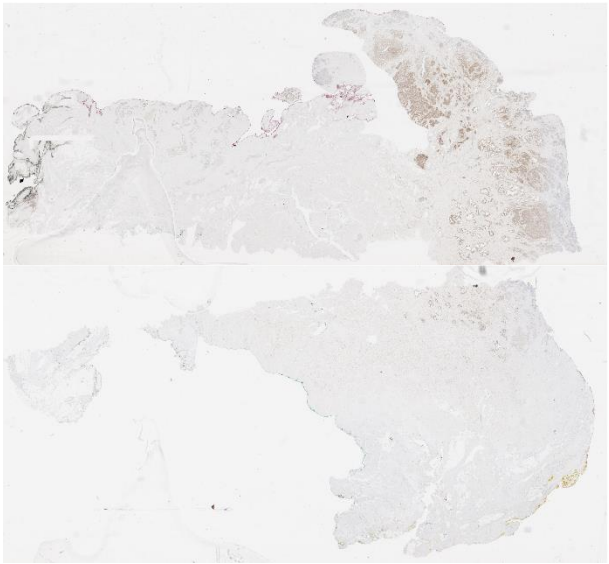

B)

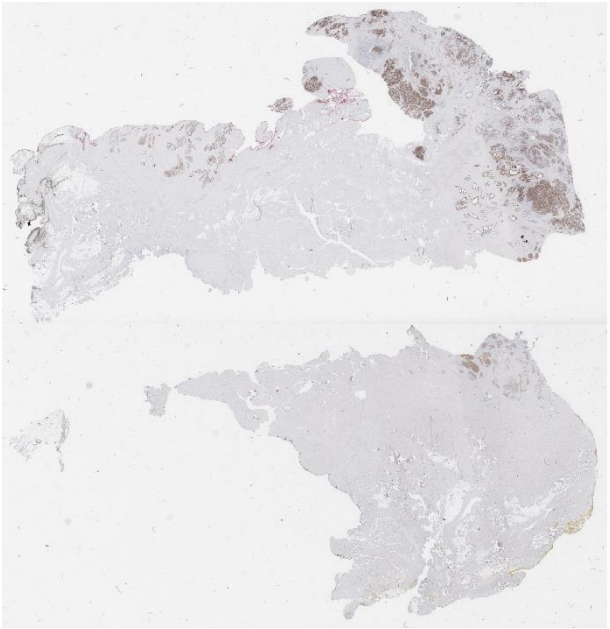

C)

Patient N.30 (ID: 16D)

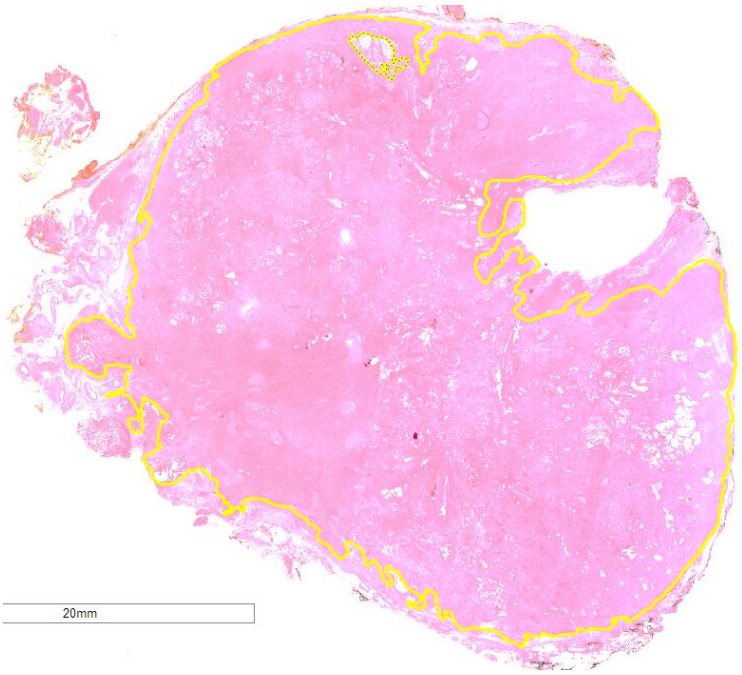

A)

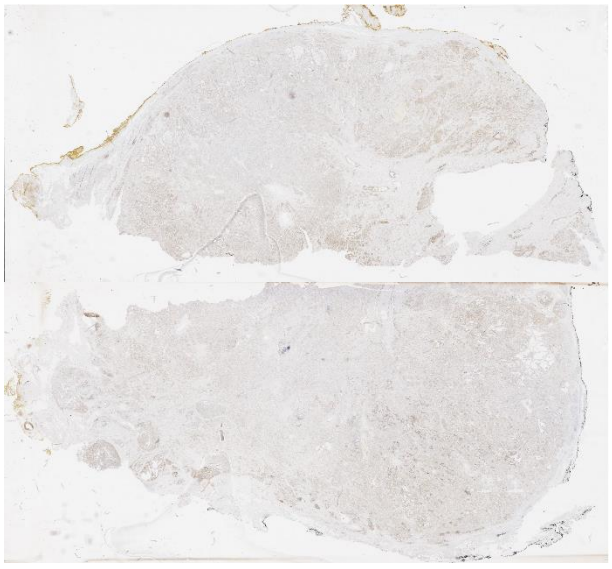

B)

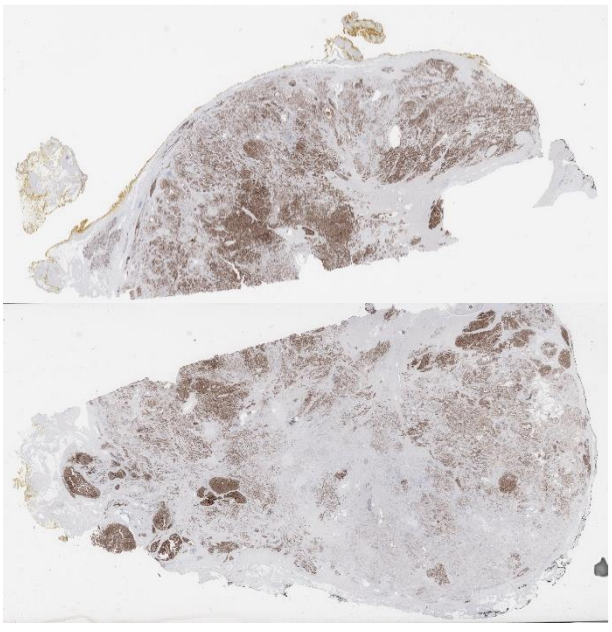

C)

Patient N.31 (ID: 19B)

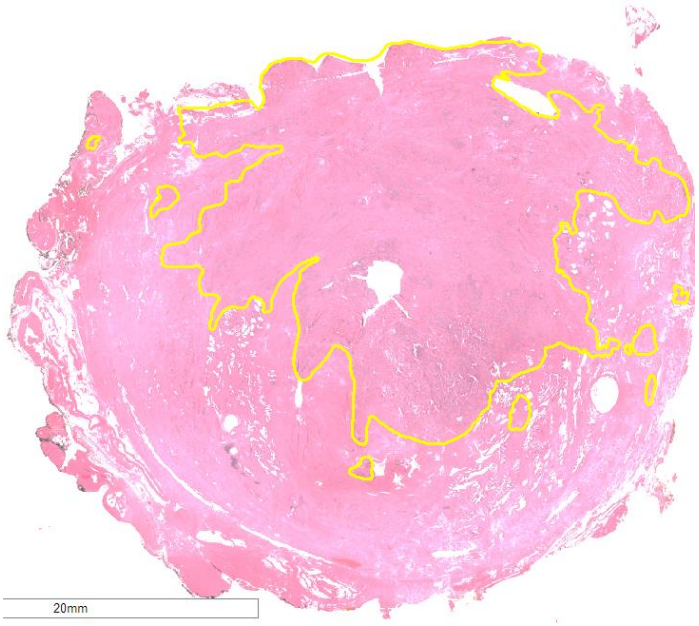

A)

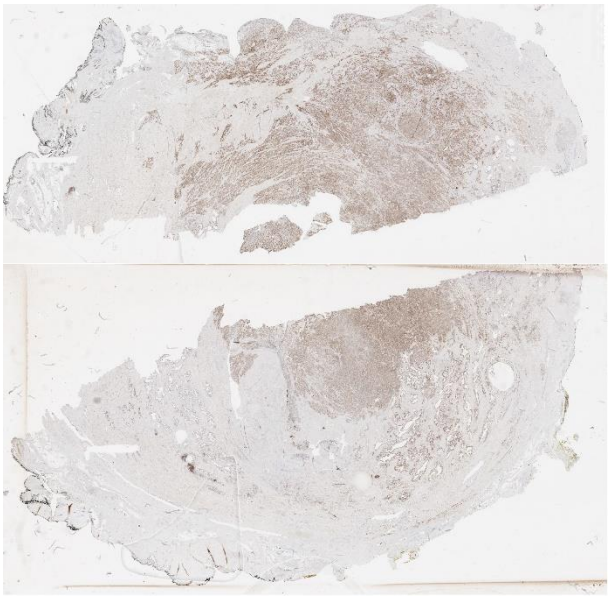

B)

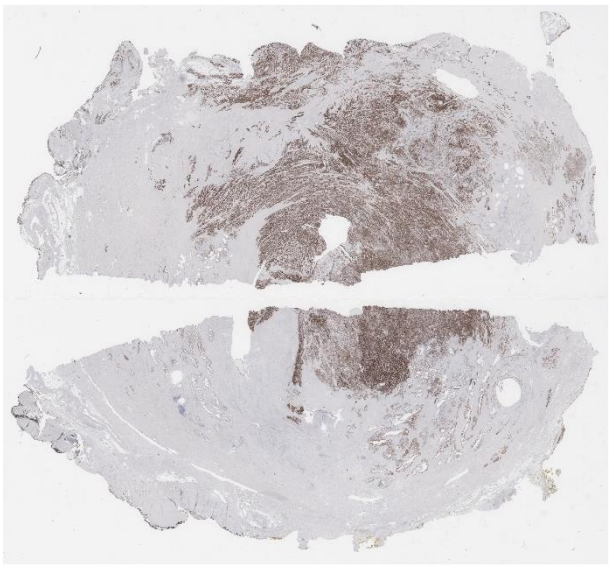

C)

11 Danksagung

"Ever tried. Ever failed. No matter. Try again. Fail again. Fail better."

Samuel Beckett

Getreu dem Zitat von Samuel Beckett hatte auch die Anfertigung dieser Dissertation ihre Höhen und Tiefen. Deswegen möchte ich mich im Folgenden gerne bei den Menschen bedanken, ohne deren Beteiligung und Unterstützung dies nicht möglich gewesen wäre.

Mein besonderer Dank gilt meiner Doktormutter Frau Prof. Dr. Susanne Kossatz für die ausgezeichnete Betreuung und die enorme Unterstützung bei der Umsetzung der gesamten Arbeit. Ich hätte mir keine bessere Zusammenarbeit vorstellen können.

Des Weiteren möchte ich mich bei meiner Betreuerin Dr. med. Marianne Reiser bedanken, die mich im Rahmen meiner Dissertation mit ihrer Expertise unterstützt hat. Vielen Dank, dass Du geduldig alle meine Zeichnungen in den Präparaten durchgeschaut und verbessert hast.

Außerdem möchte ich Hui Wang und Prof. Dr. med. Matthias Eiber Danke sagen, die durch ihre Zusammenarbeit und das Bereitstellen von Präparaten einen Teil der Analysen ermöglicht haben.

Bei meinen Schwestern Susanne und Nane und meinem Freund Andi möchte ich mich von ganzem Herzen für die Durchsicht und sprachliche Korrektur der Arbeit bedanken. Die Gewissheit, dass Ihr immer für mich da seid, ist für mich die größte Hilfe.

Meinen Freunden Anne und Laura danke ich für ihren emotionalen Support und ihre Bereitschaft, Zeit und Aufmunterungen in jeder Lebenslage beizusteuern.

Last, but not least möchte ich meinen Eltern danken, die durch ihre Unterstützung und Ermutigungen überhaupt möglich gemacht haben, dass ich ein so langes Studium und diese Promotion abschließen konnte. Vielen Dank!